Effect of HDAC9 Deficiency on Atherosclerosis and Stroke
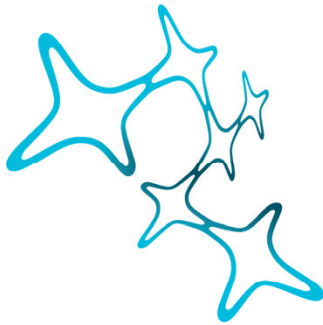

Sepiede Azghandi

Dissertation at the Graduate School of Systemic Neurosciences
at the Ludwig-Maximilians-Universität München

Effect of HDAC9 Deficiency on Atherosclerosis and Stroke

submitted by

Sepiede Azghandi

11th of August 2015

For Dominik

and

my parents

Table of Contents

Abbreviations

ACA	Anterior cerebral artery
ApoE	Apolipoprotein E
BCA	Brachiocephalic artery
BMT	Bone marrow transplantation
CAD	Coronary artery disease
CBF	Cerebral blood flow
CCA	Common carotid artery
CCR2	CC-chemokine receptor 2
CLC	Contralateral cortex
CLS	Contralateral striatum
CXCL1	Chemokine (C-X-C motif) ligand 1
DT	Diphtheria toxin
ELISA	Enzyme-linked immunosorbent assay
FACS	Fluorescence-activated cell sorting
FoxP3	Forkhead box P3
GAPDH	Glyceraldehyde 3-phosphate dehydrogenase
GWAS	Genome-wide association study
H&E	Hematoxylin and eosin
HAT	Histone acetyltransferase
HDAC9	Histone deacetylase 9
HDRP	Histone deacetylase-related protein
HPRT	Hypoxanthine-guanine phosphoribosyl-transferase
IC	Infarct core
IFN-γ	Interferon-γ
IL-10	Interleukin-10
LDL	Low-density lipoprotein
LDLR	Low-density lipoprotein receptor
LVS	Large vessel stroke
MCA	Middle cerebral artery
MCAo	Middle cerebral artery occlusion
MCP-1	Monocyte chemoattractant protein-1
MEF2	Myocyte enhancer factor 2
oxLDL	Oxidized LDL
PBMCs	Peripheral blood mononuclear cells

PComA	Posterior communicating artery
PFA	Paraformaldehyde
PIR	Peri-infarct region
Rag-1	Recombination activating gene 1
ROI	Region of interest
SCA	Subclavian artery
SCID	Severe combined immunodeficiency
SMC	Smooth muscle cell
SNP	Single nucleotide polymorphism
TGF-β	Transforming growth factor-β
TOAST	Trial of organization 10172 in acute stroke treatment
tPA	Tissue plasminogen activator
Tregs	Regulatory T cells
TUNEL	Terminal deoxynucleotidyl transferase dUTP nick end labeling
VCAM-1	Vascular cell adhesion molecule-1

1 Summary

In a genome-wide association study for ischemic stroke, the so far strongest risk locus for large vessel stroke was identified in the histone deacetylase 9 (*HDAC9*) gene region at chromosome 7p21.1. HDAC9 mRNA levels were found to be increased in peripheral blood mononuclear cells of healthy risk allele carriers of the lead SNP rs2107595, suggesting that increased HDAC9 expression enhances the risk for large vessel stroke. These findings make HDAC9 a promising candidate gene for atherosclerosis and stroke. In this thesis, we investigated the consequences of HDAC9 deficiency on atherosclerosis and ischemic stroke outcome.

ApoE deficient mice (ApoE$^{-/-}$) were used as a model for atherosclerosis. We analyzed the effects of HDAC9 deficiency on atherosclerotic plaque size in ApoE deficient mice at different ages and on different diets. Compared to HDAC9$^{+/+}$ApoE$^{-/-}$ mice, HDAC9$^{-/-}$ApoE$^{-/-}$ mice showed reduced atherosclerotic lesion sizes and less advanced lesions, when they were fed a chow diet. However, no difference was observed in more advanced atherosclerosis after a high-cholesterol Western-type diet, indicating a protective role of HDAC9 deficiency in early atherogenesis. Immunological analyses by flow cytometry showed a shift in monocyte populations from classical, inflammatory monocytes to more resident monocytes in HDAC9$^{-/-}$ApoE$^{-/-}$ mice. Moreover, T cell analysis revealed a reduction in effector memory T cells in chow fed HDAC9$^{-/-}$ApoE$^{-/-}$ mice, indicating decreased activation and migration of T cells. These findings suggest that both innate and adaptive immunity play an important role in the atheroprotective effect of HDAC9 deficiency.

For ischemic stroke outcome, we used a transient focal ischemia model which is based on the occlusion of the middle cerebral artery (MCAo) for one hour, using a filament inserted via the internal carotid artery. In contrast to the protective effect of HDAC9 deficiency in atherosclerosis, HDAC9$^{-/-}$ mice showed increased infarct volumes and more severe neurological deficits 24 hours as well as 7 days after MCAo. TUNEL staining revealed increased cell death in peri-ischemic areas of HDAC9$^{-/-}$ mice, indicating a protective role of HDAC9 in the brain parenchyma.

Our results suggest a pro-atherogenic but neuroprotective role of HDAC9. Specific pharmacological inhibition of HDAC9 might be a promising strategy to prevent atherosclerosis, but not to improve ischemic stroke outcome. Thus, potential effects of HDAC9 inhibitors on the brain have to be considered.

2 Introduction

2.1 Stroke

Epidemiology

Stroke is the second most common cause of death worldwide (Lozano et al., 2012). In the United States, every 40 seconds someone has a stroke and every 4 minutes someone dies of a stroke (Mozaffarian et al., 2015). Incidence for stroke varies between countries, ranging worldwide from 60 to 504 cases per 100,000 people per year (Feigin et al., 2014). In 2010, stroke was at the third rank of major causes for reduced disability-adjusted life years (DALYs, the sum of years of life lost and years lived with disability) (Murray et al., 2012). The lifetime risk for stroke is 1 out of 5 women and 1 out of 6 men (Seshadri and Wolf, 2007). In 2010, total European costs for stroke were 64.1 billion Euros (Olesen et al., 2012). Stroke is an increasing health problem worldwide because of demographic changes confronting us with an aging population.

Stroke is characterized by neurological deficits which are based on an acute focal injury of the central nervous system due to a vascular cause (Sacco et al., 2013) and can be subdivided into ischemic (80%) and hemorrhagic stroke (20%). While hemorrhagic stroke results from a rupture of a vessel leading to extravasation of blood, ischemic stroke is caused by the narrowing or occlusion of a brain supplying artery, for example due to an embolus or a local thrombus.

Ischemic stroke subtypes

Based on the mechanism causing the vessel occlusion, ischemic stroke can be classified according to the pathophysiological Trial of Organization 10172 in Acute Stroke Treatment (TOAST) criteria as cardioembolic stroke, large vessel stroke (LVS), small vessel occlusion (lacunes), stroke of other determined etiology or stroke of undetermined etiology (Adams et al., 1993) (Figure 1). Cardioembolic stroke is induced by an embolus arising from the heart, for example as a result of atrial fibrillation. In patients with LVS one of the major brain arteries or branch cortical arteries is occluded or has a significant stenosis (> 50%) by atherosclerotic plaques. Stroke due to small vessel disease (microangiopathy of the small cerebral vessels including small arteries, arterioles, capillaries and venules) is characterized

by subcortical or brainstem infarcts (diameter less than 1.5 cm), collectively called lacunar infarcts.
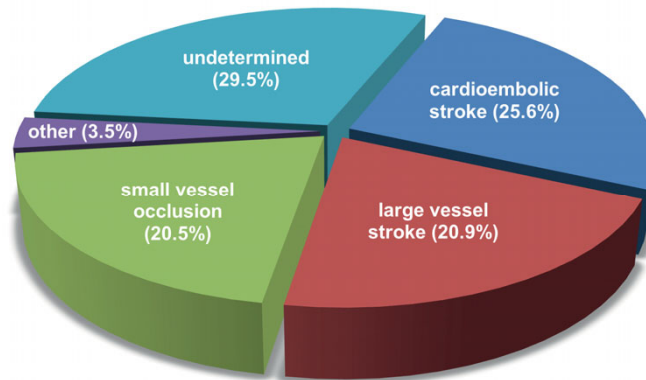
Figure 1. Etiology of ischemic stroke.
Frequencies are taken from the Stroke Data Bank of the German Stroke Foundation (Grau et al., 2001).

Therapy of ischemic stroke

In acute ischemic stroke, the most effective treatment after exclusion of a hemorrhagic cause by CT (computed tomography) scan is thrombolysis by recombinant tissue plasminogen activator (tPA) to recanalize the vessel and reperfuse the brain (The National Institute of Neurological Disorders and Stroke rt-PA Stroke Study Group, 1995). The time window of only 4.5 hours after stroke onset is essential for this therapy (Hacke et al., 2008). Recent studies showed that tPA in combination with stent retriever thrombectomy improves functional outcome in comparison to tPA medication alone, which is a breakthrough in acute stroke management (Jovin et al., 2015; Saver et al., 2015). As secondary prevention of recurrent stroke, patients receive antiplatelet agents such as aspirin and dipyridamole, statins for treating hypercholesterolemia and anticoagulants in case of atrial fibrillation. When stenosis of the symptomatic carotid artery is at least 70%, carotid endarterectomy is performed (Donnan et al., 2008). Specific treatment options for stroke are still limited, since disease mechanisms are poorly understood.

Genetics of ischemic stroke

Ischemic stroke is a heterogeneous multifactorial disease. Modifiable risk factors (hypertension, smoking, diabetes, atrial fibrillation and obesity) and acquired risk factors (age, gender and race-ethnicity) can explain part of the stroke risk, but from twin and family studies we know that also genetic factors play a substantial role (Goldstein et al., 2006). Twin studies showed that the concordance rate for stroke is fivefold higher in monozygotic twins than in dizygotic twins (Brass et al., 1992). The heritability of ischemic stroke is estimated at 37.9%, but varies for the different subtypes: 40.3% for LVS, 32.6% for cardioembolism, and 16.1% for small vessel disease (Bevan et al., 2012). These differences emphasize the importance of stroke subtyping for identifying genetic associations.

To discover novel genetic components influencing ischemic stroke risk, two approaches are commonly used: candidate-gene association studies (Hirschhorn et al., 2002) and genome-wide association studies (GWAS) (Wang et al., 2005). Both approaches make use of common (frequency >1%) genomic variants usually affecting a single nucleotide (single nucleotide polymorphisms, SNPs) to identify disease risk genes. The majority of these variants has no consequences on protein sequences or expression. However, some of them are located in coding regions and can cause amino acid exchanges altering protein structure, others are situated in regulatory regions and might influence gene expression. In both cases, this might result in an increased disease risk. In the candidate-gene approach the frequencies of variants in a known gene are compared between stroke patients and controls, but in the past only very few hits have been successfully replicated, probably due to small sample sizes, poor stroke subtype classification and study design (Dichgans and Markus, 2005). Therefore, current research focuses more and more on GWAS in order to identify risk loci in complex diseases. Here a large number of variants from the whole genome are compared between cases and controls. Some of them might have an impact for example on stroke risk by affecting conventional risk factors such as hypertension (Marteau et al., 2005) or by modulating diseases including atherosclerosis (Lusis et al., 2004; Stylianou et al., 2012). But they could also influence infarct size or stroke outcome, making GWAS a highly promising approach to identify novel risk factors.

2.2 A new risk locus for large vessel stroke - the 7p21.1 region

As part of the International Stroke Genetics Consortium and the Wellcome Trust Case Control Consortium 2, we recently contributed to a GWAS conducted on ischemic stroke (Bellenguez et al., 2012). 495,851 SNPs were analyzed in 3,548 stroke cases and 5,972 controls, all of European ancestry. Stroke cases were classified according to the TOAST classification into LVS, cardioembolism, and small vessel disease. Previous risk loci for cardioembolic stroke (*PITX2* and *ZFHX3*) (Gretarsdottir et al., 2008; Gudbjartsson et al., 2009; Lemmens et al., 2010) and one locus for LVS (9p21.3) (Gschwendtner et al., 2009) could be replicated. Additionally, a novel locus for LVS at the 7p21.1 region - the strongest risk locus for this stroke subtype to date - was identified and replicated in an independent cohort (Bellenguez et al., 2012). The METASTROKE collaboration could confirm this novel risk locus in a combined data set from available GWAS with 12,389 stroke cases and 62,004 controls from 15 different populations, all of European ancestry (Traylor et al., 2012). In the METASTROKE study, the rs2107595 SNP was the most significant variant with a *P*-value of 2.03×10^{-12}. The population attributable risk was estimated to be 4.5%, the odds ratio was 1.39 (95% CI: 1.27 - 1.53) and the risk allele frequency was 16% (Traylor et al., 2012). The 7p21.1 locus encompasses the 3'-end of the histone deacetylase 9 (*HDAC9*) gene and the intergenic region between *HDAC9* and its neighboring genes, *TWIST1* and *FERD3L* (Figure 2).
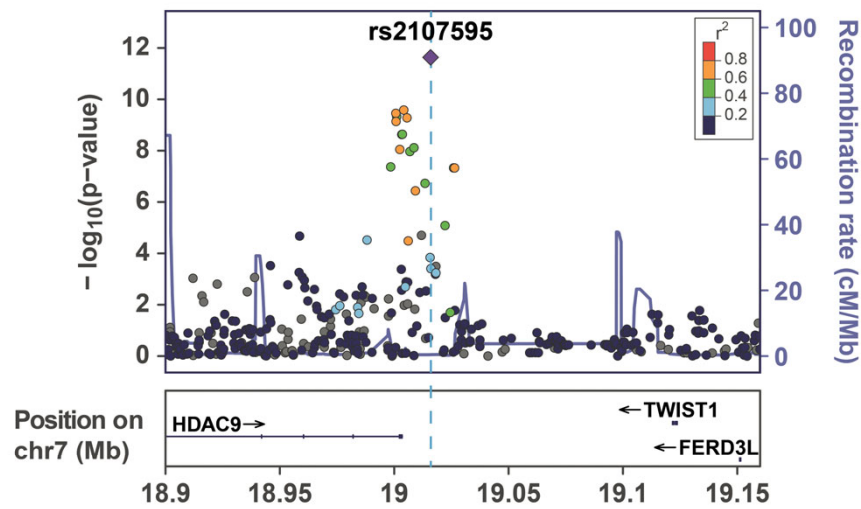
Figure 2. Plot of association signals in the 7p21.1 region.
rs2107595, the lead SNP from the METASTROKE data set (Traylor et al., 2012), and all other associated signals are located at the 3'-end of the *HDAC9* gene and in the intergenic region between *HDAC9* and the neighboring genes, *TWIST1* and *FERD3L*. Figure adapted from Azghandi et al., 2015.

The same locus was found by the CARDIOGRAM Consortium to be associated with coronary artery disease (CAD) and myocardial infarction (Deloukas et al., 2013). This is in line with the strong overlap of genetic susceptibility between ischemic stroke, especially LVS, and CAD (Dichgans et al., 2014). Moreover, several variants within the 7p21.1 region show association with both conditions, indicating that they act through a shared mechanism. Since LVS and CAD are both primarily caused by atherosclerosis, the 7p21.1 region likely represents a risk locus for this disease.

2.3 Atherosclerosis

Development of atherosclerotic plaques

Atherosclerosis is the major contributor to cardiovascular disease including stroke and myocardial infarction. It is a progressive inflammatory disease of the arterial wall characterized by accumulation of intra- and extracellular lipids and fibrous material in the inner lining of arteries, the tunica intima. The word "atherosclerosis" is derived from the Greek words "athera" (gruel) and "sklerosis" (hardening). Until the 1970s atherosclerosis has been considered as a disease of lipid deposition since there is a strong correlation

between hyperlipidemia and atherosclerosis (Ross and Harker, 1976). But in the past decades the involvement of both innate and adaptive immunity became clear.

Atherosclerosis develops in several steps (Figure 3). The anatomy of a normal arterial wall is shown in Figure 3A. The initiating step in atherosclerosis is endothelial activation due to endothelial injury, hyperlipidemia or pro-inflammatory mediators. Low-density lipoprotein (LDL) infiltrating the tunica intima can be modified by oxidation and induces an inflammatory response of the endothelium (Skalen et al., 2002; Hansson, 2005). This subendothelial retention of lipoproteins by the extracellular matrix leads to the expression of endothelial adhesion molecules (Nakashima et al., 1998) and the recruitment of leukocytes to the tunica intima (Figure 3B). Monocytes infiltrate the intima, differentiate into tissue macrophages and take up lipoproteins, including oxidized LDL. These macrophages become foam cells, a histological term derived from their lipid laden, foamy appearance. Early atherosclerotic lesions, called "fatty streaks", consist of subendothelial accumulation of foam cells (Figure 3C) and can already be found in the aorta of children in the first decade of life (Lusis, 2000). These lesions have no clinical relevance, but they can progress to advanced lesions which form mainly at branch points of arteries because of blood flow turbulences (Lusis, 2000). Advanced lesions are characterized by a fibrous cap formed by smooth muscle cells and extracellular matrix, a lipid-rich necrotic core and surrounding leukocytes of the innate and adaptive immunity (Figure 3D and 3E).

The necrotic core consists of dying foam cells which release their lipid content and thereby contribute to the excess of extracellular lipids in the lesion. Smooth muscle cells migrate from the tunica media into the intimal lesion, secreting extracellular matrix components and thereby increasing the lesion size. Initially, the atherosclerotic plaque grows into the direction of the tunica adventitia, but after reaching a critical point it grows toward the blood vessel lumen resulting in a decrease in vessel diameter. A plaque can grow gradually until it reduces the blood flow in a vessel, leading to a stenosis. But the most important complication of atherosclerosis is plaque rupture, which exposes procoagulant material often leading to a local thrombus or an embolus occluding a distal artery. The thickness of the fibrous cap, grade of inflammation, and necrotic core size are critical parameters for rupture-prone, so called vulnerable plaques (Finn et al., 2010).
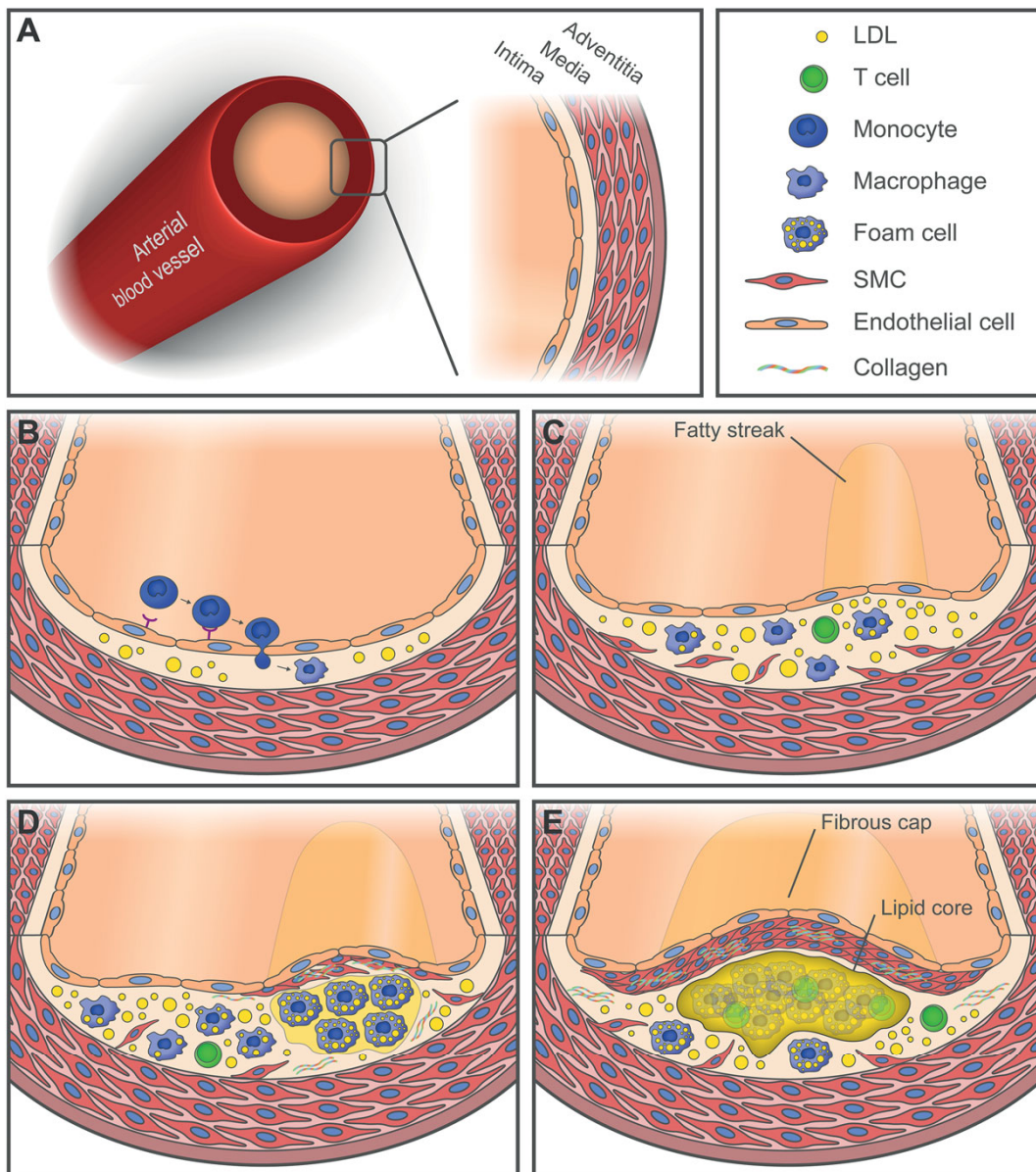
Figure 3. Stages in the development of atherosclerosis.
A, Scheme of a normal, healthy artery consisting of three layers, the tunica intima with the endothelium, the tunica media with vascular smooth muscle cells (SMCs), and the tunica adventitia with connective tissue. **B,** The initial step of atherogenesis is the expression of endothelial adhesion molecules after endothelial activation, the subsequent adhesion and migration of monocytes into the tunica intima and their differentiation into macrophages. **C,** Macrophages phagocytose lipoprotein particles, become foam cells and form so-called fatty streaks. SMCs migrate out of the tunica media into the tunica intima. **D,** SMCs produce extracellular matrix molecules such as collagen and start to form a fibrous cap. **E,** Apoptosis of foam cells and SMCs leads to the formation of a necrotic core with extracellular lipids. An advanced atheroma develops with a fibrous cap covering the necrotic, lipid core.

Mouse models of atherosclerosis

Animal models of atherosclerosis have been developed in a variety of species including rabbits, pigs and non-human primates. However, the most important and most commonly used laboratory model is the mouse (Getz and Reardon, 2012). Under normal conditions wild-type mice do not develop atherosclerotic lesions, but deletion of the apolipoprotein E (*ApoE*) gene leads to spontaneous atherosclerotic plaque formation (Plump et al., 1992; Nakashima et al., 1994). Atherogenesis in this model is accelerated by feeding a high-cholesterol diet, for example a Western-type diet (Figure 4). Another mouse model for atherosclerosis is based on low-density lipoprotein receptor (LDLR) deficiency. These mice have to be fed a high-cholesterol diet to develop atherosclerotic plaques. Although the sites of lesion formation in both mouse models (aortic root, aortic arch and brachiocephalic artery) are different from humans (coronary, carotid and periphery arteries) (Getz and Reardon, 2012), plaque types and phases of their development are highly comparable (Figure 4). However, the process of atherothrombosis due to plaque rupture cannot be studied in mouse models since vulnerable plaques do not develop. Nevertheless, the results of studies in mouse models have strongly advanced our understanding of atherosclerotic processes. Both the ApoE$^{-/-}$ and the LDLR$^{-/-}$ model are widely used to test therapeutic options for atherosclerosis or, after breeding them to other transgenic or knockout mice, to study the role of different factors, e.g. components of the immune system in atherogenesis. In addition, bone marrow transplantation into ApoE$^{-/-}$ or LDLR$^{-/-}$ mice can be performed to investigate the contribution of bone marrow derived cells. Collectively, advantages of possible genetic manipulation as well as short breeding times and relatively low costs for husbandry in comparison to other mammalian species make the mouse the most frequently used and favored model in atherosclerosis research.
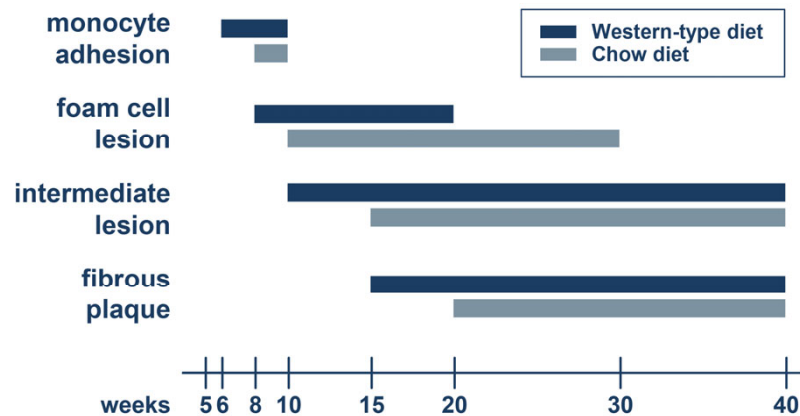
Figure 4. Timeline of atherosclerotic lesion development in ApoE deficient mice.
Feeding a high cholesterol Western-type diet accelerates atherogenesis in comparison to a standard chow diet (adapted from Nakashima et al., 1994).

Role of the immune system in atherosclerosis

The immune system plays an important role in the initiation, the progression, and the rupture of atherosclerotic lesions. The perception of atherosclerosis as a chronic inflammatory disease has replaced the earlier concept which focused entirely on lipid metabolism (Weber et al., 2008). A wide range of immune cell mediated cascades promote atherosclerosis. For instance, vascular cell adhesion molecule-1 (VCAM-1) has a major role in the initiation of atherosclerosis as an early endothelial-leukocyte adhesion molecule (Cybulsky and Gimbrone, 1991; Cybulsky et al., 2001). VCAM-1 selectively binds monocytes and lymphocytes, the predominant leukocyte subtypes in atherosclerotic plaques, and its expression increases in response to hypercholesterolemia at lesion-prone sites of the aorta (Nakashima et al., 1998). Diphtheria toxin (DT)-mediated depletion of monocytes in a CD11b-DT receptor transgenic mouse model led to a significant reduction of early plaque formation, whereas DT application had no effect on size and composition of established plaques, suggesting that monocytes play an important role in early atherogenesis (Stoneman et al., 2007). Different subsets of monocytes can be distinguished according to their expressed chemokine receptors: the short-lived inflammatory (CX_3CR1^{low} $CCR2^+$ $Ly6C^{hi}$) subset and the resident subset (CX_3CR1^{hi} $CCR2^-$ $Ly6C^{low}$) which represent patrolling monocytes on healthy endothelium and react immediately to an infection by inducing an early immune response (Auffray et al., 2007; Weber et al., 2008). It has been shown that hypercholesterolemia increases numbers of blood circulating $Ly6C^{hi}$ monocytes, which

infiltrate lesions of atherosclerotic mice (Swirski et al., 2007). Chemokines like the monocyte chemoattractant protein-1 (MCP-1/CCL2) play an important role in the recruitment and migration of monocytes into the tunica intima. Absence of MCP-1 or its receptor, CC-chemokine receptor 2 (CCR2) leads to decreased atherosclerotic lesion formation in experimental atherosclerosis models (Boring et al., 1998; Gu et al., 1998). Monocytes in the tunica intima differentiate to macrophages in response to macrophage colony-stimulating factor (M-CSF), produced by endothelial and smooth muscle cells (Rajavashisth et al., 1990).

Besides monocytes/macrophages, T cells, dendritic cells, mast cells, B cells, and neutrophils are present in atherosclerotic plaques. Macrophages and CD4+ T helper cells as well as CD8+ cytotoxic T cells are the predominant immune cell types of human atherosclerotic plaques (Jonasson et al., 1986; Stemme et al., 1992). Initially, it was thought that T cells are not playing a major role in atherosclerosis based on studies showing that ApoE$^{-/-}$ mice with a strongly compromised immune system - because of inactivation of the recombination activating gene 1 (Rag-1) - have unchanged atherosclerotic lesion sizes when fed a Western-type diet. But when a normal chow diet was used, they showed a 42% reduction in lesion size (Dansky et al., 1997). Similarly, immunodeficient ApoE$^{-/-}$/scid/scid mice show a 73% reduction in lesion size under chow diet (Zhou et al., 2000). An adoptive transfer of CD4+ T cells into ApoE$^{-/-}$/scid/scid mice aggravates atherosclerosis to almost the same degree as in immunocompetent ApoE$^{-/-}$ mice. Type 1 T helper (T$_H$1) cells are the most prevalent T cell subtype in human atherosclerotic lesions (Frostegard et al., 1999) and the pro-inflammatory cytokine interferon-γ (IFN-γ), which is secreted by T$_H$1 cells, appears to be proatherogenic (Whitman et al., 2000; Zhou et al., 2000). Analysis of the T cell antigen receptors expressed in atherosclerotic lesions showed a restricted pattern, suggesting oligoclonal T cell expansion and specific antigen processes in atherosclerosis (Paulsson et al., 2000). Isolated T cells from human atherosclerotic plaques react to oxLDL, making this metabolite a prime candidate antigen for atherosclerosis specific inflammatory processes (Stemme et al., 1995).

But some immune cell types and cytokines from the adaptive immunity show also atheroprotective properties like regulatory T cells (Tregs) and their cytokines interleukin-10 (IL-10) and transforming growth factor β (TGF-β). Tregs are T cells with immunosuppressive functions and essential for maintaining self-tolerance and the prevention of autoimmunity.

They can be generated in the thymus as naturally occurring Tregs or induced in the periphery from naïve CD4+ T cells (Ait-Oufella et al., 2014). Tregs are characterized by the expression of the forkhead/winged helix transcription factor FoxP3. It was shown that inhibition or deficiency of the Treg cytokines IL-10 and TGF-β aggravates atherosclerosis (Mallat et al., 1999; Mallat et al., 2001). Furthermore, depletion of Tregs by neutralizing antibody treatment or by diphtheria toxin increases atherosclerosis significantly (Ait-Oufella et al., 2006; Klingenberg et al., 2013), making Tregs an interesting target for therapeutic intervention.

In the last years, also the role of neutrophils has been intensely investigated in atherosclerosis. It could be shown that neutrophils are present in early and advanced atherosclerotic lesions in experimental mouse models (van Leeuwen et al., 2008; Drechsler et al., 2010; Rotzius et al., 2010) as well as in human atherosclerotic plaques (Ionita et al., 2010). Plasma levels of neutrophil granule proteins such as myeloperoxidase (MPO) are candidates for biomarkers, for example to predict coronary artery disease risk (Zhang et al., 2001).

In summary, the immune system is a major driver of atherosclerosis development and represents an important target for therapeutic intervention. However, the molecular players involved in the inflammatory processes contributing to atherosclerosis are incompletely described. The GWAS approach is highly suited to identify novel treatment targets for atherosclerosis.

2.4 Candidate genes at the 7p21.1 locus

The 7p21.1 locus is the so far strongest risk locus for large vessel stroke. However, all identified SNPs are localized in intronic or intergenic regions making an explanation for the underlying molecular mechanisms difficult. The 7p21.1 region contains three potential candidate genes, *HDAC9*, *TWIST1* and *FERD3L* (see Figure 2).

TWIST1 and *FERD3L* code for transcription factors of the helix-loop-helix family involved in cell differentiation processes during embryogenesis. The factor Nato3 encoded by the *FERD3L*-gene is dynamically expressed in the floor plate of the neural tube during both midbrain (Ono et al., 2010) and spinal cord development (Mansour et al., 2014). TWIST1 plays an important role in the differentiation of mesenchymal stem cells in chondrocytes, adipocytes and osteoblasts (Miraoui and Marie, 2010). Additionally, pathological conditions

of TWIST1 are known. Mutations in humans cause the autosomal dominant Saethre-Chotzen syndrome (SCS), also called acrocephalosyndactyly III (ACS III), which is characterized by facial dysmorphism, limb abnormalities, and craniosynostosis (El Ghouzzi et al., 1999).

HDAC9 belongs to the evolutionary conserved family of histone deacetylases (HDACs) which together with the histone acetyltransferases (HATs) regulate the acetylation of histone and non-histone proteins and play important roles in several physiological and pathological conditions (Haberland et al., 2009). HDAC9 is mainly expressed in the heart, brain, and muscle. HDACs are also known to be involved in inflammation and immunity (Shakespear et al., 2011), which play an important role in atherosclerosis.

To investigate which of the three genes might be responsible for the association of the 7p21.1 locus with LVS, my colleague Caroline Prell-Schicker quantified their mRNA levels in peripheral blood mononuclear cells (PBMCs) of healthy blood donors. HDAC9, but not TWIST1 or FERD3L, was found to be elevated in risk allele carriers of the lead SNP rs2107595 (see Figure 5 and manuscript 1 of this thesis) (Azghandi et al., 2015). This made *HDAC9* the most promising candidate gene in the 7p21.1 region and indicated that it has an atherogenic role.
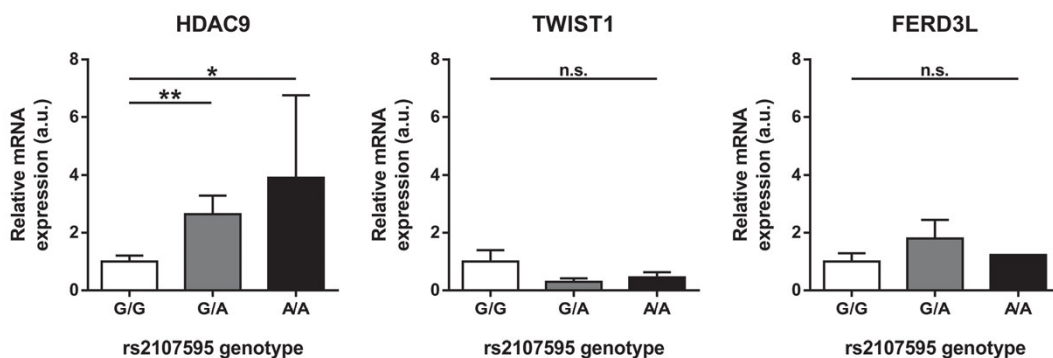
Figure 5. Expression levels of HDAC9, but not of TWIST1 and FERD3L, are increased in peripheral blood mononuclear cells of healthy homozygous and heterozygous risk allele (A) carriers.
Relative mRNA expression levels of HDAC9, TWIST1 and FERD3L in healthy subjects in respect to the rs2107595 genotype. *$P<0.05$, **$P<0.01$, n.s. not significant. Figure from Azghandi et al., 2015.
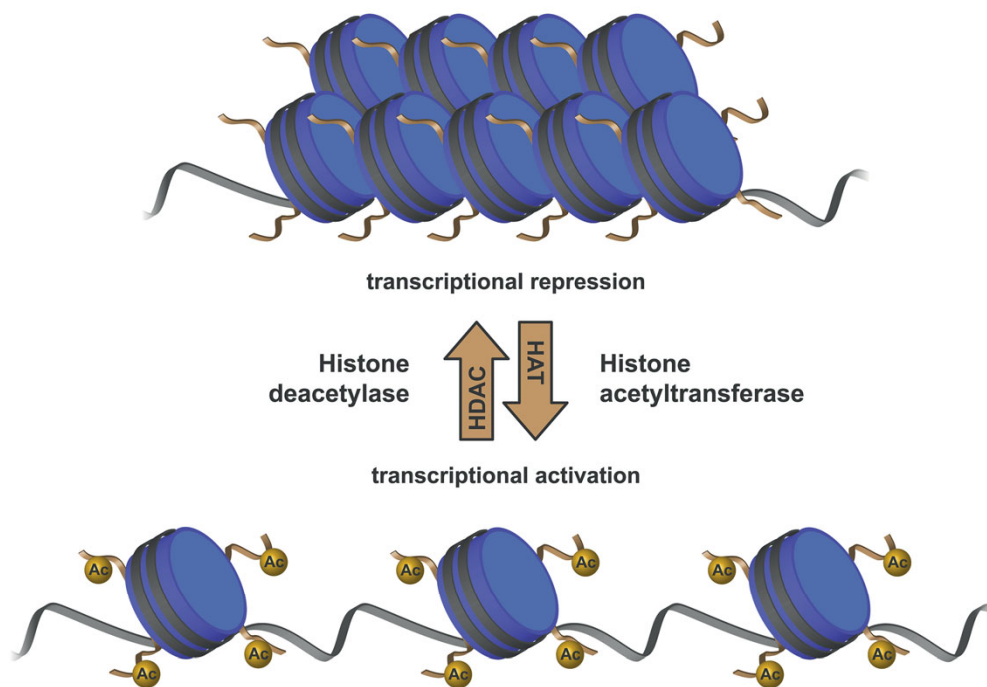
2.5 Histone deacetylases

Histones are the most important components of chromatin and thus major regulators of gene transcription. Within their N-terminal domains they contain a number of positively charged basic amino acids which interact with the negatively charged DNA backbone to promote chromatin condensation. Such compacted DNA is inaccessible for binding factors and thus transcriptionally silent. Posttranslational modification of histones such as acetylation and methylation has been known since the 1960s to control chromatin structure (Allfrey et al., 1964). For example acetylation of the ε-amino group of lysine residues within histone tails relaxes chromatin structure by neutralizing the positive charge. This results in increased accessibility of genomic DNA for transcription regulating factors (Shahbazian and Grunstein, 2007). Two families of enzymes, the histone deacetylases (HDACs) and histone acetyltransferases (HATs), regulate the acetylation and deacetylation of histones (Figure 6), but also of non-histone proteins including transcription factors and heat shock proteins. One of their main functions is the regulation of chromatin remodeling and gene expression (Shahbazian and Grunstein, 2007). HDACs and HATs are regulating diverse developmental processes, but are also involved in physiological and pathological processes in the adult organism (Haberland et al., 2009).

Classification of HDACs

The 18 members of the HDAC family can be grouped into four classes (I, II, III and IV), based on sequence homology and domain organization. Class I, II and IV are the classical HDACs which use Zn^{2+} as a cofactor whereas class III HDACs, the sirtuins 1-7, are NAD^+ dependent (Shakespear et al., 2011). Class I consists of HDAC1, HDAC2, HDAC3 and HDAC8 which localize to the nucleus and are expressed ubiquitously. HDAC9 belongs, together with HDAC4, HDAC5 and HDAC7, to class IIa HDACs which have an N-terminal binding domain mediating the interaction with transcriptional repressors and activators such as myocyte enhancer factor 2 (MEF2) (Haberland et al., 2009). Class IIa HDACs can shuttle between the nucleus and cytoplasm, a process regulated by phosphorylation through kinases such as calcium/calmodulin-dependent protein kinase (CaMK) and binding of 14-3-3 proteins (McKinsey et al., 2000). In contrast to class I HDACs, class IIa HDACs have a more restricted tissue expression pattern, for example HDAC5 and HDAC9 show a strong expression in the brain, the heart, and the muscle (Zhang et al., 2002; Chang et al., 2004). Furthermore, it

was shown that class IIa HDACs have a lower deacetylase activity in comparison to class I HDACs (Lahm et al., 2007). However, class IIa HDACs can recruit class I HDACs, thereby acquiring increased enzymatic capacity (Fischle et al., 2002). The class IIb HDACs encompass HDAC6 and HDAC10. HDAC6 is a cytoplasmic HDAC with two deacetylase domains which interacts with cytoskeletal proteins, e.g. tubulin (Matsuyama et al., 2002). Class IV HDACs consist of HDAC11 about which little is known.

Figure 6. Histone deacetylases and histone acetyltransferases.
Histone acetylation is controlled by two families of enzymes, the histone deacetylases and the histone acetyltransferases. Positively charged ε-amino groups of lysine residues within histone tails interact with the negatively charged DNA backbone to promote compaction of the chromatin structure. Acetylation of these groups disrupts interactions and results in chromatin relaxation which is required for transcription to occur. Deacetylation reverses this process resulting in transcriptional repression.

HDAC functions

The roles of HDACs were studied in several disease models including cardiovascular diseases such as cardiac hypertrophy and neointima formation as well as neurological diseases such as Huntington`s disease and stroke. Cardiac hypertrophy is a response of cardiomyocytes to stimuli like hypertension or valvular dysfunction. Deficiency of the

class IIa HDACs 5 and 9 was shown to promote cardiac hypertrophy (Zhang et al., 2002; Chang et al., 2004). In contrast, pan HDAC inhibitors and class I selective HDAC inhibitors can prevent and even reverse cardiac hypertrophy suggesting that class I HDACs oppose class II function in the regulation of cardiac hypertrophy (Kook et al., 2003; Kee et al., 2006). The role of HDACs was also studied in vascular smooth muscle cells and endothelial cells which are both important cell types for atherosclerosis and neointima formation. HDAC inhibition prevents mitogen-induced proliferation of smooth muscle cells by inducing G_1 cell cycle arrest (Findeisen et al., 2011). Furthermore, different HDAC inhibitors attenuated neointima formation *in vivo* (Findeisen et al., 2011; Kee et al., 2011), making HDACs an interesting target for vascular remodeling and atherosclerosis. HDAC3 has prosurvival functions in endothelial cells and knockdown of HDAC3 in endothelial cells of aortic isografts leads to severe atherosclerosis and vessel rupture, demonstrating that HDAC3 is critical for endothelial cell function (Zampetaki et al., 2010). HDAC4 was shown to be associated with carotid intima-media thickness, indicating an involvement of HDAC4 in atherosclerosis (Lanktree et al., 2009).

Besides beneficial effects in cancer and cardiovascular diseases, HDAC inhibitors show neuroprotective properties in neurological and neurodegenerative diseases (Kazantsev and Thompson, 2008), like Huntington`s disease (Ferrante et al., 2003; Kazantsev and Thompson, 2008) and stroke (Faraco et al., 2006; Kim et al., 2007). Several HDAC inhibitors led to reduced infarct volumes and ameliorated functional outcome in experimental animal stroke models (Kim et al., 2007; Langley et al., 2008). Proposed mechanisms include suppression of inflammation (Kim et al., 2007) and increased expression of neuroprotective factors like heat shock protein 70 (Hsp70), B-cell lymphoma 2 (Bcl-2), gelsolin and phosphorylated Akt (Faraco et al., 2006; Kim et al., 2007; Yildirim et al., 2008).

Inhibition of HDACs is a promising approach to control pathological processes. Several HDAC inhibitors have been developed and already tested in preclinical models and clinical trial settings. Known inhibitors can be subdivided into four classes, the hydroxamic acids, short chain fatty acids, cyclic tetrapeptides, and benzamides. Most of the currently available HDAC inhibitors inhibit multiple members of the HDAC family and are thus mostly non-selective. HDAC inhibitors were originally found as anticancer therapeutics by inducing apoptosis, differentiation, but also by reducing proliferation and angiogenesis (Falkenberg and Johnstone, 2014). Some HDAC inhibitors have already been approved for therapeutic

treatment, e.g. suberoylanilide hydroxamic acid (SAHA, vorinostat) for cutaneous T-cell lymphoma (Marks and Breslow, 2007) or the short chain fatty acid valproic acid (VPA) for epilepsy (Marson et al., 2007).

Thus, there is substantial evidence from the literature about the role of HDACs in cardiovascular and neurological conditions. In combination with our mRNA expression data from PBMCs (Figure 5) this motivated us to focus on *HDAC9* as the most promising risk gene within the 7p12.1 locus.

2.6 HDAC9

HDAC9 is mainly expressed in the brain, heart and skeletal muscle. Global HDAC9 deficient mice were already generated in 2002 by the group of Eric N. Olsen to study the role of HDAC9 in suppressing cardiac hypertrophy (Zhang et al., 2002). By homologous recombination with a targeting vector, exon 4 and most of exon 5 of *HDAC9*, which encode the MEF2 binding domain, were deleted. Homozygous HDAC9$^{-/-}$ mice are viable, but they develop cardiac hypertrophy with advanced age or in response to stress signals such as pressure overload or activated calcineurin (Zhang et al., 2002). This pathological condition is caused by derepression of MEF2, a transcription factor expressed in myocytes and a key regulator of cardiac hypertrophy. Interestingly, the MEF2-interacting transcriptional repressor (MITR), a HDAC9 splice variant, can also repress MEF2 activity despite lacking the deacetylase domain, indicating that the catalytic activity is not essential for regulating cardiac hypertrophy (Zhang et al., 2002).

Several studies suggest an important role of HDACs on Treg function. Administration of HDAC inhibitors increases the production and the function of FoxP3-positive Tregs in the human and in the murine system (Tao et al., 2007; Akimova et al., 2010). Moreover, HDAC9 seems to regulate FoxP3-mediated suppression of Tregs. Tao et al. could show that the number of FoxP3 positive T cells was increased in lymphoid tissues of HDAC9 knockout mice. HDAC9 deficient Tregs were found to be more suppressive than wild-type Tregs and showed increased FoxP3 acetylation (Tao et al., 2007). In line with this, HDAC9 deficient mice were protected in several autoimmune disease models like colitis (de Zoeten et al., 2010; Yan et al., 2011).

In addition to LVS and CAD, the *HDAC9* gene region (7p21.1) has also been associated with carotid intima-media thickness and with carotid plaque presence (Markus et al., 2013). Furthermore, HDAC9 was expressed in human vascular smooth muscle end endothelial cells and HDAC9 expression was increased in human carotid, aortic, and femoral atherosclerotic plaques (Markus et al., 2013). This represented additional evidence for a role of HDAC9 in atherogenesis.

3 Project design

3.1 Aims of the thesis

The 7p21.1 locus is the strongest risk locus for LVS to date (Bellenguez et al., 2012) and has also been associated with CAD (Deloukas et al., 2013) and carotid intima-media thickness (Markus et al., 2013). This provided strong evidence for a role of this locus in atherosclerosis. On the basis of mRNA studies in human PBMCs and the described role of HDACs in cardiovascular and neurological diseases, *HDAC9* was selected as the most likely disease-causing gene within the risk locus. Due to the significant increase in HDAC9 mRNA levels in risk allele carriers of the lead SNP, we hypothesized that HDAC9 deficiency could have beneficial effects. This was in line with published findings demonstrating neuroprotective effects of HDAC inhibitors. The goal of this PhD project was to study the consequences of HDAC9 deficiency in a mouse knockout model. First, a potential role in the cardiovascular system was investigated using an established mouse model for atherosclerosis. Second, HDAC9 deficient mice were subjected to transient middle cerebral artery occlusion (MCAo) to analyze effects on ischemic stroke.

In particular, this thesis had the following objectives:

A. ***To determine the influence of HDAC9 deficiency on atherosclerotic plaque formation.***
HDAC9 deficient mice were crossed with ApoE knockout mice, a widely used animal model for atherosclerosis. The parameters atherosclerotic plaque size, immune cell infiltration, and plaque stages were analyzed. The results are presented in manuscripts 1 and 2.

B. ***To determine the influence of HDAC9 deficiency on immune cell homeostasis.***
Flow cytometric analysis was used in manuscript 2 to study the distribution of different immune cell types in HDAC9 deficient mice.

C. ***To examine the role of HDAC9 deficiency in ischemic stroke.***
In manuscript 3, HDAC9 deficient mice were subjected to transient MCAo. Infarct size, neurological status and other parameters of stroke outcome were analyzed.

3.2 Experimental strategy

All animal studies were done on littermates, using HDAC9 heterozygous mice as breeders. Two different mouse lines were used. On the one hand, the HDAC9 deficient mice without ApoE deficiency were investigated (HDAC9$^{-/-}$ mice and their wild-type littermates, HDAC9$^{+/+}$ mice) and on the other hand, the HDAC9 deficient mice which were crossed to atherosclerosis-prone ApoE deficient mice (HDAC9$^{-/-}$ApoE$^{-/-}$ mice and their wild-type littermates HDAC9$^{+/+}$ApoE$^{-/-}$ mice).

Objective A and B: To determine the influence of HDAC9 deficiency on atherosclerotic plaque formation and immune cell homeostasis

Atherosclerotic plaque size was analyzed in the aortic root and the aortic arch in chow and Western-type diet fed HDAC9$^{-/-}$ApoE$^{-/-}$ mice and their wild-type littermates. First, I had to establish all techniques including dissection, histological analyses, and flow cytometry in our institute. When the mice reached the right age, they were anesthetized, blood was taken for the immunological analyses and the vessels were perfused with the vasodilator nitroprusside to achieve maximal vasodilation. The aortic arch with the main branching arteries (right and left subclavian and common carotid arteries) (Figure 7A) was dissected and analyzed histologically (Figure 7B). Additionally, the heart was taken out and cut at the level of the aortic valves (Figure 7C). Besides plaque size, plaque stages, and immune cell infiltration were analyzed. The distribution of different immune cell types was studied by flow cytometric analysis (Figure 7D) of the blood and the spleen. Besides HDAC9-ApoE double knockout mice, HDAC9 deficient mice without ApoE deficiency were examined in the immunological analyses to be able to discriminate the HDAC9 effect without disease from the effect in combination with atherosclerosis.
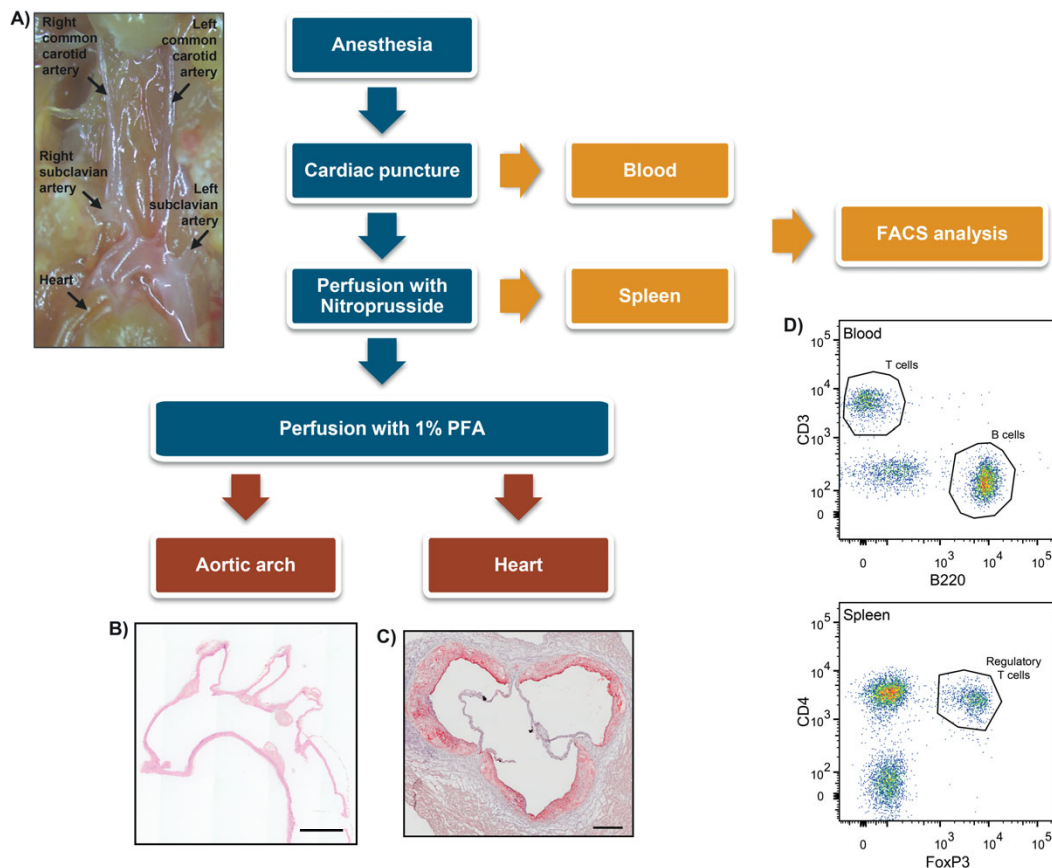
Figure 7. Work flow for atherosclerotic plaque (Objective A) and FACS analysis (Objective B) in HDAC9-ApoE double-knockout mice.
After anesthetizing the mouse, blood is taken out by cardiac puncture and vessels are perfused with the vasodilator nitroprusside. The spleen is removed, followed by perfusion with 1% paraformaldehyde (PFA) for fixation and dissection of the aortic arch and the heart. In **A,** the main branching arteries of the aortic arch are shown. In **B,** and **C,** examples of an H&E stained aortic arch section and an Oil Red O stained aortic valve section are depicted. In **D,** examples of fluorescence-activated cell sorting (FACS) analysis of the blood and the spleen are presented.

Objective C: To examine the role of HDAC9 deficiency in ischemic stroke.

For this objective, HDAC9 deficient mice without ApoE deficiency were used to study the effect of HDAC9 in stroke without the involvement of atherosclerosis. The transient middle cerebral artery occlusion model was used which is based on the occlusion of the middle cerebral artery (MCA) for one hour using a silicone-coated monofilament inserted via the internal carotid artery (Figure 8). Infarct volume, neurological status, edema formation, and other parameters of stroke outcome were analyzed in HDAC9 deficient mice and their wild-type littermates.
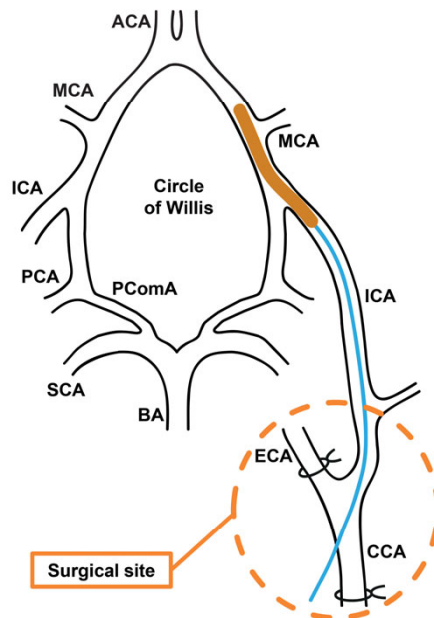
Figure 8. The middle cerebral artery occlusion (MCAo) model (Objective C).
The left common and external carotid arteries are ligated and a silicone-coated monofilament is inserted via the internal carotid artery. After one hour of ischemia, reperfusion is initiated by removing the filament. Anterior cerebral artery (ACA); basilar artery (BA); common carotid artery (CCA); external carotid artery (ECA); internal carotid artery (ICA); middle cerebral artery (MCA); posterior cerebral artery (PCA); posterior communicating artery (PComA); superior cerebellar artery (SCA).

4 Manuscript 1

Deficiency of the Stroke Relevant *HDAC9* Gene Attenuates Atherosclerosis in Accord With Allele-Specific Effects at 7p21.1

Sepiede Azghandi, BSc*[1]; Caroline Prell, Dipl.Biol.*[1]; Sander W. van der Laan, MSc[2]; Manuela Schneider, DVM[1]; Rainer Malik, PhD[1]; Kerstin Berer, PhD[3]; Norbert Gerdes, PhD[4]; Gerard Pasterkamp, MD, PhD[2]; Christian Weber, MD[4]; Christof Haffner, PhD[1]; Martin Dichgans, MD[1,5]

[1] Institute for Stroke and Dementia Research, Klinikum der Universität München, Munich, Germany

[2] Divisions Heart & Lungs and Laboratories & Pharmacy, University Medical Center Utrecht, the Netherlands

[3] Department of Neuroimmunology, Max Planck Institute of Neurobiology, Martinsried, Germany

[4] Institute for Cardiovascular Prevention, Ludwig-Maximilians-University, Munich, Germany

[5] Munich Cluster for Systems Neurology (SyNergy), Munich, Germany

* Sepiede Azghandi and Caroline Prell contributed equally to this work.

Author contributions:

SA designed, acquired and analyzed the mouse experiments; CP acquired and analyzed the human gene expression data; SWvDL acquired and analyzed human atherosclerotic plaque data. MS, RM and KB worked as technical consultants and edited the manuscript. NG, GP, CW, CH and MD designed the study and edited the manuscript. SA, CP and MD wrote the manuscript.

Abstract

Background and Purpose: Recent genome-wide association studies identified the *HDAC9* gene region as a major risk locus for large vessel stroke and coronary artery disease (CAD). However, the mechanisms linking variants at this locus to vascular risk are poorly understood. In this study, we investigated the candidacy and directionality of HDAC9 in atherosclerosis and analyzed associations between risk alleles at 7p21.1 and plaque characteristics.

Methods: Allele-dependent expression of HDAC9 was analyzed in human peripheral blood mononuclear cells (PBMCs) of healthy donors. Effects of HDAC9 deficiency on atherosclerotic plaques were investigated in 18- and 28-week-old ApoE$^{-/-}$ mice by histology and immunohistochemistry. We further performed detailed plaque phenotyping and genotyping of rs2107595, the lead SNP in METASTROKE, in carotid endarterectomy samples of 1,858 subjects from the Athero-Express Study.

Results: Gene expression studies in PBMCs revealed increased mRNA levels of *HDAC9* but not of neighboring genes (*TWIST1/FERD3L*) in risk allele carriers of rs2107595. Compared to HDAC9$^{+/+}$ApoE$^{-/-}$ mice, HDAC9$^{-/-}$ApoE$^{-/-}$ mice exhibited markedly reduced lesion sizes throughout atherosclerotic aortas and significantly less advanced lesions. The proportion of Mac3-positive macrophages was higher in plaques from HDAC9$^{-/-}$ApoE$^{-/-}$ mice, but this was largely due to a lower proportion of advanced lesions. Analysis of human atherosclerotic plaques revealed no association between rs2107595 and specific plaque characteristics.

Conclusions: Our results suggest that *HDAC9* represents the disease-relevant gene at the stroke and CAD risk locus on 7p21.1 and that risk alleles in this region mediate their effects through elevated HDAC9 expression. Targeted inhibition of HDAC9 might be a viable strategy to prevent atherosclerosis.

Introduction

Stroke and coronary artery disease (CAD) are among the most common causes of premature death and loss of disability-adjusted life years worldwide.[1,2] About a quarter of all strokes are classified as large vessel stroke (LVS) most of which are attributed to atherosclerosis. LVS shares many risk factors with CAD and both conditions have a strong heritable component.[3,4]

In a genome-wide association study (GWAS) we recently identified the histone deacetylase 9 (*HDAC9*) gene region on chromosome 7p21.1 as the strongest risk locus for LVS to date.[5,6] Variants at this locus were subsequently shown to be also associated with CAD[7] and common carotid intima media thickness (IMT)[8] suggesting that the effects of the 7p21.1 region are mediated through atherosclerosis.

rs2107595, the lead SNP in METASTROKE,[6] is located 3' to the *HDAC9* gene. The next two genes, *TWIST1* and *FERD3L*, reside 100 kb downstream to rs2107595 whereas other genes are more than 500 kb away. Histone deacetylases (HDACs) mediate the acetylation of histones and non-histone proteins together with histone acetylases.[9] The balance between acetylation and deacetylation plays a critical role in gene expression mechanisms during embryonic development and disease states in later life.[10] HDAC9 has been implicated in immune-mediated mechanisms and is expressed in various cell types relevant to atherosclerosis including inflammatory, vascular endothelial and smooth muscle cells.[8,11,12] Hence, *HDAC9* represents a strong candidate gene for atherosclerosis. However, there are no expression data supporting the candidacy of *HDAC9* over other genes at 7p21.1. Also, the relationship between risk variants in this region and plaque morphology remains to be determined. We thus investigated samples from healthy subjects and patients undergoing carotid endarterectomy.[13] We further tested the hypothesis that deficiency of HDAC9 attenuates atherosclerosis in mice.

Materials and Methods

Allele carrier status and mRNA expression

DNA and RNA were isolated from peripheral blood mononuclear cells (PBMCs) of healthy donors (43 male, 34 female, age 65.3±20.8 [mean±SD] years). Carrier status at rs2107595 was determined by direct sequencing. RNA was isolated using PAXgene Blood RNA Kit (PreAnalytiX GmbH) according to the manufacturer`s protocol. For each sample, 800 ng of DNase-treated RNA were converted into cDNA (Omniscript RT Kit, Qiagen) using Oligo dT(15) primer. For quantitative real-time PCR cDNAs were diluted with water 1:9 and analyzed using TaqMan Gene Expression Assays (ABI Bioscience) for human *HDAC9*, *TWIST1*, *FERD3L* and *RPLP0*. Measurements were performed in triplicates. Results for target genes were normalized to the reference gene *RPLP0* and to a calibrator sample. All subjects provided written informed consent.

Atherosclerotic plaque analysis in mice

All animal protocols were approved by the government of Upper Bavaria. HDAC9$^{-/-}$ mice from E. Olson[14] were provided by Laurent Schaeffer (Université Lyon) and were crossed with ApoE deficient mice (The Jackson Laboratory) to generate HDAC9$^{-/-}$ApoE$^{-/-}$ mice. Mice had *ad libitum* access to food and water and were housed under a 12 h light-dark cycle. All experiments were done on male littermates fed a standard chow diet to sensitively capture the effect of HDAC9 on spontaneous rather than aggravated and accelerated atherosclerosis induced by western-type diet. Animals were sacrificed at age 18 or 28 weeks (n = 8-13 for each genotype and time point) by an overdose of ketamine and xylazin. Blood was obtained by cardiac puncture from the right ventricle and plasma was used for cholesterol measurements using a colorimetric assay (Cayman Chemical Company). The arterial tree was perfused through the left ventricle with 6 ml phosphate buffered saline (PBS, containing sodium nitroprusside (1 mg/ml, Sigma-Aldrich)) to achieve vasodilation and 10 ml 1% paraformaldehyde (PFA) for tissue fixation. The aortic arch and its main branch points were removed and fixed for 24 h in a 1% PFA solution.

To evaluate atherosclerotic lesion size, a total of 8 cryosections (8 μm) extending cranially through the aortic valves at 104 μm intervals were cut. Lesion area per cross-section and relative area of lesions were quantified. Relative lesion area was calculated for each section as R% = (100 × L/A), where L is lesion area and A is area inside the external elastic lamina.

The relative lesion area was expressed as the mean of four consecutive sections (104 μm - 416 μm) per mouse. We further measured plaque sizes of the aortic arch of 28-week-old mice. The aortic arch was embedded in paraffin and cut into consecutive 4 μm sections. Four sections at 20 μm intervals were chosen for plaque analysis. Sections were stained with hematoxylin and eosin (H&E) and lesion areas of the total aorta as well as individual lesions at the main branch points and the curvature were measured by AxioVision Software (Zeiss, Germany). The number of plaques per arch was counted. Atherosclerotic lesions were classified as initial or advanced using the Virmani classification.[15] The number of nuclei and the acellular core area per plaque in the brachiocephalic artery were quantified. Immunohistochemistry was performed on paraffin sections of the aortic arch (n = 8-13 for each phenotype). A Mac3 monoclonal antibody (1:100 dilution, M3/84, BD Bioscience) to detect macrophages and an isotype matched control antibody were used. Antibodies were titrated to optimal performance and applied to PFA-fixed paraffin sections of the aortic arch followed by detection using an ABC peroxidase kit and DAB substrate (both from Vector Laboratories). The stainings were quantified by ImageJ Software and the number of Mac3-positive cells per lesion was divided by the total number of cells per lesion, as determined by number of nuclei per lesion.

All experiments and data analysis were performed under blinded conditions for the genotype.

rs2107595 and human atherosclerotic plaques

Human carotid atherosclerotic plaques (N=1,858) were obtained from the Athero-Express Study, an ongoing, longitudinal, multi-center study collecting carotid atherosclerotic plaques from patients with significant (>70%) stenosis who undergo carotid endarterectomy.[13,16] The medical ethics committee of the participating centers approved the study and written informed consent was obtained from all patients.

Immunohistochemical plaque phenotyping was performed as described elsewhere.[13,16] In brief, carotid plaques were divided into segments of 5 mm thickness. The culprit lesion was defined and used for immunohistochemical staining. Calcification (hematoxylin & eosin, H&E) and collagen content (picrosirius red) were semi-quantitatively defined as no or minor vs. moderate/heavy staining as previously described.[13,16] Atheroma size was defined as less than or more than 10% fat content (H&E and picrosirius red). We quantitatively scored

macrophages (CD68) and smooth muscle cells (α-actin) as percentage plaque area. We also determined the presence of intraplaque hemorrhage (H&E) and counted the number of vessel per 3-4 hotspots (CD34).

Genotyping was done in two batches using Affymetrix arrays. rs2107595 was imputed using phased data from HapMap 2 (release 22, b36) as a reference. Quality control (QC) was performed according to standard procedures. Detailed description of genotyping, quality control and imputation is provided in the online-only Data Supplement.

Statistical analysis

For the human mRNA expression data and the murine plaque analysis, GraphPad Prism 5 (GraphPad Software) and SigmaPlot 12.5 (Systat Software Inc.) were used for statistical analysis. Groupwise comparisons (n>2) were performed using a nonparametric Kruskal-Wallis test followed by a Mann-Whitney test. Pairwise comparisons were performed using a Mann-Whitney test. Differences were considered statistically significant at *P*<0.05. Data are expressed as mean±SEM.

For statistical analysis of the Athero-Express data quantitative histological phenotypes were normalized through natural log (LN) transformation; outliers deviating more than ±3 SD from the LN-transformed mean were removed. Genetic analyses were corrected for age, sex, 10 principal components, year of surgery and a dummy variable representing the two genotyping batches, assuming an additive genetic model. Linear and logistic regression models were used for quantitative and binary phenotypes, respectively. IBM SPSS Statistics version 20 (release 20.0.0, IBM Corp., Armonk, NY, USA) was used for statistical analyses of baseline characteristics. PLINK v1.7 and Golden Helix SNP & Variation Suite v8.1.5 (Golden Helix, Inc., Bozeman, MT, USA) were used for genetic analyses. Our power to detect an association between rs2107595 and individual plaque phenotypes at a significance level of 0.05 [0.005] with a sample size of 1,400, an effect size of 0.182 and a minor allele frequency of 20% was >90% [>75%] for quantitative phenotypes. For binary phenotypes our power to detect an OR of 1.20 (corresponding to an effect size of 0.182) was between 20% [4%] (for collagen) and 54% [23%] (for intraplaque hemorrhage). To account for testing multiple phenotypes the level of statistical significance was set at 0.005.

Results

rs2107595 risk allele carriers show increased HDAC9 mRNA expression in PBMCs

rs2107595, the lead SNP in METASTROKE,[6] is situated in the intergenic region between *HDAC9* and *TWIST1/FERD3L* and co-localizes with both Deoxyribonuclease I (DNase I) hypersensitivity clusters and histone modification hotspots (UCSC Genome Browser,[17] genome build hg18, Figure 1A), suggesting a possible involvement of this variant in gene regulation.
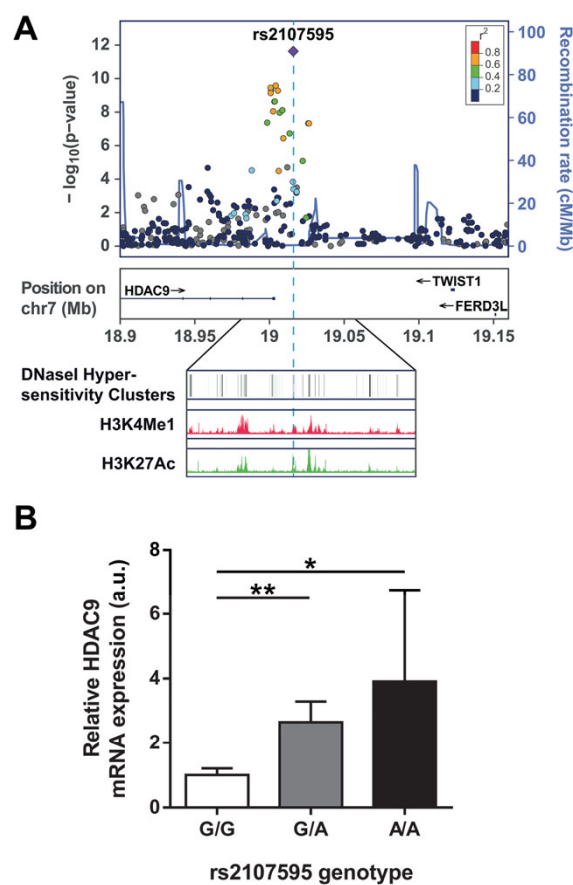
Figure 1. HDAC9 mRNA levels are significantly elevated in risk allele carriers of the lead SNP (rs2107595) found to be associated with large vessel stroke. **A**, Regional association plot of the *HDAC9* gene region showing association signals around rs2107595 for LVS in the METASTROKE dataset.[6] **Top**, SNPs are colored based on their correlation with rs2107595, which has the smallest *P*-value in the region. **Bottom**, DNase I hypersensitivity clusters and histone modification hotspots (H3K4Me1, H3K27Ac). **B**, Relative mRNA expression of HDAC9 in human PBMCs for different genotypes of rs2107595. HDAC9 mRNA levels are significantly elevated in homozygous and heterozygous carriers of the risk allele (A) with a gene dosage effect (GG n=51, GA n=22, AA n=4). Results represent mean±SEM. *$P<0.05$, **$P<0.01$ (Kruskal-Wallis test $P=0.003$, followed by Mann-Whitney test).

We thus measured mRNA expression levels of HDAC9, TWIST1 and FERD3L in PBMCs from healthy donors. HDAC9 mRNA levels were significantly increased in homozygous and heterozygous carriers of the risk allele (rs2107595A) with a gene dosage effect (Figure 1B). In contrast, mRNA levels of the adjacent genes *TWIST1* and *FERD3L* did not correlate with allele carrier status at rs2107595 (Figure I in the online-only Data Supplement), suggesting that variants at this locus regulate HDAC9 expression and that the effects of this locus on stroke risk might be mediated through elevated HDAC9 expression.

HDAC9 deficiency reduces atherosclerotic lesion size in mice

To test the hypothesis that HDAC9 deficiency attenuates atherogenesis and to refine its influence on plaque composition, we crossed HDAC9$^{-/-}$ mice with ApoE$^{-/-}$ mice and fed them a normal chow diet. HDAC9$^{-/-}$ApoE$^{-/-}$ mice showed a significant reduction of atherosclerotic lesion size at both 18 weeks and 28 weeks of age in aortic valve sections (Figure 2A and 2B) as well as in aortic arch sections (Figure 2C and 2D).

A significant reduction in plaque area was also found in the brachiocephalic artery and aortic curvature (Figure IIA in the online-only Data Supplement). The number of plaques in the aortic arch was significantly reduced (Figure IIB in the online-only Data Supplement).
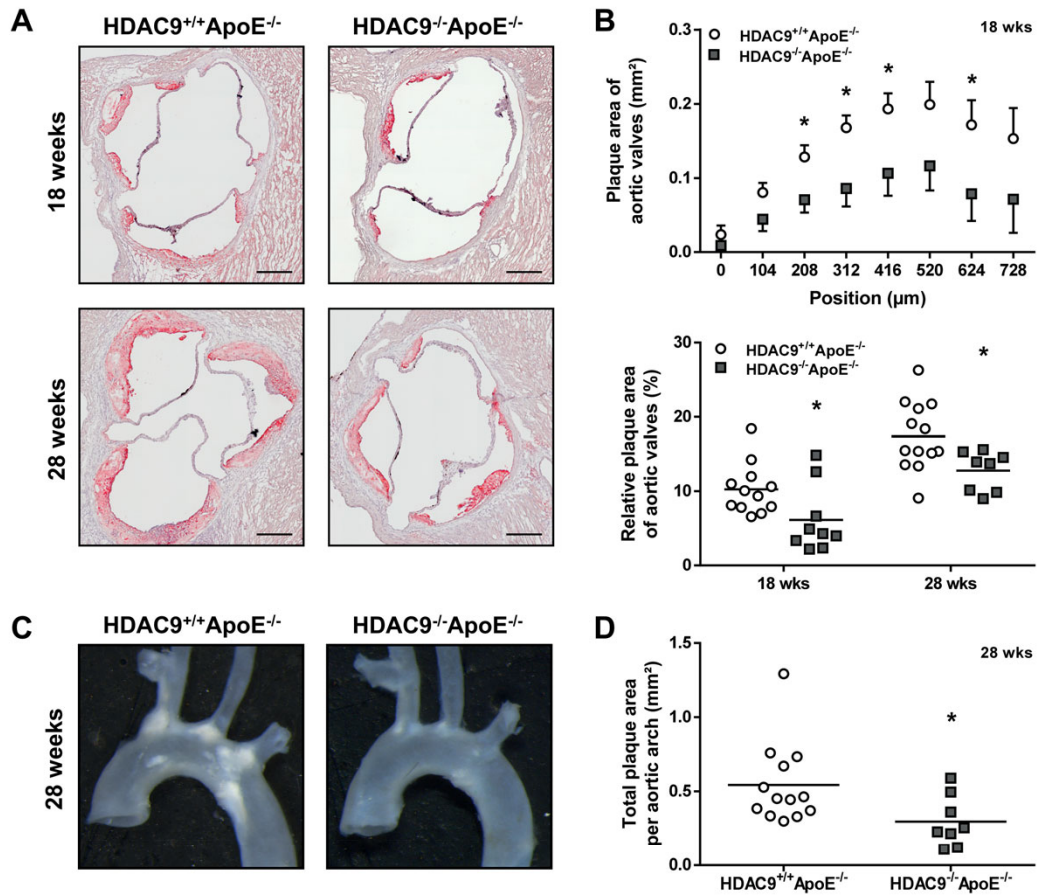
Figure 2. HDAC9 deficiency reduces atherosclerotic plaque size in ApoE deficient mice. **A**, Representative images showing Oil-Red O- and hematoxylin stained cryosections from the proximal aorta of HDAC9$^{+/+}$ApoE$^{-/-}$ and HDAC9$^{-/-}$ApoE$^{-/-}$ mice at 18 and 28 weeks of age. Scale bars: 250 µm. **B**, Absolute plaque areas at different distances from the aortic valves of 18-week-old mice (**top**) and relative plaque area (in relation to the area inside of the external elastic lamina) (**bottom**). **C**, Representative images showing dissected aortic arches of 28-week-old mice. **D**, Total plaque area in the aortic arch of 28-week-old mice. Values represent mean plaque area for each mouse; n = 8-13 for each genotype and time point; $*P<0.05$; $**P<0.01$ vs. wildtype (Mann-Whitney test).

Next, we categorized atherosclerotic lesion stage using the Virmani classification.[15] We distinguished intimal xanthomas consisting mainly of foam cells from advanced atheromas characterized by fibrous cap and acellular areas. In brachiocephalic artery plaques (Figure 3A and 3B) only 2 out of 8 HDAC9$^{-/-}$ApoE$^{-/-}$ mice showed acellular areas compared to 12 out of 13 HDAC9$^{+/+}$ApoE$^{-/-}$ ($P<0.01$) (Figure 3C). The reduction in acellular cores corresponded to the increased number of nuclei per lesion area in HDAC9$^{-/-}$ApoE$^{-/-}$ mice (Figure 3D).

Figure 3. HDAC9 deficiency affects composition of atherosclerotic plaques in the brachiocephalic artery (BCA) of 28-week-old mice. **A**, Overview of aortic arch. Orange rectangle indicates region of interest for plaque analysis in the BCA. **B**, Representative images of H&E stained plaques are shown. **C**, Acellular core per lesion area in the BCA. **D**, Nuclei per lesion area in the BCA. n = 8-13 for each genotype; scale bars: 100 μm; *$P<0.05$; **$P<0.01$ vs. wildtype (Mann-Whitney test); BCA brachiocephalic artery, CCA common carotid artery, SCA subclavian artery, Curv. aortic curvature.

Analysis of the entire aorta likewise revealed a lower proportion of advanced lesions in HDAC9-deficient mice (HDAC9$^{+/+}$ApoE$^{-/-}$: 43±7%; HDAC9$^{-/-}$ApoE$^{-/-}$: 12±6%; [mean±SEM]; Figure 4A). In addition, immunostaining for Mac3 showed a higher proportion of macrophages in plaques from HDAC9$^{-/-}$ApoE$^{-/-}$ mice (Figure 4B and 4C). However, after exclusion of advanced lesions no difference of Mac3 infiltration was observed. Plasma cholesterol levels measured at 18 and 28 weeks did not differ between HDAC9$^{-/-}$ApoE$^{-/-}$ and HDAC9$^{+/+}$ApoE$^{-/-}$ mice (Figure IIC in the online-only Data Supplement).
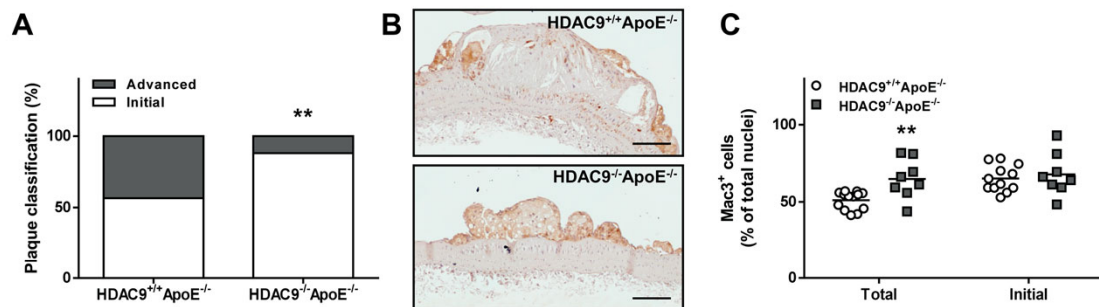
Figure 4. HDAC9 deficiency affects stages and composition of atherosclerotic plaques in the aorta of 28-week-old mice. **A**, Classification of aortic arch lesions according to their stage of atherosclerosis. Initial plaques (intimal xanthomas and pathological intimal thickenings); advanced plaques (fibrous cap atheromas). **B**, Immunostaining for Mac3 and quantification of Mac3-positive cells in all plaques in the total aorta and in initial plaques only (following exclusion of advanced atheromas). n = 8-13 for each genotype; scale bars: 100 µm; *P<0.05; **P<0.01 vs. wildtype (Mann-Whitney test).

rs2107595 has no discernable effect on plaque morphology in humans

To explore potential associations between risk alleles at *HDAC9* and specific advanced plaque characteristics we genotyped 1,858 subjects with available detailed plaque phenotyping from Athero-Express. 1,439 subjects passed quality control. Their demographic and clinical characteristics are presented in Table I in the online-only Data Supplement. There was no significant association between rs2107595 and specific plaque characteristics in the overall sample (Table 1) or when analysis was restricted to patients with asymptomatic plaques, symptomatic plaques or stroke (Table II in the online-only Data Supplement).

Table 1. Association of rs2107595 with plaque phenotypes in the Athero-Express Study (*N*=1,439).

MAF	OR	ß	95% CI	SEM	*P*	Phenotype	*N*
0.800	1.129	NA	0.93-1.38	NA	0.215	calcification	705/700
0.800	0.877	NA	0.69-1.12	NA	0.284	collagen	1129/277
0.800	1.164	NA	0.94-1.44	NA	0.162	atheroma size	1018/389
0.800	1.211	NA	0.99-1.48	NA	0.058	intraplaque hemorrhage	849/557
0.800	NA	0.120	NA	0.089	0.176	macrophages	1403
0.800	NA	-0.071	NA	0.064	0.261	smooth muscle cells	1375
0.797	NA	-0.036	NA	0.037	0.329	vessel density	1216

MAF: major allele frequency; odds ratios (OR) and effect sizes (ß) are relative to the major allele (G) on genome build 36; *P*-values are two-sided. Phenotype: calcification and collagen are coded as no or minor vs. moderate heavy staining, atheroma size is coded as <10% vs. >10% fat content, intraplaque hemorrhage as no vs. yes, macrophages and smooth muscle cells are natural log (LN)-transformed percentages of plaques, and vessel density is the LN-transformed average intraplaque vessel density per 3-4 hotspots. *N* is the number of patients analyzed for the respective plaque phenotype. SEM: standard error of the mean; NA: not applicable.

Discussion

This study provides converging evidence that *HDAC9* represents the disease-relevant gene at the stroke and CAD risk locus on 7p21.1 and that risk alleles at this locus mediate their effects through increased HDAC9 expression.

Our finding of elevated HDAC9 mRNA expression in risk allele carriers of rs2107595, the lead SNP in METASTROKE, is consistent with recent data from the ENCODE project showing that the majority of disease-associated variants are located in regulatory regions and control genes within a distance of ±500 kb. rs2107595 resides inside a DNase I hypersensitivity cluster and histone modification hotspot. In fact, rs2107595A is predicted to disrupt a consensus sequence for an E2F3-binding site (TRANSFAC database,[18] data not shown), a transcription factor forming a repressor complex with Rb-proteins, thus raising the possibility that this variant is implicated in gene regulation. However, the exact mechanism by which genetic variation at this locus regulates HDAC9 expression remains to be determined. *TWIST1* and *FERD3L*, the only other genes nearby, exhibited no allele-dependent mRNA expression and are thus less likely to be implicated in locus-specific effects. However, because our expression analyses were restricted to PBMCs, we cannot exclude regulatory effects in other cell types.

Complementing our expression data, we found deficiency of HDAC9 to attenuate atherogenesis in ApoE$^{-/-}$ mice. The reduction of atherosclerotic lesion size reaching up to 45% in 28-week-old animals, was present throughout all segments of the aortic arch (aortic valves, curvature, branching arteries) and already significant in 18-week-old animals. Staging of lesions further revealed that HDAC9$^{-/-}$ApoE$^{-/-}$ mice had significantly less advanced lesions compared to HDAC9$^{+/+}$ApoE$^{-/-}$ mice. Together, these findings demonstrate a strong effect of HDAC9 expression on atherogenesis. The higher proportion of Mac3-positive macrophages in plaques from HDAC9$^{-/-}$ApoE$^{-/-}$ mice likely reflects the lower proportion of acellular areas that are typical for advanced lesions as there was no difference of Mac3 infiltration when we restricted our analyses to intimal xanthomas. Hence, we found no obvious influence of HDAC9 deficiency on plaque morphology.

In accordance with our findings in mice, no significant association between rs2107595 and specific plaque characteristics was found in human carotid plaques from the Athero-Express Study. Importantly, our power to detect an association with macrophage count, smooth muscle cell count, and vessel density was over 75%. Hence, we are confident that we would

have captured any prominent effect on these plaque phenotypes. However, our power to detect associations with binary plaque phenotypes was limited. Thus, we cannot exclude allele-specific effects on collagen content, atheroma size, calcification, and intraplaque hemorrhage. Interestingly, a recent meta-analysis of population-based cohorts revealed an association of rs2107595 with carotid IMT measured by ultrasound.[8] Taken together, these data suggest that HDAC9 expression promotes early atherogenesis rather than accelerating progression to vulnerable plaques. However, we cannot exclude skewing of macrophage polarization from M1 to M2 phenotype as previously reported.[19]

The precise mechanisms by which elevated HDAC9 expression promotes atherogenesis and vascular risk remain to be determined. A recent study found that targeted depletion of HDAC9 in bone marrow cells attenuates atherogenesis in LDLr$^{-/-}$ mice.[19] HDAC9 was further shown to repress cholesterol efflux in macrophages. However, whether the changes in macrophages give rise to atherosclerotic lesion formation remains speculative. Given the widespread expression of HDAC9 in multiple cell types there are several mechanisms by which elevated HDAC9 expression could promote atherosclerosis. For example, HDAC9 has been shown to inhibit FOXP3 expression and the function of regulatory T cells,[20] which protect against atherosclerosis.[21,22]

Our findings imply that targeting HDAC9 may be a viable strategy to prevent atherosclerosis progression. Broad-spectrum HDAC inhibitors have multiple off-target effects and exacerbate atherosclerosis.[23] Selective inhibitors of class IIa HDACs have recently been developed but not yet sufficiently tested *in vivo*.[24] Given the pleiotropic role of class IIa HDACs developing inhibitors with selectivity for HDAC9 seems the most promising approach to specifically target atherosclerotic lesion formation.

In conclusion, this study provides mechanistic insights how genetic variation in the *HDAC9* gene region, a major risk locus for LVS and CAD, promotes atherosclerosis. Moreover, our findings suggest that selective pharmacological inhibition of HDAC9 may be an effective strategy to prevent atherosclerosis and its clinical manifestations.

Acknowledgments

Sources of Funding

Disclosures

None

References

1. Bonita R. Epidemiology of stroke. *Lancet*. 1992;339:342-344
2. Lozano R, Naghavi M, Foreman K, Lim S, Shibuya K, Aboyans V, et al. Global and regional mortality from 235 causes of death for 20 age groups in 1990 and 2010: A systematic analysis for the global burden of disease study 2010. *Lancet*. 2012;380:2095-2128
3. Bevan S, Traylor M, Adib-Samii P, Malik R, Paul NL, Jackson C, et al. Genetic heritability of ischemic stroke and the contribution of previously reported candidate gene and genomewide associations. *Stroke*. 2012;43:3161-3167
4. Dichgans M. Genetics of ischaemic stroke. *Lancet Neurol*. 2007;6:149-161
5. Bellenguez C, Bevan S, Gschwendtner A, Spencer CC, Burgess AI, Pirinen M, et al. Genome-wide association study identifies a variant in hdac9 associated with large vessel ischemic stroke. *Nat Genet*. 2012;44:328-333
6. Traylor M, Farrall M, Holliday EG, Sudlow C, Hopewell JC, Cheng YC, et al. Genetic risk factors for ischaemic stroke and its subtypes (the metastroke collaboration): A meta-analysis of genome-wide association studies. *Lancet Neurol*. 2012;11:951-962
7. Deloukas P, Kanoni S, Willenborg C, Farrall M, Assimes TL, Thompson JR, et al. Large-scale association analysis identifies new risk loci for coronary artery disease. *Nat Genet*. 2013;45:25-33
8. Markus HS, Makela KM, Bevan S, Raitoharju E, Oksala N, Bis JC, et al. Evidence hdac9 genetic variant associated with ischemic stroke increases risk via promoting carotid atherosclerosis. *Stroke*. 2013;44:1220-1225
9. Shahbazian MD, Grunstein M. Functions of site-specific histone acetylation and deacetylation. *Annu Rev Biochem*. 2007;76:75-100

10. Haberland M, Montgomery RL, Olson EN. The many roles of histone deacetylases in development and physiology: Implications for disease and therapy. *Nat Rev Genet*. 2009;10:32-42

11. Shakespear MR, Halili MA, Irvine KM, Fairlie DP, Sweet MJ. Histone deacetylases as regulators of inflammation and immunity. *Trends Immunol*. 2011;32:335-343

12. Kaluza D, Kroll J, Gesierich S, Manavski Y, Boeckel JN, Doebele C, et al. Histone deacetylase 9 promotes angiogenesis by targeting the antiangiogenic microrna-17-92 cluster in endothelial cells. *Arterioscler Thromb Vasc Biol*. 2013;33:533-543

13. Verhoeven BA, Velema E, Schoneveld AH, de Vries JP, de Bruin P, Seldenrijk CA, et al. Athero-express: Differential atherosclerotic plaque expression of mrna and protein in relation to cardiovascular events and patient characteristics. Rationale and design. *Eur J Epidemiol*. 2004;19:1127-1133

14. Zhang CL, McKinsey TA, Chang S, Antos CL, Hill JA, Olson EN. Class ii histone deacetylases act as signal-responsive repressors of cardiac hypertrophy. *Cell*. 2002;110:479-488

15. Virmani R, Kolodgie FD, Burke AP, Farb A, Schwartz SM. Lessons from sudden coronary death: A comprehensive morphological classification scheme for atherosclerotic lesions. *Arterioscler Thromb Vasc Biol*. 2000;20:1262-1275

16. van den Borne P, van der Laan SW, Bovens SM, Koole D, Kowala MC, Michael LF, et al. Leukotriene b4 levels in human atherosclerotic plaques and abdominal aortic aneurysms. *PLoS One*. 2014;9:e86522

17. Rosenbloom KR, Sloan CA, Malladi VS, Dreszer TR, Learned K, Kirkup VM, et al. Encode data in the ucsc genome browser: Year 5 update. *Nucleic Acids Res*. 2013;41:D56-63

18. Wingender E, Chen X, Hehl R, Karas H, Liebich I, Matys V, et al. Transfac: An integrated system for gene expression regulation. *Nucleic Acids Res*. 2000;28:316-319

19. Cao Q, Rong S, Repa JJ, Clair RS, Parks JS, Mishra N. Histone deacetylase 9 represses cholesterol efflux and alternatively activated macrophages in atherosclerosis development. *Arterioscler Thromb Vasc Biol*. 2014;34:1871-1879

20. Tao R, de Zoeten EF, Ozkaynak E, Chen C, Wang L, Porrett PM, et al. Deacetylase inhibition promotes the generation and function of regulatory t cells. *Nat Med*. 2007;13:1299-1307

21. Ait-Oufella H, Salomon BL, Potteaux S, Robertson AK, Gourdy P, Zoll J, et al. Natural regulatory t cells control the development of atherosclerosis in mice. *Nat Med*. 2006;12:178-180

22. Klingenberg R, Gerdes N, Badeau RM, Gistera A, Strodthoff D, Ketelhuth DF, et al. Depletion of foxp3+ regulatory t cells promotes hypercholesterolemia and atherosclerosis. *J Clin Invest*. 2013;123:1323-1334

23. Choi JH, Nam KH, Kim J, Baek MW, Park JE, Park HY, et al. Trichostatin a exacerbates atherosclerosis in low density lipoprotein receptor-deficient mice. *Arterioscler Thromb Vasc Biol*. 2005;25:2404-2409

24. Lobera M, Madauss KP, Pohlhaus DT, Wright QG, Trocha M, Schmidt DR, et al. Selective class iia histone deacetylase inhibition via a nonchelating zinc-binding group. *Nat Chem Biol*. 2013;9:319-325

Supplemental Methods

Human carotid plaque studies

Genotyping

We performed two genome-wide association (GWA) experiments in 1,858 consecutive patients from Athero-Express Study. DNA was extracted from whole blood or carotid plaques following standardized protocols. The first experiment was performed in the Athero-Express Genomics Study 1 (AEGS1; n=836 patients recruited between 2002 and 2007) and was carried out by AROS Applied Biotechnology (Denmark) under study number A318 using the Affymetrix Genome-Wide Human SNP Array 5.0 (SNP5) chip (Affymetrix Inc., Santa Clara, CA, USA). The second experiment was performed in the Athero-Express Genomics Study 2 (AEGS2; n=1,022 patients recruited between 2002 and 2013). These samples were genotyped at the Genomic Analysis Center, Helmholtz Center Munich (Germany) using the Affymetrix Axiom GW CEU 1 Array (AxM).

Genotyping quality control and imputation

Quality control (QC) was performed according to standard procedures. Genotype calling was conducted using the standard settings of Affymetrix Genotyping Console 4.0 Software (GCOS4) and the proper algorithm for each chip (BRLMM-P for SNP5 and Axiom GT1 for AxM, respectively). Subsequent QC included the following steps: We first excluded samples with low average genotype calling and gender discrepancies (compared to clinical data) based on GCOS4 metrics. Next, data were filtered on 1) individual (sample) call rate > 97%, 2) SNP call rate > 97%, 3) minor allele frequencies > 3%, 4) average heterozygosity rate ± 3.0 SD, 5) relatedness (pi-hat > 0.20), 6) Hardy–Weinberg Equilibrium (HWE *P*-value < 1.0×10^{-6}), and 7) population stratification (based on HapMap 2, release 22, b36) by excluding samples deviating more than 6 standard deviations from the average in 5 iterations during principal component analysis and by visual inspection. All subjects were of self-reported European ancestry, which was confirmed through PCA. After QC 657 and 869 samples from AEGS1 and AEGS2 respectively, were available for imputation. A total of 403,789 markers in AEGS1 and 535,983 in AEGS2 were included before imputation. Autosomal missing genotypes

were imputed in both datasets using phased data from the HapMap 2 project[1] (release 22, b36) and BEAGLE[2] v3.3.2 (31 October 2011).

Statistical analysis

For statistical analysis quantitative histological phenotypes were normalized through natural log (LN) transformation; outliers deviating more than ±3 SD from the LN-transformed mean were removed. Genetic analyses were corrected for age, sex, 10 principal components, year of surgery and a dummy variable representing the two genotyping batches, assuming an additive genetic model. Linear and logistic regression models were used for quantitative and binary phenotypes, respectively. IBM SPSS Statistics version 20 (release 20.0.0, IBM Corp., Armonk, NY, USA) was used for statistical analyses of baseline characteristics. PLINK[3] v1.7 and Golden Helix SNP & Variation Suite v8.1.5 (Golden Helix, Inc., Bozeman, MT, USA) were used for genetic analyses. Our power to detect an association between rs2107595 and individual plaque phenotypes at a significance level of 0.05 [0.005] with a sample size of 1,400, an effect size of 0.182 and a minor allele frequency of 20% was >90% [>75%] for quantitative phenotypes. For binary phenotypes our power to detect an OR of 1.20 (corresponding to an effect size of 0.182) was between 20% [4%] (for collagen) and 54% [23%] (for intraplaque hemorrhage). To account for testing multiple phenotypes the level of statistical significance was set at 0.005.

Supplemental Tables

Table I. Demographic characteristics of the Athero-Express Study.

| Characteristic	
Total sample, *N*	1,439
Age in years, mean (SD)	68.31 (9.31)
Sex, male, %	67.89
Mean arterial pressure (SD), mmHg	106.71 (15.86)
Total cholesterol (SD), mmol/l	4.72 (1.24)
Smoking, %	34.26
Diabetes mellitus, %	22.79
BMI (SD), kg/m2	26.29 (3.86)
Time since last cerebrovascular event, median (IQR), days	43.50 (18-92)
Index event, %	
Asymptomatic	28.42
Symptomatic	70.95
Transient ischemic attack	44.34
Stroke	26.62

SD: standard deviation. *IQR*: interquartile range.

Table II. Association of rs2107595 with plaque phenotypes in patient subgroups from the Athero-Express Study.

MAF	OR	95% CI	*P*	Phenotype	*N*
asymptomatic (*N*=409)					
0.800	0.786	0.53-1.16	0.229	calcification	234/168
0.799	1.024	0.63-1.67	0.926	collagen	339/63
0.799	1.146	0.78-1.69	0.496	atheroma size (10%)	268/135
0.799	1.698	1.16-2.49	0.007	intraplaque hemorrhage	229/173
0.799	1.347	0.97-1.88	0.079	macrophages	399
0.801	0.868	0.70-1.07	0.188	smooth muscle cells	397
0.791	1.015	0.89-1.16	0.825	vessel density	354
symptomatic (*N*=1,021)					
0.801	1.230	0.98-1.55	0.077	calcification	469/525
0.802	0.768	0.58-1.02	0.072	collagen	787/208
0.802	1.169	0.90-1.51	0.234	atheroma size (10%)	742/253
0.802	1.082	0.85-1.37	0.520	intraplaque hemorrhage	616/379
0.802	1.078	0.87-1.33	0.482	macrophages	995
0.801	0.947	0.81-1.10	0.487	smooth muscle cells	969
0.801	0.954	0.87-1.04	0.297	vessel density	858
stroke (*N*=383)					
0.800	1.404	0.96-2.05	0.081	calcification	175/198
0.800	0.720	0.44-1.19	0.201	collagen	306/67
0.800	1.159	0.76-1.78	0.499	atheroma size (10%)	276/97
0.801	0.809	0.54-1.21	0.307	intraplaque hemorrhage	232/140
0.800	1.178	0.85-1.63	0.324	macrophages	374
0.802	1.048	0.83-1.32	0.693	smooth muscle cells	364
0.809	0.954	0.82-1.12	0.559	vessel density	317

MAF: major allele frequency; odds ratios (OR) are relative to the major allele (G) on genome build 36; *P*-values are two-sided. Phenotype: calcification and collagen are coded as no or minor vs. moderate heavy staining, atheroma size is coded as <10% vs. >10% fat content, intraplaque hemorrhage (IPH) as no vs. yes, macrophages and smooth muscle cells are natural log (LN)-transformed percentages of plaques, and vessel density is the LN-transformed average intraplaque vessel density per 3-4 hotspots. *N* is the number of patients analyzed for the respective plaque phenotype. *Asymptomatic*: includes patients with significant stenosis (>50%) or ocular events (including amaurosis fugax or retinal infarction) but no history of transient ischemic attack (TIA) or stroke prior to carotid endarterectomy (CEA). *Symptomatic*: includes patients with a history of TIA or stroke prior to CEA.

Supplemental Figures
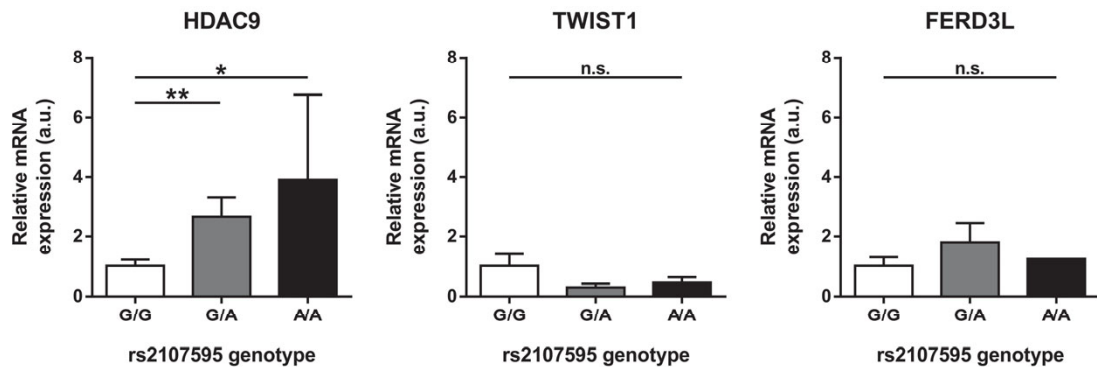
Figure I. Relative mRNA expression of HDAC9, TWIST1 and FERD3L in human PBMCs for different genotypes of rs2107595. HDAC9 mRNA levels are significantly elevated in homozygous and heterozygous carriers of the risk allele (A) with a gene dosage effect (GG n=51, GA n=22, AA n=4). For TWIST1 (GG n=23, GA n=3, AA n=4) and FERD3L (GG n=23, GA n=3, AA n=1) no correlation with allele carrier status was found. Results represent mean±SEM. *$P<0.05$, **$P<0.01$ (Kruskal-Wallis test followed by Mann-Whitney test).
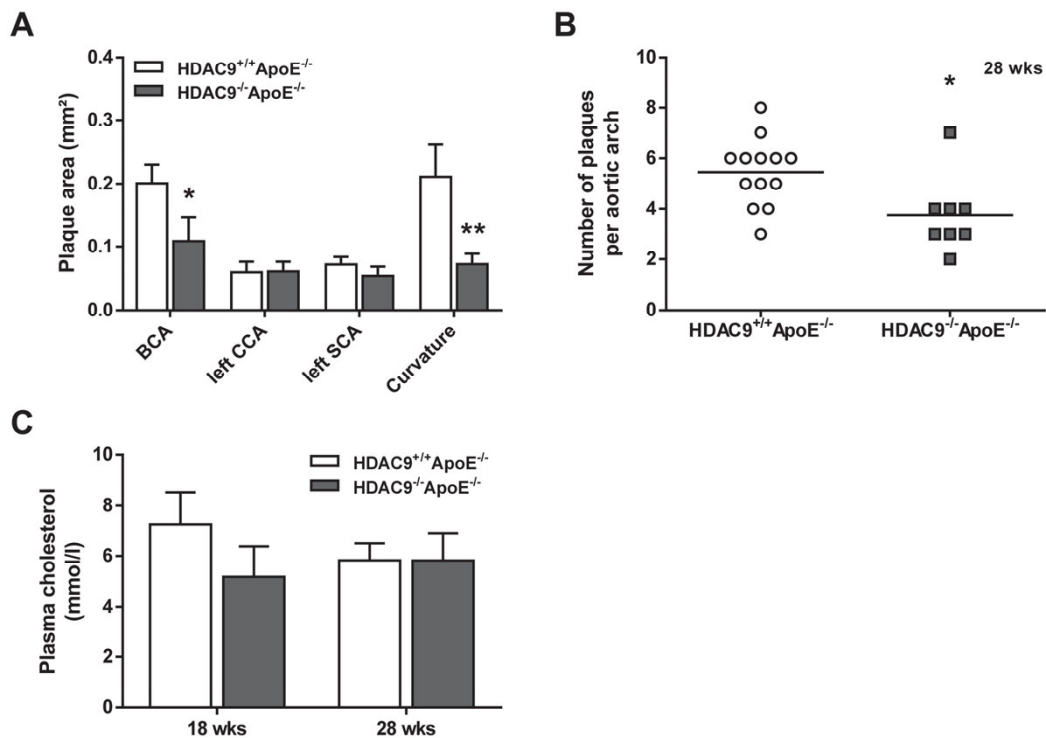
Figure II. A, Plaque area of the main branches and the curvature of the aorta in 28-week-old mice. **B**, Number of plaques per aortic arch. **C**, Plasma cholesterol in 18 and 28-week-old male mice. Results represent mean±SEM. n = 8-13 for each genotype and time point; *$P<0.05$; **$P<0.01$ vs. wildtype (Mann-Whitney test). BCA brachiocephalic artery, CCA common carotid artery, SCA subclavian artery.

Supplemental References

1. International HapMap C, Frazer KA, Ballinger DG, Cox DR, Hinds DA, Stuve LL, et al. A second generation human haplotype map of over 3.1 million snps. *Nature*. 2007;449:851-861
2. Browning BL, Browning SR. A unified approach to genotype imputation and haplotype-phase inference for large data sets of trios and unrelated individuals. *Am J Hum Genet*. 2009;84:210-223
3. Purcell S, Neale B, Todd-Brown K, Thomas L, Ferreira MA, Bender D, et al. Plink: A tool set for whole-genome association and population-based linkage analyses. *Am J Hum Genet*. 2007;81:559-575

5 Manuscript 2

Effect of HDAC9 Deficiency on Atherosclerosis and Immune Cell Homeostasis

Sepiede Azghandi, BSc[1]; Dominik Bühler, BSc[1]; Kerstin Berer, PhD[2]; Martin Dichgans, MD[1,3]; Christof Haffner, PhD[1]

[1] Institute for Stroke and Dementia Research, Klinikum der Universität München, Munich, Germany

[2] Department of Neuroimmunology, Max Planck Institute of Neurobiology, Martinsried, Germany

[3] Munich Cluster for Systems Neurology (SyNergy), Munich, Germany

Author contributions:

SA designed the studies, performed and analyzed the experiments, and wrote the manuscript. DB worked as technical consultant and edited the manuscript. KB and CH contributed to writing of the manuscript. KB, MD and CH designed and supervised the study.

Abstract

Cardiovascular diseases including stroke and ischemic heart disease belong to the most common causes for mortality worldwide. Atherosclerosis is the underlying pathology for these diseases. We could recently demonstrate that deficiency of histone deacetylase 9 (HDAC9), which was identified as a risk gene for large vessel stroke and coronary artery disease, is atheroprotective in a mouse atherosclerosis model. The aim of the current study was to investigate the effect of HDAC9 deficiency on atherosclerotic plaque size, immune cell infiltration and immune cell distribution in mice using different dietary settings. We could show that HDAC9 deficiency mainly affects early atherogenesis by delaying the development of progressed atherosclerotic lesions. Using a Western-type diet, where lesions are in a more advanced stage, atherosclerotic lesion size was comparable between $HDAC9^{+/+}ApoE^{-/-}$ and $HDAC9^{-/-}ApoE^{-/-}$ mice. Flow cytometry analysis revealed a shift in monocyte populations from classical, inflammatory monocytes to resident monocytes. Furthermore, frequencies of monocytes/macrophages were reduced in the spleen of HDAC9 deficient mice. In addition, T cell analysis revealed that chow fed $HDAC9^{-/-}ApoE^{-/-}$ mice harbored significantly less effector memory T cells suggesting a decreased activation and mobilization of T cells in HDAC9 deficient mice. These findings support our hypothesis that both innate as well as adaptive immune responses play an important role in the atheroprotective effect mediated by HDAC9 deficiency. Inhibition of HDAC9 seems to be a promising therapeutic strategy for the prevention of atherosclerosis by modulating the immune system.

Introduction

Cardiovascular diseases including ischemic heart disease and stroke are major causes of mortality worldwide.[1] In recent genome-wide association studies (GWAS), the histone deacetylase 9 (*HDAC9*) gene region (7p21.1) was associated with large vessel stroke (LVS)[2,3] and coronary artery disease (CAD).[4] In the LVS study, the variant rs2107595, which locates just downstream of the *HDAC9* gene, was identified as the lead single nucleotide polymorphism (SNP).[3] HDAC9 belongs to the family of histone deacetylases (HDACs) which consists of 18 members grouped in 4 classes.[5] HDAC9 is a class IIa HDAC which in contrast to class I HDACs are characterized by a tissue-specific expression - for HDAC9 mainly in the heart, the brain and the immune system - as well as by an N-terminal domain mediating interactions with transcription factors and transport proteins.[5-7]

Both LVS and CAD are mainly caused by atherosclerosis. We and others could recently demonstrate that HDAC9 deficiency is atheroprotective using two different murine models for atherosclerosis, ApoE$^{-/-}$ and LDLR$^{-/-}$ mice, respectively.[8,9] While Cao et al. showed a reduction of lesion sizes in HDAC9$^{-/-}$LDLR$^{-/-}$ mice fed with a Western-type diet for 16 weeks,[9] we made a similar observation in aortic valves and the aortic arch of HDAC9$^{-/-}$ApoE$^{-/-}$ mice at two different time points (18 and 28 weeks of age) and under a normal chow diet.[8] Furthermore, we observed that HDAC9 deficiency led to significantly more initial lesions consequently showing increased macrophage infiltrations. These results are well in line with the increased HDAC9 mRNA levels we measured in peripheral blood mononuclear cells (PBMCs) of individuals carrying the rs2107595 risk allele.[8]

Atherosclerosis is a chronic inflammatory disease of the arterial wall. Both innate and adaptive immunity play an important role in the initiation and progression of atherosclerotic lesions.[10] The predominant immune cells in atherosclerotic lesions are macrophages and T cells. Recent studies have demonstrated an involvement of HDAC3 and HDAC7 in macrophage polarization,[11-13] as well as on T cell function, especially on regulatory T cells.[14,15] Cao et al. observed in HDAC9 deficient macrophages an increased cholesterol efflux via the transporter proteins ABCA1 and ABCG1 and a polarization to the more anti-inflammatory M2 phenotype.[9] A limitation of this study was the exclusive *ex vivo* approach using bone marrow derived or peritoneal macrophages, stimulated and analyzed in cell culture experiments, while the involvement of other immune cell types, such as T cells, was neglected. The aim of the current study was to determine the effect of HDAC9

deficiency on atherosclerotic plaque size and immune cell homeostasis after feeding different diets.

Materials and Methods

Animals

All animal protocols were approved by the government of Upper Bavaria. HDAC9^{-/-} mice from E. Olson[7] were crossed with ApoE deficient mice (The Jackson Laboratory) to generate HDAC9^{-/-}ApoE^{-/-} mice. Mice had *ad libitum* access to food and water and were housed in a specific pathogen-free animal facility under a 12 h light-dark cycle. All experiments were performed on male littermates fed a standard chow diet for 18 or 28 weeks or a Western-type diet (21.2% fat, 0.2% cholesterol, and 33.2% sugar, ssniff) for 10 weeks, starting at 8 weeks of age. All experiments and data analysis were performed in a blinded fashion. Following primers were used for HDAC9 genotyping:

5'-CAATTGACTATGCGGCTCT-3' (wt forward),

5'-AGGCATGCTGGGGATGCGGTGGGC-3' (ko forward),

5'-CCTTCCATATAAAACCAACTCC-3' (reverse).

Bone Marrow Transplantation

Bone marrow cells were isolated from femur and tibia of 10-week-old male HDAC9^{+/+}ApoE^{-/-} mice or HDAC9^{-/-}ApoE^{-/-} littermates and $1x10^7$ bone marrow cells were injected intravenously into lethally irradiated 6-week-old male ApoE deficient mice. For two weeks after the transfer, animals were treated with 1 g/L neomycin (Sigma-Aldrich). After additional two weeks of recovery, mice were fed a Western-type diet for 10 weeks.

Tissue Harvesting

Mice were anesthetized using ketamine and xylazine. Blood was obtained by cardiac puncture. The arterial tree was perfused through the left ventricle with phosphate buffered saline (PBS), containing 1 mg/ml sodium nitroprusside (Sigma-Aldrich) for vasodilation. The spleen was removed prior to perfusion with 10 ml of 1% paraformaldehyde (PFA). The aortic arch was dissected and fixed for 24 hours in 1% PFA solution. Half the spleen was used to prepare a single cell suspension by mechanical disruption using a 40 µm nylon mesh

(BD Falcon). For RNA expression analysis, the other half of the spleen was incubated in RNAlater (QIAGEN) at 4°C overnight, shock-frozen on dry ice the next day and stored at -80°C.

Plaque Size and Immunohistochemistry Analysis

Atherosclerotic plaque size at the aortic valves and in the aortic arch was quantified as previously described.[8] In the Western-type diet fed mice, the acellular core area of the plaque at the brachiocephalic artery (BCA) was measured on two aortic arch sections at a distance of 40 μm by using the Axiovision software (Zeiss).

Immunohistochemistry was performed on heart cryosections at the level of the aortic valves. We used a rat anti-CD45 monoclonal antibody (1:200 dilution, 30-F11, BD Pharmingen) to detect all infiltrated leukocytes and a Syrian hamster anti-CD3 monoclonal antibody (1:50 dilution, 500A2, BD Pharmingen) to detect T cells. Antibodies were titrated to optimal performance and applied to acetone-fixed cryosections of the aortic valves. Goat secondary antibodies (Vector Laboratories) were used, followed by detection with an ABC peroxidase kit and DAB substrate (both from Vector Laboratories). Stainings were quantified using ImageJ Software. The CD45+ stained area and the number of CD3+ cells inside the plaque or the lamina were divided by the lesion area.

Flow Cytometry Analysis

Flow cytometry analysis was performed on single cell suspensions of spleen or leukocytes isolated from blood. Cells were stained in FACS buffer (1x PBS with 0.5% Bovine Serum Albumin and 0.01% sodium azide) with the following fluorochrome-labeled antibodies against: CD45 (eFluor450, 30-F11, eBioscience), CD3 (FITC, 145-2C11, eBisocience), CD11b (PerCp-Cy5.5, M1/70, eBioscience), Ly6G (PE, 1A8, BD Pharmingen), Ly6C (APC, 1G7.G10, Miltenyi), CD11c (PE-Cy7, N418, eBioscience), CD4 (APC-H7, GK1.5, BD Pharmingen), CD8 (eFluor450, 53-6.7, eBioscience), CD44 (APC, IM7, eBioscience), CD62L (PE-Cy7, Mel-14, eBioscience), and FoxP3 (PE, FJK-16a, eBioscience). Intracellular staining for FoxP3 was performed using the anti-mouse/rat FoxP3 Staining Set (eBioscience). Samples were acquired on the FACSVerse (BD Biosciences) and data analysis was done using FlowJo software (Tree Star).

Real-time PCR

Total RNA from spleens of 28-week-old chow fed HDAC9$^{-/-}$ApoE$^{-/-}$ mice and their wild-type littermates was isolated by RNeasy Lipid Tissue Mini Kit (QIAGEN). cDNA was prepared from 1 µg RNA using the Omniscript RT Kit (QIAGEN) and diluted 1:5. For expression analysis of interferon-γ (IFN-γ), a reaction mix of 12 µl, including 2 µl cDNA, 200 nM IFN-γ-specific primers (IFN-γ forward: 5'-TCAAGTGGCATAGATGTGGAAGAA-3'; IFN-γ reverse: 5'- TGGCTCTGCAGGATTTTCATG-3') and Brilliant II SYBR Green QPCR Master Mix (Agilent Technologies) was used. For CXCL1, CXCL2 and CXCL5, PrimeTime Mini qPCR Assays from Integrated DNA Technologies were used. Real-time PCR was performed on 384-well plates using the LightCycler 480 (Roche Diagnostics). Glyceraldehyde 3-phosphate dehydrogenase (GAPDH) was used as a house-keeping gene. Measurements were performed in triplicates. Data were analyzed based on the comparative threshold cycle method with the following formula: Relative mRNA expression level = $2^{-\Delta\Delta C_t}$;

$\Delta\Delta C_t = \Delta C_{t, target} - \Delta C_{t, calibrator}$; $\Delta C_t = C_{target-gene} - C_{t, GAPDH.}$

Average C_t values of wild-type mice were used as calibrator.

ELISA

Splenocytes were cultured in the presence of anti-CD3 (1 µg/ml, 500A2, BD Biosciences) or anti-CD3 plus anti-CD28 (0.5 µg/ml, 37.51, eBioscience). After 48 hours of stimulation, cell culture supernatants were collected and frozen at -20°C. Cytokine levels were measured by matching antibody pairs for IFN-γ (BD Pharmingen), IL-17 (eBioscience) and IL-10 (R&D).


Statistical analysis

GraphPad Prism 6 (GraphPad Software) and SigmaPlot 12.5 (Systat Software Inc.) were used for statistical analysis. Pairwise comparisons were performed using the Mann-Whitney test. Differences were considered statistically significant at *P*<0.05. Data are expressed as mean ± SEM.

Results and Discussion

Deficiency of HDAC9 has mainly an effect on early atherogenesis

To test the effect of HDAC9 deficiency on atherosclerosis at various time points using different dietary settings, several groups of HDAC9$^{-/-}$ApoE$^{-/-}$ mice and their wild-type littermates were analyzed (Figure 1). Recently, we showed the influence of HDAC9 deficiency on atherosclerotic plaque size in ApoE deficient mice fed a normal chow diet.[8] At both 18 and 28 weeks of age, HDAC9$^{-/-}$ApoE$^{-/-}$ animals showed a significant reduction of atherosclerotic lesion size in the aortic valves as well as in the aortic arch. In addition, we observed that HDAC9 deficiency led to significantly less advanced lesions, and a pronounced infiltration of macrophages. However, after exclusion of advanced atheromas, we no longer observed any differences in the numbers of infiltrating macrophages into initial lesions.[8] In the current study, we analyzed infiltration of leukocytes (CD45+ cells) as well as T cells (CD3+ cells) in aortic valve sections of 28-week-old HDAC9$^{-/-}$ApoE$^{-/-}$ mice. There were no differences, neither in the overall leukocyte infiltration (Supplementary Figure S1A) nor in the number of T cells that migrated into the lamina or the plaque (Supplementary Figure S1B). In addition to 18- and 28-week-old animals fed a normal chow diet, we also added a third group of Western-type diet fed mice and a fourth group of bone marrow transplanted mice to our analysis (Figure 1).
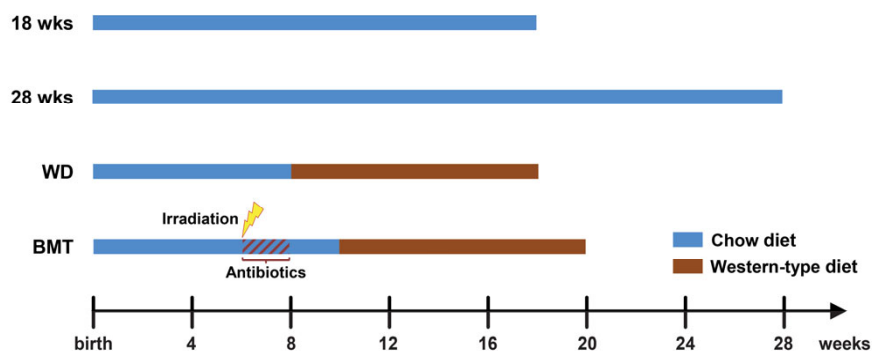
Figure 1. Study design. Four groups of mice were analyzed. The first two groups, 18- and 28-week-old HDAC9$^{-/-}$ApoE$^{-/-}$ mice and their wild-type littermates were fed a normal chow diet. The third group of mice was fed a high cholesterol Western-type diet for 10 weeks, starting at an age of 8 weeks. The fourth group consisted of ApoE$^{-/-}$ mice which received bone marrow from HDAC9$^{-/-}$ApoE$^{-/-}$ or from HDAC9$^{+/+}$ApoE$^{-/-}$ donors after irradiation. After two weeks of antibiotics and two additional weeks of recovery, the mice were fed a Western-type diet for 10 weeks.

To test the hypothesis whether immune cells are responsible for the atheroprotective effect seen in HDAC9 deficient mice, we transplanted bone marrow from HDAC9^{-/-}ApoE^{-/-} mice or wild-type littermates to lethally irradiated ApoE^{-/-} mice and after four weeks of recovery, mice were fed a Western-type diet for 10 weeks. No differences in atherosclerotic plaque size were observed in Western-type diet fed mice or in bone marrow transplanted animals, neither on the level of the aortic valves (Figure 2) nor in the aortic arch (Supplementary Figure S2). Since plaque sizes were comparable between Western-type diet fed HDAC9^{-/-}ApoE^{-/-} mice and wild-type littermates, we could not address the question whether HDAC9 deficiency in immune cells is sufficient for the atheroprotective effect.

For proteins important in adaptive immunity it is already known that they often only show an effect on atherosclerosis when ApoE deficient mice are fed a chow diet and not a Western-type diet. For example, lymphocyte deficient Rag-1 knockout mice on an ApoE deficient background showed a reduction in lesion size of almost 50% when fed a normal chow diet, but no difference when fed a Western-type diet.[16] Similar experiments were performed by Song et al. in LDLR deficient mice, analyzing the effect of Rag-1 deficiency after different durations of Western-type diet feeding.[17] After 8 weeks on Western-type diet, Rag1^{-/-}LDLR^{-/-} mice displayed a reduction of 54% in lesion size, while after 12 or 16 weeks, no reduction in lesion size was observed any longer.[17] Histological analysis demonstrated a lower complexity of lesions in Rag1^{-/-}LDLR^{-/-} mice, which had mainly initial foam cell lesions, indicating an involvement of lymphocytes in early atherogenesis.[17]

These findings from Rag-1 deficient mice are comparable to our data obtained in HDAC9 deficient animals. The biggest reduction of lesion size in HDAC9 deficient mice was seen at 18 weeks of age on chow diet. However, the difference was becoming smaller with time (40% reduction in 18-week-old vs. 26.5% reduction in 28-week-old HDAC9^{-/-}ApoE^{-/-} mice in comparison to HDAC9^{+/+}ApoE^{-/-} mice), indicating a delay of atherogenesis by HDAC9 deficiency. This is supported by histological data from our previous study showing more initial lesions in HDAC9^{-/-}ApoE^{-/-} mice.[8]
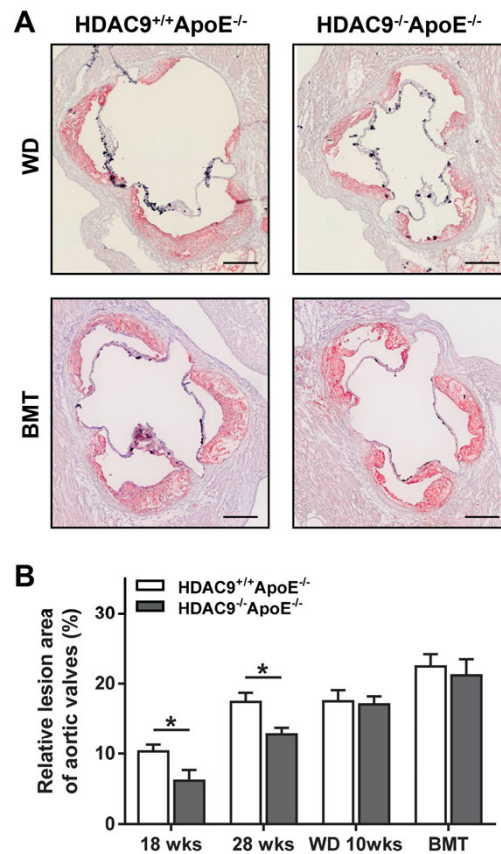
Figure 2. HDAC9 deficiency has no effect on atherosclerotic plaque size in Western-type diet fed mice. A, Representative images showing Oil-Red O- and hematoxylin-stained cryosections from the proximal aorta of HDAC9$^{+/+}$ApoE$^{-/-}$ and HDAC9$^{-/-}$ApoE$^{-/-}$ mice fed a Western-type diet (WD) or after bone marrow transplantation (BMT). Scale bars: 250 μm. **B**, Quantification of the relative lesion area (in relation to the area inside the external elastic lamina) demonstrates a significant reduction of atherosclerosis in 18- and 28-week-old HDAC9$^{-/-}$ApoE$^{-/-}$ mice on chow diet in comparison to their wild-type littermates,[8] but no differences in Western-type diet and bone marrow transplanted mice. Results represent mean ± SEM; n = 7-13 for each genotype and time point; *$P<0.05$ vs. wild-type (Mann-Whitney test).

To further validate this finding, we analyzed the amount of acellular cores in the brachiocephalic artery of Western-type diet mice. In contrast to 28-week-old HDAC9 deficient mice on chow diet, which showed a significant reduction of acellular cores,[8] no difference in the acellular cores was observed in HDAC9$^{-/-}$ApoE$^{-/-}$ mice compared to wild-type littermates fed a Western-type diet (Figure 3). These findings indicate an involvement of HDAC9 in early atherogenesis. To answer the question if HDAC9 deficiency in immune cells is sufficient for an atheroprotective effect, it is necessary to perform a bone marrow

transplantation in ApoE deficient mice fed a normal chow diet or a Western-type diet for a shorter duration.
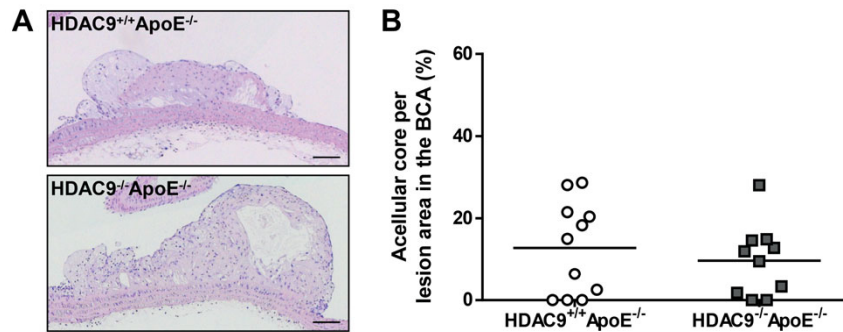
Figure 3. Western-type diet fed HDAC9$^{-/-}$ApoE$^{-/-}$ mice have similar proportions of acellular cores in atherosclerotic lesions as wild-type littermates. A, Representative images of atherosclerotic plaques in the brachiocephalic artery (BCA) of HDAC9$^{-/-}$ApoE$^{-/-}$ and HDAC9$^{+/+}$ApoE$^{-/-}$ mice. Scale bars: 100 μm**. B**, Quantification of acellular core per lesion area in the BCA of Western-type diet fed HDAC9$^{-/-}$ApoE$^{-/-}$ mice and their wild-type littermates. n = 10-11 for each genotype.

HDAC9 deficiency affects monocyte populations in atherosclerotic mice

To study the distribution of different leukocyte subpopulations in HDAC9 deficient mice during atherosclerosis, flow cytometry analysis of the spleen and the blood was performed with specific immune cell markers. Blood leukocyte analysis did not reveal differences in the leukocyte populations investigated (data not shown). HDAC9$^{-/-}$ApoE$^{-/-}$ mice on chow as well as on Western-type diet had a lower percentage of monocytes/macrophages (CD11b+Ly6G-) in the spleen (Figure 4A and 4B). Moreover, when we compared the classical, pro-inflammatory Ly6C+ monocytes with non-classical, resident Ly6C- monocytes, a shift toward the latter population was observed in HDAC9 deficient mice (Figure 4 and Supplementary Figure S3), a finding in line with the observed reduction in lesion size. This shift in Ly6C was only observed in HDAC9$^{-/-}$ApoE$^{-/-}$ mice but not in HDAC9 single knockout mice (Supplementary Figure S3D), indicating that it represents a disease-specific effect. Differences were also detected in neutrophil percentages (CD11b+Ly6G+). However, these were not consistent between 18- and 28-week-old mice (Figure 4A and Supplementary Figure S3A). HDAC9 deficient mice showed no differences in CD11c+ dendritic cells (data not shown). Additionally, we also checked the expression of different cytokines and chemokines which are important for macrophage and neutrophil function/migration in

spleens from 28-week-old mice. Expression of IFN-γ, CXCL1, CXCL2 and CXCL5 was comparable between HDAC9$^{+/+}$ApoE$^{-/-}$ and HDAC9$^{-/-}$ApoE$^{-/-}$ mice (Supplementary Figure S4).
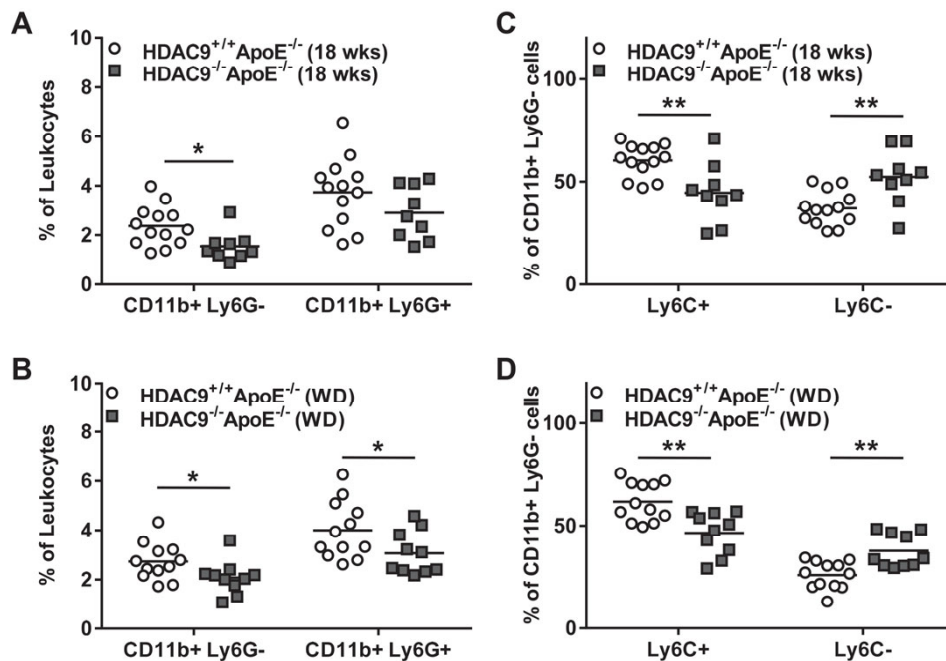
Figure 4. HDAC9$^{-/-}$ApoE$^{-/-}$ mice show reduced monocyte numbers and a shift to more Ly6C negative, non-classical, resident monocytes. Flow cytometric analysis of spleens from 18-week-old and Western-type diet (WD) fed HDAC9$^{+/+}$ApoE$^{-/-}$ and HDAC9$^{-/-}$ApoE$^{-/-}$ mice. **A** and **B**, Frequencies of monocytes/macrophages (CD11b+Ly6G-) and neutrophils (CD11b+Ly6G+) (% of leukocytes). **C** and **D**, Frequencies of Ly6C+ and Ly6C- monocytes/macrophages (% of CD11b+Ly6G- cells). n = 9-13 mice for each genotype per group. *P<0.05; **P<0.01.

HDAC9$^{-/-}$ApoE$^{-/-}$ mice have a modest decrease in regulatory T cells

To investigate possible effects of HDAC9 deficiency on cells of the adaptive immune system, we analyzed T cell populations by flow cytometry. We detected no differences in the frequencies of T cells (CD3+), the T helper cell subpopulation (CD4+) or the cytotoxic T cell subpopulation (CD8+) (Figure 5A, 5B, Supplementary Figure S5A and S5B). Surprisingly, we measured a modest decrease in regulatory T cells (CD4+FoxP3+) in our HDAC9$^{-/-}$ApoE$^{-/-}$ mice on chow and on Western-type diet (Figure 5C, 5D and Supplementary Figure S5C), but not in HDAC9 deficient mice without ApoE deficiency (Supplementary Figure S5D).
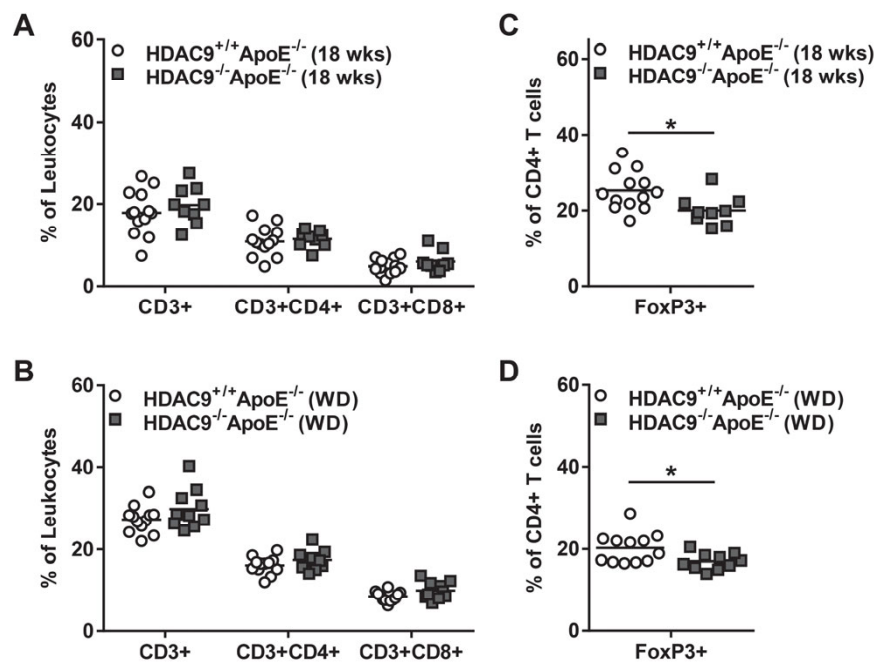
Figure 5. HDAC9$^{-/-}$ApoE$^{-/-}$ mice show a modest decrease in regulatory T cells. Flow cytometric analysis of spleens from 18-week-old and Western-type diet (WD) fed HDAC9$^{+/+}$ApoE$^{-/-}$ and HDAC9$^{-/-}$ApoE$^{-/-}$ mice. **A** and **B**, Frequencies of T cells (CD3+), T helper cells (CD3+CD4+) and cytotoxic T cells (CD3+CD8+) (% of leukocytes). **C** and **D**, Frequencies of CD4+FoxP3+ regulatory T cells. n = 9-13 mice for each genotype per group. *$P<0.05$.

These findings are in contrast to previously published data by Tao et al. showing that HDAC9 deficient mice have a 50% increase in CD4+FoxP3+ T cells.[15] Different wild-type controls may account for these contradictory observations. In our study, wild-type littermates were used. It is, however, not clear which controls the Tao et al. study used for the analysis. Furthermore, only a number of 4 spleens were measured by Tao and colleagues,[15] while a minimum of 8 HDAC9$^{-/-}$ApoE$^{-/-}$ mice were used in the three different groups in our study. Nevertheless, our data do not allow the conclusion that HDAC9 has no influence on regulatory T cells, since the study by Tao et al. convincingly demonstrated that HDACs, especially HDAC9, are important for the suppressive function of regulatory T cells. Our modest decrease in regulatory T cells has probably no consequence on atherosclerosis. Nevertheless, these cells could still be more suppressive than wild-type regulatory T cells.

In addition to flow cytometry analysis, we assessed the ability of T cells to respond to antigen stimulation using the production of pro-inflammatory (IFN-γ or IL-17) or anti-inflammatory (IL-10) cytokines as a read-out system. Splenocytes from chow or Western-type diet fed HDAC9$^{-/-}$ApoE$^{-/-}$ mice showed similar patterns of cytokine secretion when

stimulated *in vitro* with anti-CD3 or anti-CD3/CD28 antibodies (Figure 6). This data suggests that despite the lack of HDAC9, antigen-presenting cells can efficiently prime T lymphocytes, that HDAC9 deficient T cells recognize and respond normally to antigen encounter and that the effector T cell response is not disturbed in HDAC9 deficient mice. Hence, other immune cells/pathways/mechanisms are responsible for the atheroprotective effect seen in HDAC9 deficient mice.
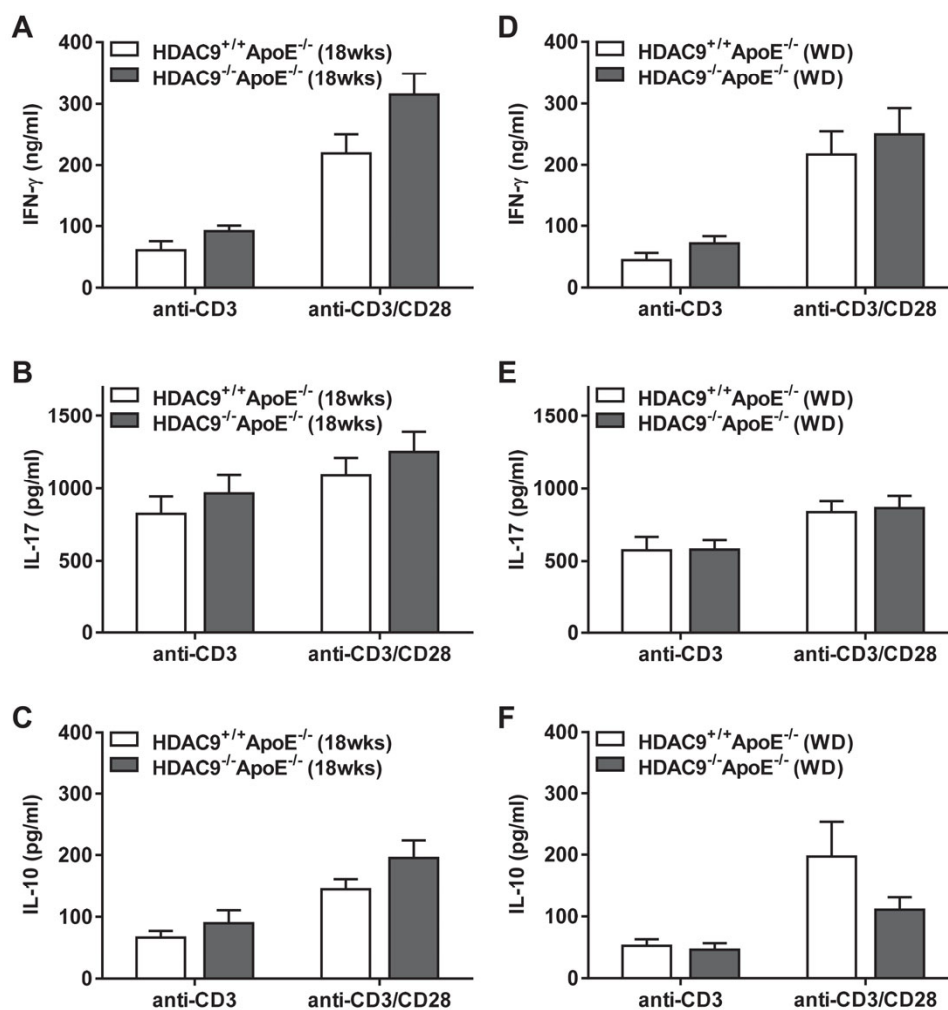
Figure 6. HDAC9 deficiency has no influence on cytokine expression of splenocytes after T cell stimulation. Splenocytes from 18-week-old and Western-type diet (WD) fed HDAC9$^{+/+}$ApoE$^{-/-}$ and HDAC9$^{-/-}$ApoE$^{-/-}$ mice were stimulated for 48 hours with anti-CD3 or anti-CD3/anti-CD28 antibodies. Levels of IFN-γ (**A** and **D**), IL-17 (**B** and **E**) and IL-10 (**C** and **F**) were measured in the supernatants by ELISA. All graphs represent mean ± SEM; n = 6-7 mice for each genotype per group.

HDAC9^{-/-}ApoE^{-/-} mice show a reduction in CD4+ effector memory T cells

Besides regulatory T cells, we also checked the memory T cell populations by using the CD44 and the CD62L (L-selectin, homing receptor) markers. Interestingly, chow fed HDAC9^{-/-}ApoE^{-/-} mice showed a decrease in effector memory T cells within the CD4+ population (Figure 7 and Supplementary Figure S6A). This difference was only observed in normal chow but not in Western-type diet fed mice (Figure 7B) or in HDAC9 deficient mice without ApoE deficiency (Supplementary Figure S6B). The decrease in effector memory T cells could explain the reduced atherosclerosis in chow fed HDAC9^{-/-}ApoE^{-/-} mice, due to less activation and mobilization of T cells. Ammirati et al. demonstrated a correlation of CD4+ effector memory T cells with the extent of atherosclerosis in animals and carotid intima-media thickness in humans.[18] These data are well in line with our findings.
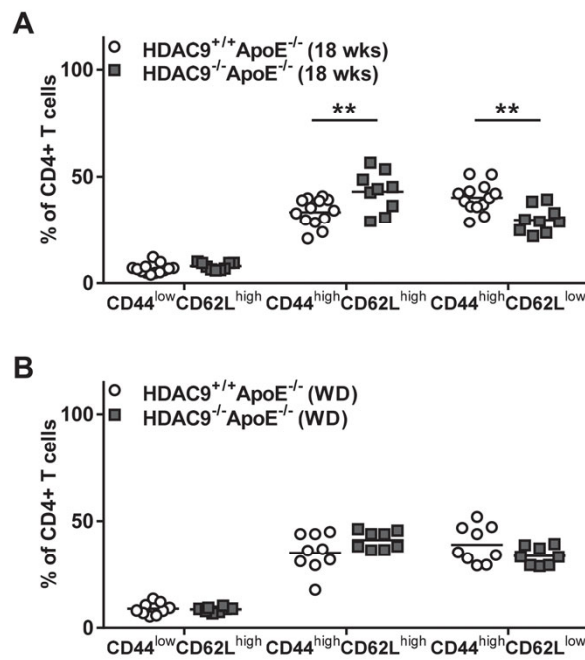
Figure 7. HDAC9^{-/-}ApoE^{-/-} mice have less effector memory T cells. Flow cytometric analysis of spleens from 18-week-old and Western-type diet (WD) fed HDAC9^{+/+}ApoE^{-/-} and HDAC9^{-/-}ApoE^{-/-} mice. **A** and **B**, Frequencies of naïve (CD44^{low}CD62L^{high}), central memory (CD44^{high}CD62L^{high}) and effector memory (CD44^{high}CD62L^{low}) T cells within the CD4+ T cell population are shown. n = 9-13 mice for each genotype per group. **P<0.01.

In conclusion, the present study highlights the importance of HDAC9 in early atherogenesis. We could show that HDAC9 deficiency leads to a delay of atheroprogression. HDAC9 deficient mice on chow diet had less advanced lesions, but similar immune cell infiltration into the plaques. We demonstrate a shift in monocyte/macrophage populations by flow cytometry which is in line with the M2 anti-inflammatory phenotype which Cao et al. could recently show in peritoneal macrophages from HDAC9$^{-/-}$LDLR$^{-/-}$ mice.[9] Besides macrophages, also T cells seem to play an important role in HDAC9 deficient mice. Chow fed HDAC9$^{-/-}$ApoE$^{-/-}$ mice show less effector memory T cells which fits to the reduced atherosclerosis in these mice. Additional functional experiments are necessary to delineate the exact mechanism and interaction of different cell types leading to the atheroprotective effect mediated by HDAC9 deficiency. HDAC9 inhibition seems to be a promising therapeutic strategy for the prevention of atherosclerosis.

Disclosures

None.

References

1. Lozano R, Naghavi M, Foreman K, Lim S, Shibuya K, Aboyans V, et al. Global and regional mortality from 235 causes of death for 20 age groups in 1990 and 2010: A systematic analysis for the global burden of disease study 2010. *Lancet*. 2012;380:2095-2128

2. Bellenguez C, Bevan S, Gschwendtner A, Spencer CC, Burgess AI, Pirinen M, et al. Genome-wide association study identifies a variant in hdac9 associated with large vessel ischemic stroke. *Nat Genet*. 2012;44:328-333

3. Traylor M, Farrall M, Holliday EG, Sudlow C, Hopewell JC, Cheng YC, et al. Genetic risk factors for ischaemic stroke and its subtypes (the metastroke collaboration): A meta-analysis of genome-wide association studies. *Lancet Neurol*. 2012;11:951-962

4. Deloukas P, Kanoni S, Willenborg C, Farrall M, Assimes TL, Thompson JR, et al. Large-scale association analysis identifies new risk loci for coronary artery disease. *Nat Genet*. 2013;45:25-33

5. Haberland M, Montgomery RL, Olson EN. The many roles of histone deacetylases in development and physiology: Implications for disease and therapy. *Nat Rev Genet*. 2009;10:32-42

6. Shakespear MR, Halili MA, Irvine KM, Fairlie DP, Sweet MJ. Histone deacetylases as regulators of inflammation and immunity. *Trends Immunol*. 2011;32:335-343

7. Zhang CL, McKinsey TA, Chang S, Antos CL, Hill JA, Olson EN. Class ii histone deacetylases act as signal-responsive repressors of cardiac hypertrophy. *Cell*. 2002;110:479-488

8. Azghandi S, Prell C, van der Laan SW, Schneider M, Malik R, Berer K, et al. Deficiency of the stroke relevant hdac9 gene attenuates atherosclerosis in accord with allele-specific effects at 7p21.1. *Stroke*. 2015;46:197-202

9. Cao Q, Rong S, Repa JJ, Clair RS, Parks JS, Mishra N. Histone deacetylase 9 represses cholesterol efflux and alternatively activated macrophages in atherosclerosis development. *Arterioscler Thromb Vasc Biol*. 2014;34:1871-1879

10. Hansson GK, Hermansson A. The immune system in atherosclerosis. *Nat Immunol*. 2011;12:204-212

11. Chen X, Barozzi I, Termanini A, Prosperini E, Recchiuti A, Dalli J, et al. Requirement for the histone deacetylase hdac3 for the inflammatory gene expression program in macrophages. *Proc Natl Acad Sci U S A*. 2012;109:E2865-2874

12. Shakespear MR, Hohenhaus DM, Kelly GM, Kamal NA, Gupta P, Labzin LI, et al. Histone deacetylase 7 promotes toll-like receptor 4-dependent proinflammatory gene expression in macrophages. *J Biol Chem*. 2013;288:25362-25374

13. Mullican SE, Gaddis CA, Alenghat T, Nair MG, Giacomin PR, Everett LJ, et al. Histone deacetylase 3 is an epigenomic brake in macrophage alternative activation. *Genes Dev*. 2011;25:2480-2488

14. Akimova T, Ge G, Golovina T, Mikheeva T, Wang L, Riley JL, et al. Histone/protein deacetylase inhibitors increase suppressive functions of human foxp3+ tregs. *Clin Immunol*. 2010;136:348-363

15. Tao R, de Zoeten EF, Ozkaynak E, Chen C, Wang L, Porrett PM, et al. Deacetylase inhibition promotes the generation and function of regulatory t cells. *Nat Med*. 2007;13:1299-1307

16. Dansky HM, Charlton SA, Harper MM, Smith JD. T and b lymphocytes play a minor role in atherosclerotic plaque formation in the apolipoprotein e-deficient mouse. *Proc Natl Acad Sci U S A*. 1997;94:4642-4646

17. Song L, Leung C, Schindler C. Lymphocytes are important in early atherosclerosis. *J Clin Invest*. 2001;108:251-259

18. Ammirati E, Cianflone D, Vecchio V, Banfi M, Vermi AC, De Metrio M, et al. Effector memory t cells are associated with atherosclerosis in humans and animal models. *J Am Heart Assoc*. 2012;1:27-41

Supplementary Figures
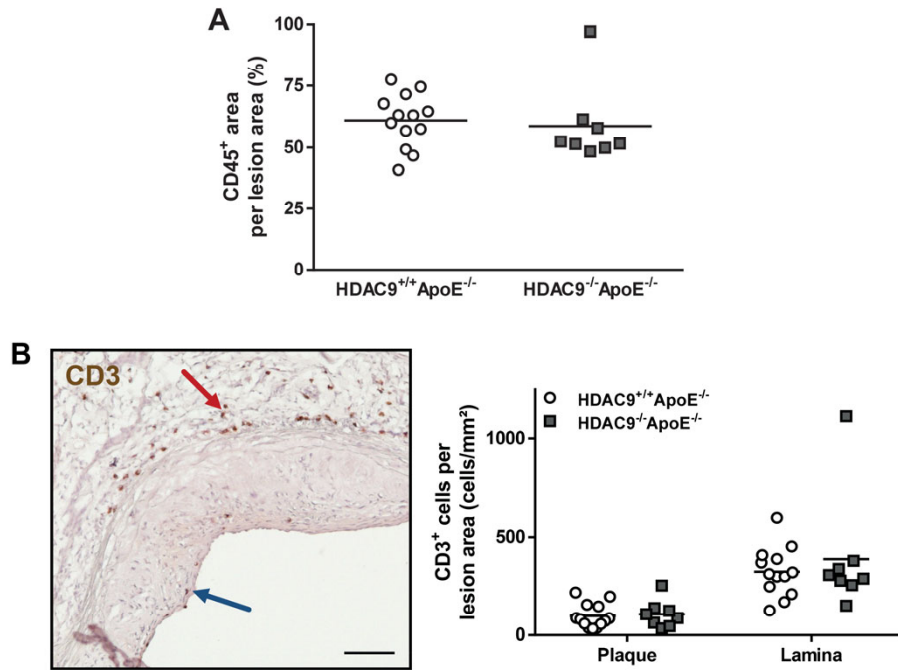
Supplementary Figure S1. HDAC9 deficiency has no effect on immune cell infiltration in atherosclerotic plaques. A, Quantification of CD45-positive stained area in atherosclerotic plaques of the aortic valves showed no difference in leukocyte infiltration between 28-week-old HDAC9$^{-/-}$ApoE$^{-/-}$ mice and their wild-type littermates. **B**, Quantification of CD3+ cells in the lamina (red arrow) and in the plaque (blue arrow) of aortic valve sections showed no difference in T cell infiltration of 28-week-old mice. Scale bars: 100 µm; n = 8-13 for each genotype.
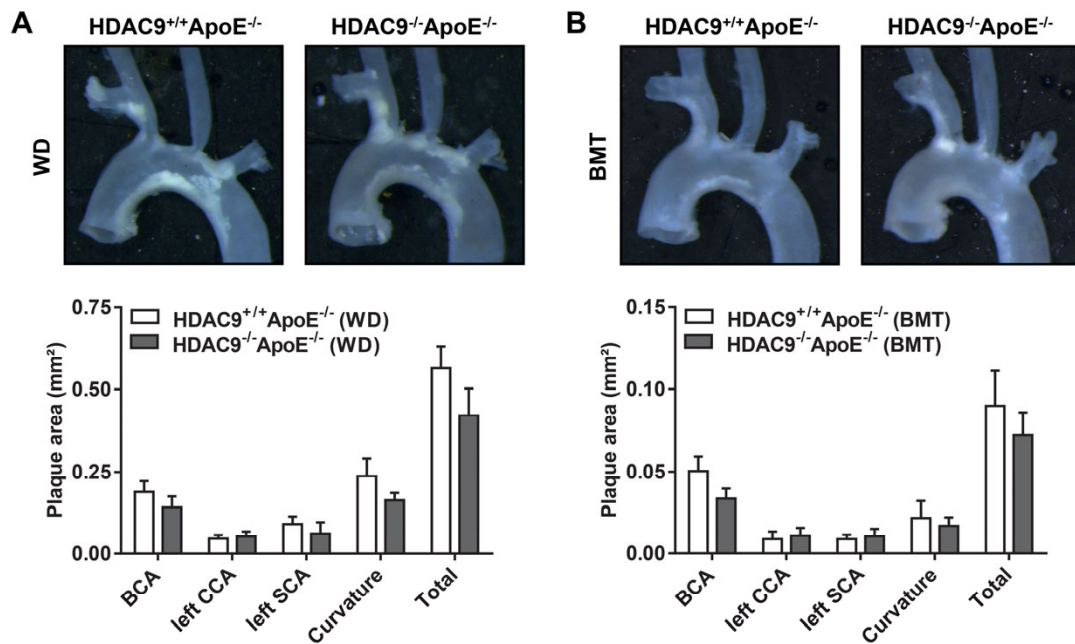
Supplementary Figure S2. HDAC9 deficiency has no effect on atherosclerotic plaque size in Western-type diet fed or bone marrow transplanted mice on Western-type diet. A, Representative images showing dissected aortic arches and quantification of lesion sizes at the main branching arteries and aortic curvature of Western-type diet (WD) fed (**A**) and bone marrow transplanted mice (BMT) (**B**). BCA brachiocephalic artery, CCA common carotid artery, SCA subclavian artery. All graphs represent mean ± SEM; n = 7-11 mice for each genotype per group.
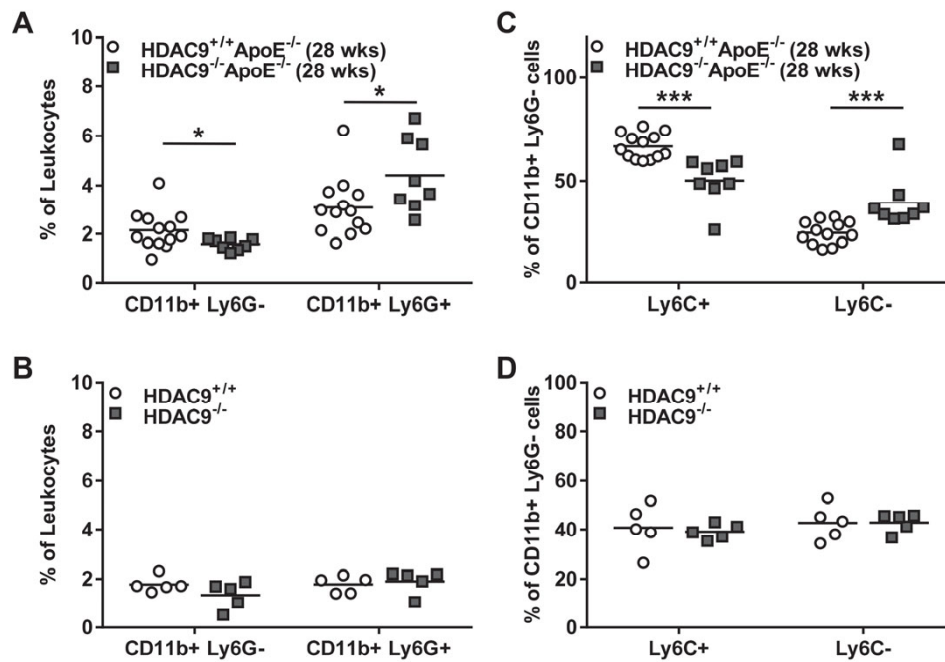
Supplementary Figure S3. HDAC9$^{-/-}$ApoE$^{-/-}$ mice show reduced monocyte numbers and a shift to more Ly6C negative, non-classical, resident monocytes. Flow cytometric analysis of spleens from 28-week-old HDAC9$^{+/+}$ApoE$^{-/-}$ and HDAC9$^{-/-}$ApoE$^{-/-}$ mice and 20-week-old HDAC9$^{+/+}$ and HDAC9$^{-/-}$ mice. **A** and **B**, Frequencies of monocytes/macrophages (CD11b+Ly6G-) and neutrophils (CD11b+Ly6G+) (% of leukocytes). **C** and **D**, Frequencies of Ly6C+ and Ly6C- monocytes/macrophages (% of CD11b+Ly6G- cells). n = 5-13 mice for each genotype per group. *$P<0.05$; ***$P<0.001$.
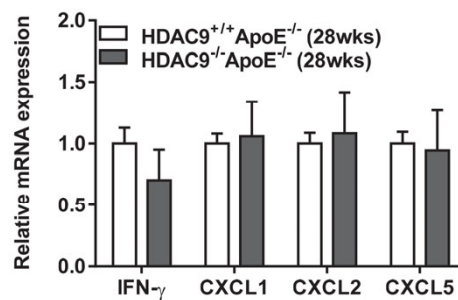
Supplementary Figure S4. HDAC9 deficiency does not influence cytokine and chemokine expression in the spleen. mRNA expression levels of IFN-γ, CXCL1, CXCL2 and CXCL5 were measured in the spleen of 28-week-old HDAC9$^{-/-}$ApoE$^{-/-}$ and HDAC9$^{+/+}$ApoE$^{-/-}$ mice. n = 8-13 mice for each genotype. All graphs represent mean ± SEM.
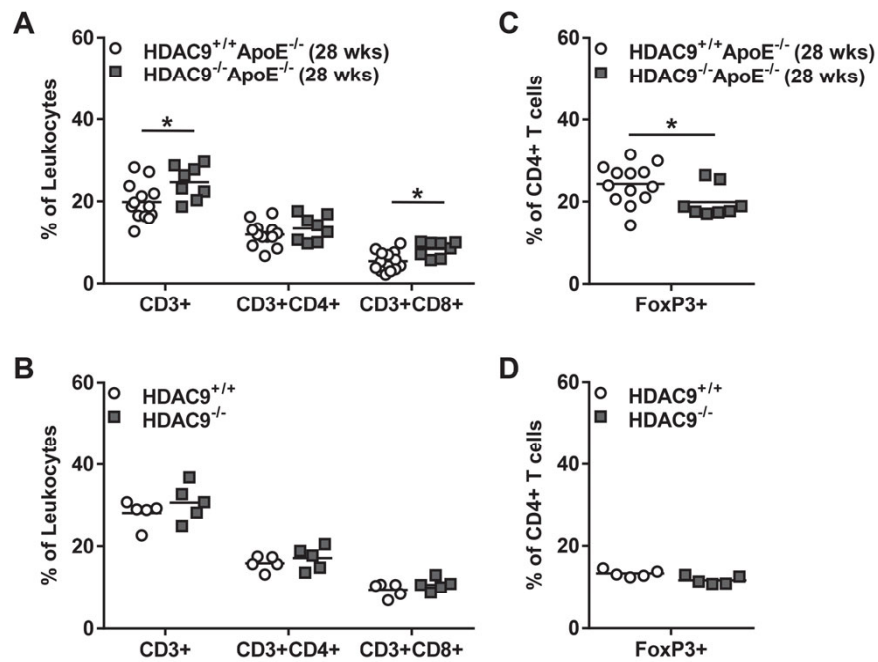
Supplementary Figure S5. HDAC9$^{-/-}$ApoE$^{-/-}$ mice show a modest decrease in regulatory T cells. Flow cytometric analysis of spleens from 28-week-old HDAC9$^{+/+}$ApoE$^{-/-}$ and HDAC9$^{-/-}$ApoE$^{-/-}$ mice and 20-week-old HDAC9$^{+/+}$ and HDAC9$^{-/-}$ mice. **A** and **B**, Frequencies of T cells (CD3+), T helper cells (CD3+CD4+) and cytotoxic T cells (CD3+CD8+) (% of leukocytes). **C** and **D**, Frequencies of CD4+FoxP3+ regulatory T cells. n = 5-13 mice for each genotype per group. *P<0.05.
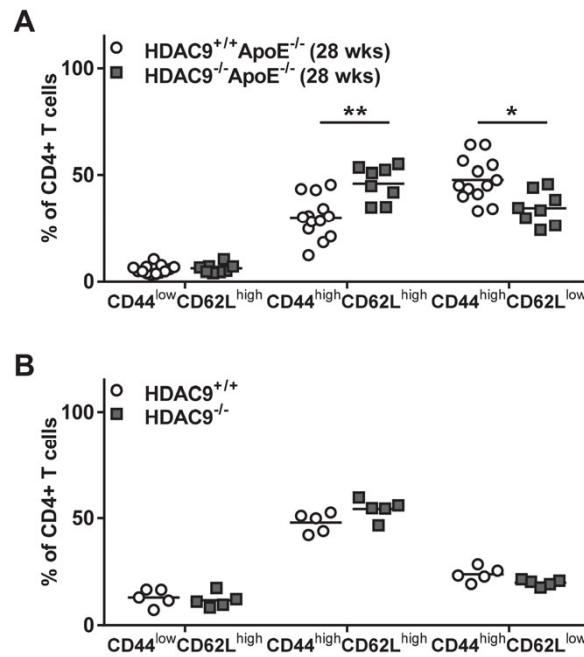
Supplementary Figure S6. HDAC9$^{-/-}$ApoE$^{-/-}$ mice have less effector memory T cells. Flow cytometric analysis of spleens from 28-week-old HDAC9$^{+/+}$ApoE$^{-/-}$ and HDAC9$^{-/-}$ApoE$^{-/-}$ mice and 20-week-old HDAC9$^{+/+}$ and HDAC9$^{-/-}$ mice. **A** and **B**, Frequencies of naïve (CD44^{low}CD62L^{high}), central memory (CD44^{high}CD62L^{high}) and effector memory (CD44^{high}CD62L^{low}) T cells within the CD4+ T cell population. n = 5-13 mice for each genotype per group. *P<0.05; **P<0.01.

6 Manuscript 3

Histone Deacetylase 9 Deficiency Worsens Brain Damage and Neurological Function after Experimental Ischemic Stroke

Sepiede Azghandi, BSc[1]; Dominik Bühler, BSc[1]; Uta Mamrak[1]; Iga Rynarzewska[1]; Manuela Schneider, DVM[1]; Christof Haffner, PhD[1]; Martin Dichgans, MD[1,2]; Nikolaus Plesnila, MD[1,2]

[1] Institute for Stroke and Dementia Research, Klinikum der Universität München, Munich, Germany

[2] Munich Cluster for Systems Neurology (SyNergy), Munich, Germany

Author contributions:

SA designed the studies, performed and analyzed the experiments, and wrote the manuscript. DB and UM performed and analyzed the experiments. IR and MS worked as technical consultants and edited the manuscript. DB and MD contributed to writing of the manuscript. NP and CH designed and supervised the study and edited the manuscript.

This manuscript has been submitted for publication.

Abstract

The histone deacetylase 9 (*HDAC9*) gene region at chromosome 7p21.1 has been identified as a major risk locus for atherosclerotic stroke and HDAC9 deficiency attenuated disease progression in experimental models of atherosclerosis in mice. Since this makes HDAC9 a potential drug target for stroke prevention, we wanted to evaluate the role of HDAC9 in acute ischemic stroke.

HDAC9 mRNA levels significantly increased, almost two-fold, in the ischemic brain 2-3 hours after 60-min of middle cerebral artery occlusion followed by reperfusion.

HDAC9 deficient mice showed significantly larger infarct volumes and increased cell death in peri-ischemic areas 24 hours after stroke. The difference in infarct volume (+40%) persisted until one week after ischemia and was accompanied by worse neurological scores. Blood pressure, arterial blood gases, plasma electrolytes, vascular anatomy, reperfusion, and brain edema formation were not different between HDAC9 deficient mice and their wild-type littermates.

Our results suggest a protective role of HDAC9 in acute ischemic stroke. Therapeutic strategies to reduce atherogenesis and, hence, stroke incidence by inhibition of HDAC9 should therefore account for potential effects in acute ischemic stroke.

Introduction

Genome-wide association studies have identified the histone deacetylase 9 (*HDAC9*) gene region (7p21.1) as the so far strongest risk locus for large vessel stroke.[1,2] Common variants at this locus were further found to be associated with coronary artery disease[3] and common carotid intima-media thickness.[4] We recently showed that the risk allele of rs2107595, the lead single nucleotide polymorphism (SNP) in METASTROKE,[2] is associated with elevated HDAC9 mRNA expression in peripheral blood mononuclear cells.[5] We and others further demonstrated that HDAC9 deficiency is atheroprotective in mouse models for atherosclerosis, making targeted inhibition of HDAC9 a potentially promising strategy for prevention of atheroprogression and, hence, large vessel stroke.[5,6]

HDAC9 belongs to the family of histone deacetylases (HDACs) which removes acetyl groups from lysine residues of histones and other non-histone proteins, thus regulating gene expression. The group of HDACs consists of 18 enzymes which can be classified according to their molecular structure, cofactors, and subcellular localization. HDAC9 is a class IIa HDAC and like all classical HDACs requires Zn^{2+} for its activity.[7,8] Acetylation homeostasis plays an important role in neuronal survival and in neurodegenerative disorders.[9,10] HDAC inhibitors have been shown to exhibit neuroprotective properties in several experimental stroke models.[11-13] Available pan HDAC inhibitors exhibit side-effects and *in vitro* studies have demonstrated potential neuroprotective effects of specific HDAC family members, including HDAC9.[14,15] Hence, there is growing interest in delineating the impact of individual HDACs on neuronal survival. To characterize the role of HDAC9 in acute ischemic stroke *in vivo*, we investigated the expression of HDAC9 in ischemic brain and subjected HDAC9 deficient mice to transient middle cerebral artery occlusion (MCAo).

Materials and Methods

All animal studies were approved by the Ethical Review Board of the Government of Upper Bavaria (protocol number 55.2-1-54-2532-187-13) and were performed in accordance with national and institutional guidelines. Male C57BL/6 (18 to 22 g, Charles River, Sulzfeld, Germany) and male, 6-week-old HDAC9 deficient (HDAC9$^{-/-}$) mice, initially generated by E. Olson[16], and their wild-type littermates were used. All surgeries, quantifications, and

analyses were done in a randomized manner and assessed by blinded investigators. The results are reported according to the ARRIVE guidelines.

Transient Middle Cerebral Artery Occlusion Model

Transient middle cerebral artery occlusion (MCAo) was performed as previously described.[17,18] 30 minutes prior to surgery, analgesia was provided with carprofen (4 mg/kg s.c.). Anesthesia was induced using 4% isoflurane in a gas mixture of 30% oxygen and 70% nitrous oxide and maintained with 1.5% isoflurane during surgery (15-20 minutes). A feedback-controlled heating pad was used to maintain body temperature at 37°C. Regional cerebral blood flow (CBF) in the MCA territory was monitored continuously using a flexible laser Doppler probe (PeriFlux System 5000, Perimed, Järfälla, Sweden) glued onto the exposed left temporal bone. After ligation of the left common and external carotid arteries, a silicone-coated 7-0 monofilament (7019PK5Re, Doccol Corporation, Sharon, MA) was introduced into the internal carotid artery and advanced further to occlude the MCA origin, resulting in a CBF drop below 25% of baseline. After occlusion, the wounds were closed and the animals were allowed to wake up. After 1 hour of MCA occlusion, mice were shortly reanesthetized and the filament was withdrawn. In sham-operated animals, the monofilament was placed into the internal carotid artery without occlusion of the MCA.

Tissue Harvesting for Expression Analyses

Brains from C57BL/6 mice sacrificed 1h, 3h, 6h, or 24h after MCA occlusion were cut in 2 mm thick coronal slices (from Bregma to Bregma -2 mm) using a brain matrix (Zivic Instruments, Pittsburgh, PA). The peri-infarct region, infarct core, contralateral cortex, and contralateral striatum were dissected (Figure 1A), incubated in RNAlater (QIAGEN, Hilden, Germany) at 4°C overnight and then shock-frozen on dry ice.

Real-time PCR

Total RNA was isolated by RNeasy Lipid Tissue Mini Kit (QIAGEN, Hilden, Germany) and cDNA was prepared from 1 µg RNA by the Omniscript RT Kit (QIAGEN, Hilden, Germany). cDNA was diluted 1:20 and added to 200 nM gene specific-primers and Brilliant II SYBR Green QPCR Master Mix (Agilent Technologies, Santa Clara, CA). A total volume of 12 µl (including 2 µl cDNA) was used. Real-time PCR was performed on 384-well plates using the

LightCycler 480 (Roche Diagnostics, Basel, Switzerland). Hypoxanthine-guanine phosphoribosyl-transferase (HPRT) was used as a house-keeping gene. Data were analyzed based on the comparative threshold cycle method with the following formula: Relative mRNA expression level = $2^{-\Delta\Delta C_t}$; $\Delta\Delta C_t = \Delta C_{t, target} - \Delta C_{t, calibrator}$; $\Delta C_t = C_{t, HDAC9} - C_{t, HPRT}$. The corresponding sample from the contralateral hemisphere was used as calibrator. Following primers were designed for Real-time PCR: 5'-CAATACCAGCAGCAGATCCA-3' and 5'-GATTGGTCCCCCTGAAGC-3' (for HDAC9); 5'-GATTAGCGATGATGAACCAGGTT-3' and 5'-CCTCCCATCTCCTTCATGACA-3' (for HPRT).

Infarct Volume Analysis

Infarct analysis was performed as previously described.[18] Briefly, mice were euthanized 24 hours or 7 days after MCAo by cervical dislocation in deep isoflurane anesthesia and brains were removed and shock-frozen on dry ice. 12 coronal cryosections (10 µm) were cut at an interval of 750 µm and then stained with cresyl violet. Infarct and hemisphere areas were measured using a calibrated microscope and AxioVision Software (Zeiss, Jena, Germany) and the infarct volume was calculated and corrected for brain edema using the following formula:

$A_{infarct, corr} = A_{contralateral\ hemisphere} - (A_{ipsilateral\ hemisphere} - A_{infarct})$;

$V_{infarct} = (A_{section1} + ... + A_{section12}) * 750\ \mu m$.

Infarct volumes are expressed as percentages of the volume of the contralateral hemisphere.

Assessment of the Vascular Anatomy in HDAC9$^{-/-}$ mice

Mice were transcardially perfused with saline and 0.5 ml India ink in deep ketamine and xylazine anesthesia. Brains were removed and the MCA territory of both hemispheres and both posterior communicating arteries (PComA) were imaged. The diameter of the PComA was scored as previously described (Score 0-3; 0 = absence of PComA, Score 3 = fully developed PComA).[18,19] The territory of the dorsal brain surface perfused by the MCA was expressed as percentage of the hemisphere surface.

Functional Outcome

A modified, five-point Bederson-test was performed as previously described.[20] Briefly, the scores were the following: 0 = normal neurological behavior; 1 = no circling, but clear asymmetry in forepaw movement, when lifted by the tail; 2 = clear circling to contralateral side, but normal posture at rest; 3 = lying on contralateral side at rest; 4 = no spontaneous movement. Scores of 0.5, 1.5 and 2.5 were assigned when an intermediate phenotype was observed. The tests were done in the evening throughout the observation period of 7 days in parallel with measurements of body weight.

Physiological Monitoring before and after MCAo

Anesthesia was induced with 4% isoflurane and continued by an intraperitoneal injection of fentanyl (0.05 mg/kg), midazolam (5 mg/kg), and medetomidine (0.5 mg/kg). After one hour, anesthesia was maintained by injecting one-third of the initial dose. Mice were oro-tracheally intubated and mechanically ventilated with a mixture of 70% air and 30% oxygen. A catheter was placed in the left carotid artery for measuring mean arterial blood pressure (MAP) continuously and electrolytes and blood gases at the beginning and the end of each experiment. MCA occlusion was performed as described above.

Brain Edema

Brains from HDAC9$^{-/-}$ mice and their wild-type littermates were removed 24 hours after MCAo. After separation of the hemispheres, the wet weight (W) of each hemisphere was measured. Thereafter, the hemispheres were incubated at 110°C in an oven for 24 hours and weighed again to determine the dry weight (D). Water content of each hemisphere was determined with the following formula: ((W-D)/W) * 100%.

TUNEL Staining

Cryosections were stained for cell death using the ApopTag Fluorescein In Situ Apoptosis Detection Kit (Merck Millipore, Darmstadt, Germany). Two brain sections at Bregma -1.5 mm and -3 mm were selected per animal. Two regions of interest (ROI) were analyzed on each section, one at the border of the MCA and ACA territory (ROI1) and one at the piriform cortex (ROI2), a region specifically prone to selective post-ischemic neuronal cell death. A counting window of 0.075 mm^2 was placed at the border of the TUNEL positive

area and only the strong TUNEL positive cells were counted by using global threshold. The quantification was done twice by two independent, blinded investigators. The averaged means of both brain sections are shown.

Statistical Analysis

Statistical analysis was performed using SigmaPlot 12.5 (Systat Software Inc., San Jose, CA). Pairwise comparisons were performed using the Mann-Whitney rank sum test. Differences were considered statistically significant at $P<0.05$. Data are presented as Box-Whisker-Plots indicating the median and the 90th, 75th, 25th, and 10th percentiles or as mean ± SEM.

Results

HDAC9 expression increases after MCAo

HDAC9 mRNA expression was analyzed at different time points after MCAo in the peri-infarct region and the infarct core of C57BL/6 mice. The peri-infarct region and the infarct core were dissected as shown in Figure 1A. Besides 24h sham, two additional control groups were used, 3h sham and naïve brains (without surgery). All control groups demonstrated the same HDAC9 baseline expression (data not shown). HDAC9 mRNA expression was significantly upregulated 1 hour and 3 hours after MCAo both in the peri-infarct region (Figure 1B) and in the infarct core (Figure 1C) (1.4-1.9 fold increase; $P<0.05$ versus 24h sham). HDAC9 expression decreased subsequently and reached 62% in the infarct core at 24 hours after MCAo ($P<0.05$ versus 24h sham; Figure 1C).
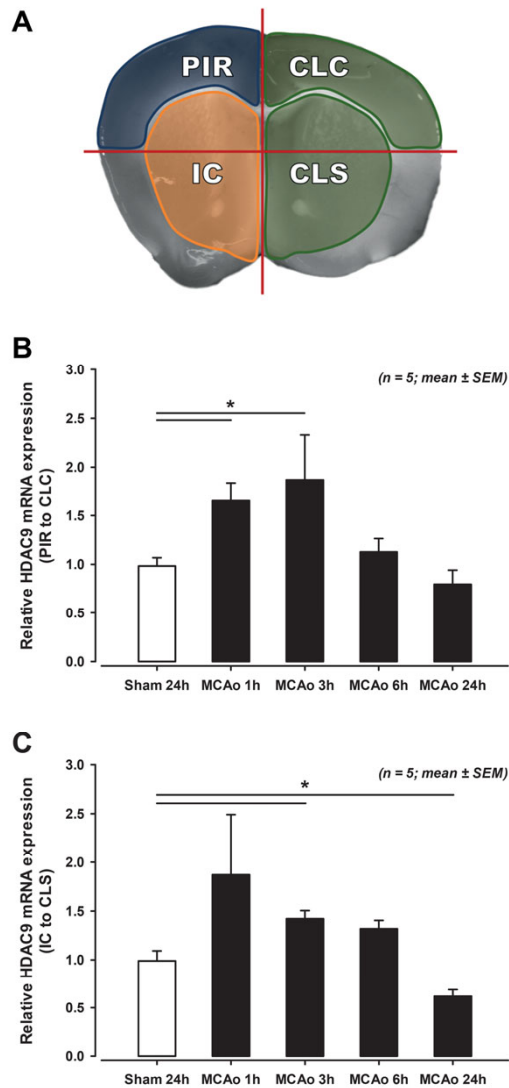
Figure 1. HDAC9 mRNA expression after MCAo in C57BL/6 mice. (**A**) Schematic drawing of how coronal brain sections were dissected for RNA analysis. CLC: contralateral cortex, CLS: contralateral striatum, IC: infarct core, PIR: peri-infarct region. (**B and C**) HDAC9 mRNA expression increased in the PIR and the IC within 1-3 hours after MCAo and decreased thereafter in comparison to the corresponding contralateral brain regions. HDAC9 expression was normalized to HPRT expression. Results represent mean ± SEM. *$P<0.05$.

HDAC9 deficiency increases infarct size 24 hours and 7 days after MCAo

To explore the effect of HDAC9 deficiency in acute ischemic stroke, HDAC9 deficient mice were subjected to 1 hour of MCA occlusion and 23 hours of reperfusion. 24 hours after MCAo, HDAC9 deficient mice showed significantly increased infarct areas at the level of the coronal sections covering the MCA territory (Figure 2A), and their overall infarct volumes were significantly larger as compared to wild-type mice (28% ± 7% and 32% ± 3% of the

contralateral hemisphere for HDAC9$^{+/+}$ and HDAC9$^{-/-}$ mice, respectively; mean ± SD; $P<0.05$; Figure 2B). In an additional group with a 7 days observation period, increased infarct volumes were still present in HDAC9 deficient mice (25% ± 8% and 35% ± 7% of the contralateral hemisphere for HDAC9$^{+/+}$ and HDAC9$^{-/-}$ mice, respectively; mean ± SD; $P<0.05$; Figure 2C and 2D); the difference between both groups was even more pronounced (+40% as compared to +14% at day 1; $P<0.05$; Figure 2D).
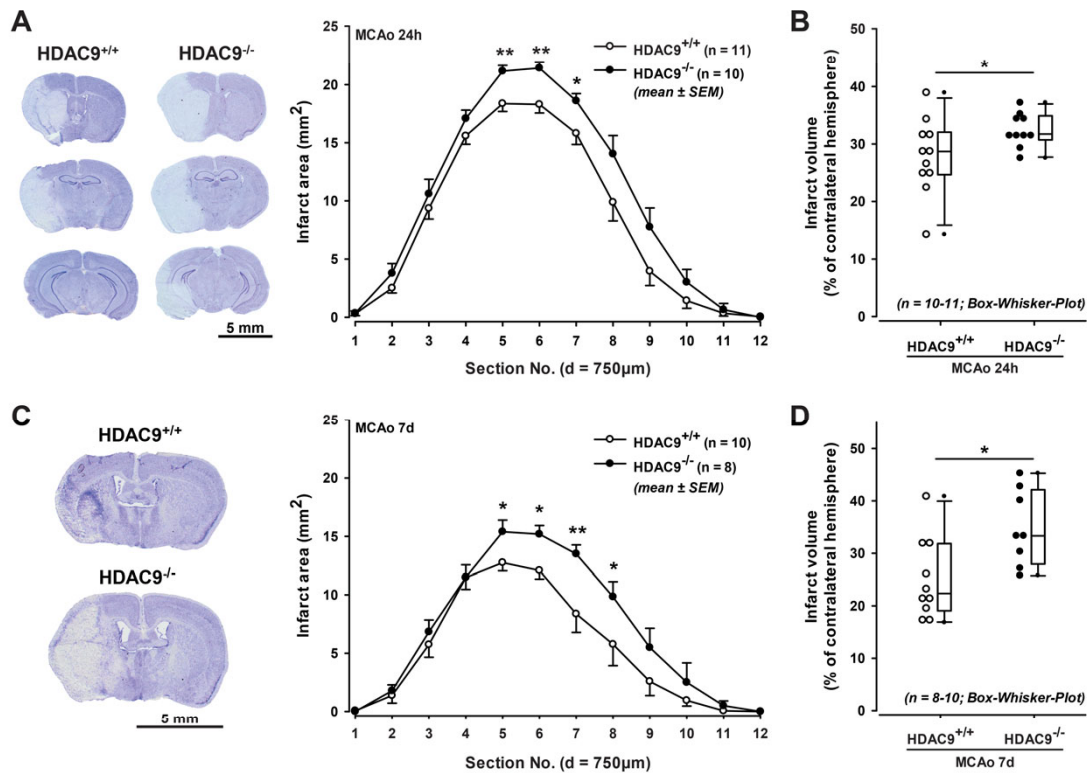
Figure 2. Infarct volume analysis 24 hours and 7 days after MCAo. (**A**) Representative sections from HDAC9$^{+/+}$ and HDAC9$^{-/-}$ mice and infarct area analysis showed larger areas of infarcted brain tissue at the level of the MCA territory on coronal sections 24 hours after MCAo in HDAC9 deficient mice. (**B**) Volumetric calculation of infarct sizes revealed significantly increased infarcts in HDAC9 deficient mice 24 hours after MCAo. (**C and D**) The difference in infarct volume between HDAC9 deficient mice and their wild-type littermates was still present and even more pronounced 7 days after MCAo (+40%). *$P<0.05$, **$P<0.01$.

To exclude that differences in vascular anatomy influence peri-infarct perfusion and, hence, infarct volume, we evaluated the vasculature in HDAC9$^{-/-}$ and HDAC9$^{+/+}$ mice by perfusion with India ink. The MCA territory as well as the degree of collateralization between the

anterior and the posterior vascular territories did not differ between HDAC9 deficient mice and their wild-type littermates (Figure 3).
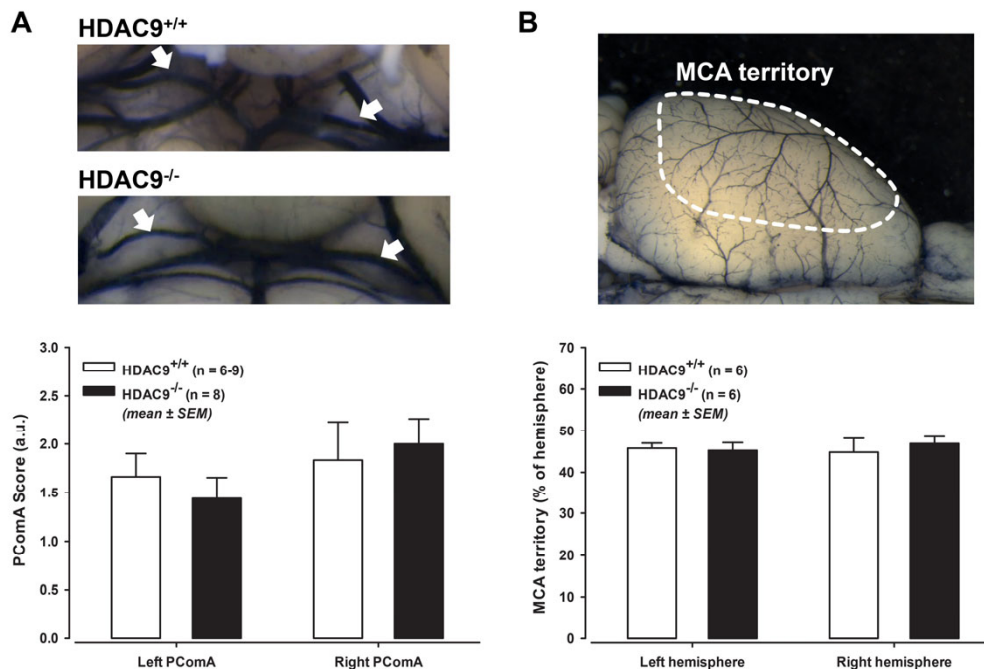
Figure 3. Characterization of vascular anatomy of HDAC9 deficient mice and their wild-type littermates by transcardial India ink perfusion. Evaluation of the diameter of the posterior communicating arteries (PComA) (**A**, arrows) and the brain surface covered by the MCA and its branches (**B**, dashed line) showed no influence of HDAC9 deficiency on vascular anatomy.

HDAC9 deficiency leads to worse outcome during 7 days survival after MCAo

Long-term functional outcome and mortality was analyzed during the 7 days observation period after MCAo. Overall, 5 out of 13 HDAC9^{-/-} mice died in comparison to 4 out of 14 HDAC9^{+/+} mice (Figure 4A; P=0.51). HDAC9^{-/-} mice showed a trend toward increased body weight loss and delayed body weight recovery during the 7 days (P=0.083 and P=0.069 for day 6 and 7; Figure 4B). Motor function was examined prior to filament removal and daily after MCAo (Supplementary Figure S1). No animal reached scores higher than 2.5. No difference in the modified Bederson score was observed at the end of the 1 hour occlusion, indicating that comparable areas of the brain were equally affected by MCAo (Figure 4C). But 24 hours after MCAo, 8 out of 13 HDAC9^{-/-} mice showed severe deficits in comparison to 5 out of 14 HDAC9^{+/+} mice (P=0.089, Figure 4C). 7 days after MCAo this difference was

even more prominent: all HDAC9$^{-/-}$ mice displayed persistent deficits while this was the case in only 4 out of 10 HDAC9$^{+/+}$ animals (*P*<0.01; Figure 4C).
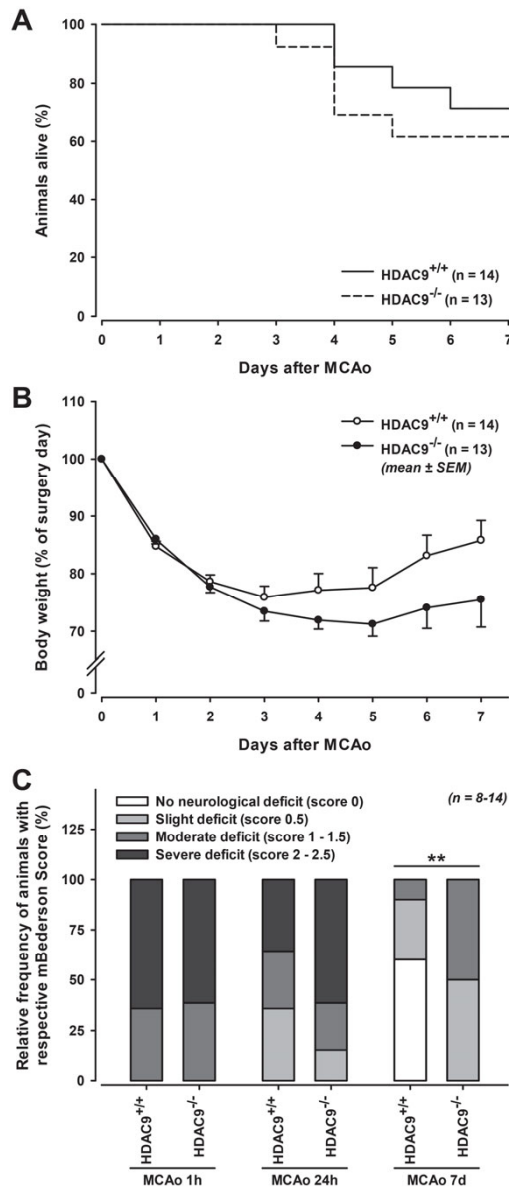
Figure 4. Outcome 7 days after MCAo. (**A**) There was no difference in mortality during the 7 days observation period. (**B**) HDAC9 deficient mice showed a trend toward worse body weight recovery compared to their wild-type littermates. (**C**) HDAC9 deficient mice showed worse functional outcome 24 hours and 7 days after MCAo. **P<0.01.

HDAC9 deficiency has no effect on cerebral blood flow, animal physiology, and brain edema formation

Monitoring of CBF during ischemia and reperfusion revealed no differences between HDAC9$^{-/-}$ and HDAC9$^{+/+}$ mice, neither in the degree of CBF reduction during ischemia nor during reperfusion (Figure 5A). Similarly, there were no differences in blood gases and mean arterial pressure before and after ischemia between groups (Supplementary Table S1). Analysis of brain edema 24 hours after MCAo showed similar brain water contents in the non-affected contralateral hemisphere (78.6% ± 0.3% for HDAC9$^{+/+}$; 78.4% ± 0.4% for HDAC9$^{-/-}$ mice; mean ± SD) and the infarcted ipsilateral hemisphere (81.0% ± 0.8% for HDAC9$^{+/+}$; 81.0% ± 0.7% for HDAC9$^{-/-}$ mice; mean ± SD), demonstrating that increased infarct volumes in HDAC9 deficient mice were not associated with increased edema formation (Figure 5B).
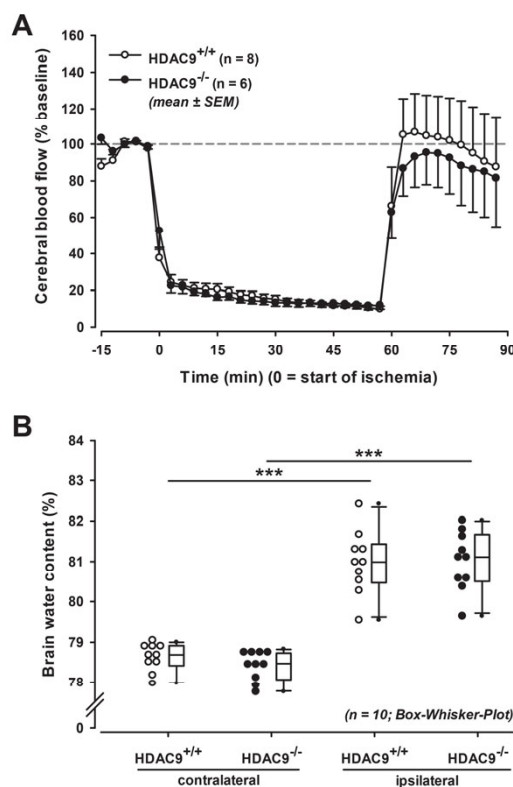
Figure 5. Post-ischemic reperfusion and edema formation. (**A**) Cerebral blood flow during ischemia and reperfusion was unaffected by HDAC9 deficiency. (**B**) Analysis of brain water content 24 hours after MCAo revealed significant edema formation in the ipsilateral hemisphere. However, HDAC9 deficiency had no influence either on basal brain water content or on the formation of ischemic brain edema. ***$P<0.001$.

HDAC9 deficiency increased the number of TUNEL positive cells in the peri-ischemic region

The differences in infarct volume and neurological score between HDAC9$^{-/-}$ and wild-type mice were more pronounced 7 days post MCAo which could be a result of increased cell death in the peri-ischemic region. We analyzed this by quantifying TUNEL positive cells 24 hours after MCAo in two regions of interest, one at the border of the MCA and ACA territory (ROI1) and one at the piriform cortex (ROI2), a region specifically prone to post-ischemic neuronal cell death. We observed significantly increased cell death in the piriform cortex of HDAC9 deficient mice as compared to wild-type littermates (ROI2 in Figure 6A and 6B).
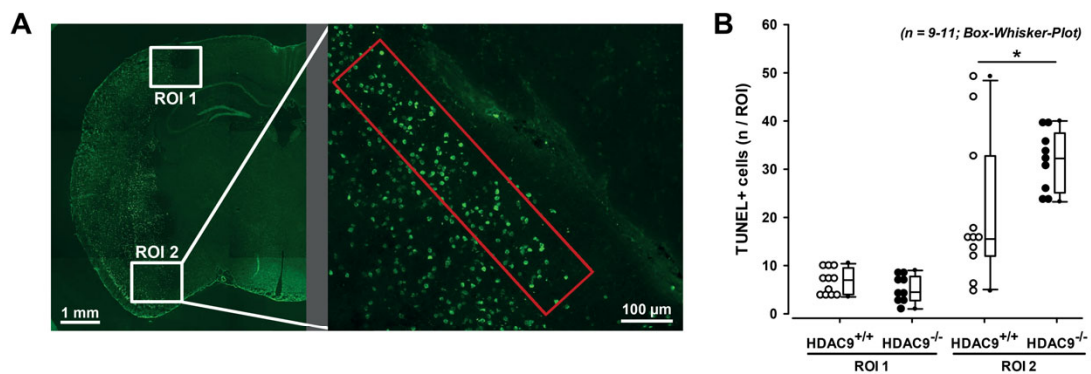
Figure 6. Quantification of the number of cells with DNA damage 24 hours after MCAo by TUNEL staining. (**A**) Representative image demonstrating the two regions of interest (ROI1 and ROI2) at the peri-ischemic region for quantification of TUNEL positive cells. (**B**) HDAC9 deficiency resulted in a significantly higher number of TUNEL positive cells in the piriform cortex (ROI2). *$P<0.05$.

Discussion

The results of the current study suggest that HDAC9 may have a neuroprotective potential after cerebral ischemia. This is demonstrated by larger infarct volumes 24 hours and 7 days after MCAo, a trend toward worse body weight recovery and a worse neurological outcome in HDAC9 deficient mice. Moreover, HDAC9 deficient mice showed increased numbers of TUNEL positive cells in peri-ischemic brain tissue. While the exact mechanisms mediating the neuroprotective effect of HDAC9 remain unclear, we could exclude differences in perfused MCAo territory or collateralization as underlying cause. Similarly, reperfusion,

physiological parameters and brain edema were similar between HDAC9 deficient mice and wild-type littermates.

The observed increase in HDAC9 expression levels in ischemic brain within the first 3 hours after MCAo is in agreement with similar results on ischemic core and penumbra lysates obtained from rats sacrificed 24 hours after transient cerebral ischemia.[21] Further evidence for a potential role of HDAC9 in neuroprotection has been provided by *in vitro* data showing that expression of the histone deacetylase-related protein (HDRP), an isoform of HDAC9 lacking the histone deacetylase domain, is reduced in rat cerebellar granule neurons when undergoing apoptosis induced by low potassium levels.[14] By overexpressing HDRP, cell death could be successfully inhibited.[14] This is well in line with our results of increased infarct volume, worse functional outcome and the elevated number of TUNEL positive cells in HDAC9 deficient mice following cerebral ischemia. One possible interpretation for the increased HDAC9 expression after experimental stroke is that HDAC9 is upregulated in order to counteract cell death signaling.

Several reports describe beneficial effects of pan HDAC inhibitors in animal models of neurodegeneration, such as Huntington disease,[22] amyotrophic lateral sclerosis,[23] spinal muscular atrophy,[24] dementia[25] and stroke.[11-13,26,27] Our current results are not necessarily contradictory to these findings, since inhibiting more than one HDAC isoform might result in pleiotropic effects obscuring the roles of individual HDACs. Moreover, a number of HDAC-associated processes, in particular those dependent on type II HDACs such as HDAC9, have been shown to not require deacetylase activity. It is therefore conceivable that pan HDAC inhibitors only marginally interfere with HDAC9 functions.

We and others recently showed an attenuation of atheroprogression in HDAC9^{-/-} mice.[5,6] These results are in line with recent genome-wide association studies which identified an association of the *HDAC9* gene region with large vessel stroke[1,2] and coronary artery disease,[3] indicating a specific involvement of HDAC9 in atherosclerosis. HDAC9 may therefore represent a promising pharmacological target for the treatment of this disease. Since, however, patients with atherosclerosis are also often affected by ischemic stroke and our results suggest a protective function of HDAC9 after cerebral ischemia, specific caution is required when developing HDAC9 inhibitors for the treatment of atherosclerosis. A possible approach could be to develop HDAC9 inhibitors which do not cross the blood-brain barrier and might thus have no or minimal effects on stroke outcome.

In summary, our current results demonstrate that HDAC9 deficiency increases cell death and worsens long-term outcome following transient cerebral ischemia. This suggests a robust and long-lasting protective role of HDAC9 in the ischemic brain which needs to be carefully considered when exploiting the anti-atherogenic potential of HDAC9 inhibitors.

Acknowledgments

Author Contribution Statement

SA designed the studies, performed and analyzed the experiments, and wrote the manuscript. DB and UM performed and analyzed the experiments. MS and IR worked as technical consultants and edited the manuscript. DB and MD contributed to writing of the manuscript. NP and CH designed and supervised the study and edited the manuscript.

Disclosure/Conflict of Interest

The authors declare no conflict of interest.

References

1. Bellenguez C, Bevan S, Gschwendtner A, Spencer CC, Burgess AI, Pirinen M *et al.* Genome-wide association study identifies a variant in HDAC9 associated with large vessel ischemic stroke. *Nat Genet* 2012; 44**:** 328-333.
2. Traylor M, Farrall M, Holliday EG, Sudlow C, Hopewell JC, Cheng YC *et al.* Genetic risk factors for ischaemic stroke and its subtypes (the METASTROKE collaboration): a meta-analysis of genome-wide association studies. *Lancet Neurol* 2012; 11**:** 951-962.
3. Deloukas P, Kanoni S, Willenborg C, Farrall M, Assimes TL, Thompson JR *et al.* Large-scale association analysis identifies new risk loci for coronary artery disease. *Nat Genet* 2013; 45**:** 25-33.
4. Markus HS, Makela KM, Bevan S, Raitoharju E, Oksala N, Bis JC *et al.* Evidence HDAC9 genetic variant associated with ischemic stroke increases risk via promoting carotid atherosclerosis. *Stroke* 2013; 44**:** 1220-1225.
5. Azghandi S, Prell C, van der Laan SW, Schneider M, Malik R, Berer K *et al.* Deficiency of the Stroke Relevant HDAC9 Gene Attenuates Atherosclerosis in Accord With Allele-Specific Effects at 7p21.1. *Stroke* 2015; 46**:** 197-202.

6. Cao Q, Rong S, Repa JJ, Clair RS, Parks JS, Mishra N. Histone deacetylase 9 represses cholesterol efflux and alternatively activated macrophages in atherosclerosis development. *Arterioscler Thromb Vasc Biol* 2014; 34**:** 1871-1879.

7. Thiagalingam S, Cheng KH, Lee HJ, Mineva N, Thiagalingam A, Ponte JF. Histone deacetylases: unique players in shaping the epigenetic histone code. *Ann N Y Acad Sci* 2003; 983**:** 84-100.

8. Haberland M, Montgomery RL, Olson EN. The many roles of histone deacetylases in development and physiology: implications for disease and therapy. *Nat Rev Genet* 2009; 10**:** 32-42.

9. Rouaux C, Jokic N, Mbebi C, Boutillier S, Loeffler JP, Boutillier AL. Critical loss of CBP/p300 histone acetylase activity by caspase-6 during neurodegeneration. *EMBO J* 2003; 22**:** 6537-6549.

10. Saha RN, Pahan K. HATs and HDACs in neurodegeneration: a tale of disconcerted acetylation homeostasis. *Cell Death Differ* 2006; 13**:** 539-550.

11. Faraco G, Pancani T, Formentini L, Mascagni P, Fossati G, Leoni F *et al.* Pharmacological inhibition of histone deacetylases by suberoylanilide hydroxamic acid specifically alters gene expression and reduces ischemic injury in the mouse brain. *Mol Pharmacol* 2006; 70**:** 1876-1884.

12. Kim HJ, Rowe M, Ren M, Hong JS, Chen PS, Chuang DM. Histone deacetylase inhibitors exhibit anti-inflammatory and neuroprotective effects in a rat permanent ischemic model of stroke: multiple mechanisms of action. *J Pharmacol Exp Ther* 2007; 321**:** 892-901.

13. Ren M, Leng Y, Jeong M, Leeds PR, Chuang DM. Valproic acid reduces brain damage induced by transient focal cerebral ischemia in rats: potential roles of histone deacetylase inhibition and heat shock protein induction. *J Neurochem* 2004; 89**:** 1358-1367.

14. Morrison BE, Majdzadeh N, Zhang X, Lyles A, Bassel-Duby R, Olson EN *et al.* Neuroprotection by histone deacetylase-related protein. *Mol Cell Biol* 2006; 26**:** 3550-3564.

15. Ma C, D'Mello SR. Neuroprotection by histone deacetylase-7 (HDAC7) occurs by inhibition of c-jun expression through a deacetylase-independent mechanism. *J Biol Chem* 2011; 286**:** 4819-4828.

16. Zhang CL, McKinsey TA, Chang S, Antos CL, Hill JA, Olson EN. Class II histone deacetylases act as signal-responsive repressors of cardiac hypertrophy. *Cell* 2002; 110**:** 479-488.

17. Plesnila N, Zhu C, Culmsee C, Groger M, Moskowitz MA, Blomgren K. Nuclear translocation of apoptosis-inducing factor after focal cerebral ischemia. *J Cereb Blood Flow Metab* 2004; 24**:** 458-466.

18. Groger M, Lebesgue D, Pruneau D, Relton J, Kim SW, Nussberger J *et al.* Release of bradykinin and expression of kinin B2 receptors in the brain: role for cell death and brain edema formation after focal cerebral ischemia in mice. *J Cereb Blood Flow Metab* 2005; 25**:** 978-989.

19. Murakami K, Kondo T, Kawase M, Chan PH. The development of a new mouse model of global ischemia: focus on the relationships between ischemia duration, anesthesia, cerebral vasculature, and neuronal injury following global ischemia in mice. *Brain Res* 1998; 780**:** 304-310.

20. Plesnila N, Zinkel S, Le DA, Amin-Hanjani S, Wu Y, Qiu J *et al.* BID mediates neuronal cell death after oxygen/ glucose deprivation and focal cerebral ischemia. *Proc Natl Acad Sci U S A* 2001; 98**:** 15318-15323.

21. He M, Zhang B, Wei X, Wang Z, Fan B, Du P *et al.* HDAC4/5-HMGB1 signalling mediated by NADPH oxidase activity contributes to cerebral ischaemia/reperfusion injury. *J Cell Mol Med* 2013; 17**:** 531-542.

22. Ferrante RJ, Kubilus JK, Lee J, Ryu H, Beesen A, Zucker B *et al.* Histone deacetylase inhibition by sodium butyrate chemotherapy ameliorates the neurodegenerative phenotype in Huntington's disease mice. *J Neurosci* 2003; 23**:** 9418-9427.

23. Petri S, Kiaei M, Kipiani K, Chen J, Calingasan NY, Crow JP *et al.* Additive neuroprotective effects of a histone deacetylase inhibitor and a catalytic antioxidant in a transgenic mouse model of amyotrophic lateral sclerosis. *Neurobiol Dis* 2006; 22**:** 40-49.

24. Avila AM, Burnett BG, Taye AA, Gabanella F, Knight MA, Hartenstein P *et al.* Trichostatin A increases SMN expression and survival in a mouse model of spinal muscular atrophy. *J Clin Invest* 2007; 117**:** 659-671.
25. Fischer A, Sananbenesi F, Wang X, Dobbin M, Tsai LH. Recovery of learning and memory is associated with chromatin remodelling. *Nature* 2007; 447**:** 178-182.
26. Yildirim F, Gertz K, Kronenberg G, Harms C, Fink KB, Meisel A *et al.* Inhibition of histone deacetylation protects wildtype but not gelsolin-deficient mice from ischemic brain injury. *Exp Neurol* 2008; 210**:** 531-542.
27. Wang Z, Tsai LK, Munasinghe J, Leng Y, Fessler EB, Chibane F *et al.* Chronic valproate treatment enhances postischemic angiogenesis and promotes functional recovery in a rat model of ischemic stroke. *Stroke* 2012; 43**:** 2430-2436.

Supplementary Information

Supplementary Figure S1
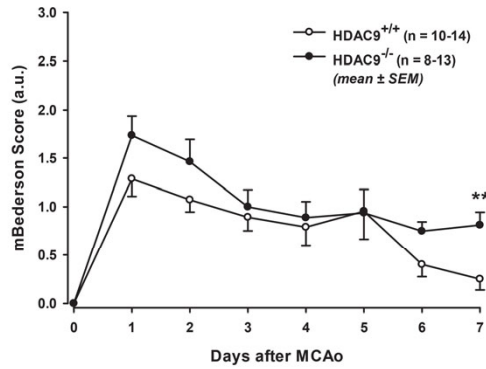
Figure S1. Daily neurological examinations resulted in a trend toward worse motor function in HDAC9 deficient mice which reached significance 7 days after MCAo. **$P<0.01$.

Supplementary Table S1. Physiological values

	before ischemia			after ischemia		
	HDAC9$^{+/+}$	HDAC9$^{-/-}$	*P* value	HDAC9$^{+/+}$	HDAC9$^{-/-}$	*P* value
MAP (mmHg)	124 ± 21	123 ± 16	n.s.	86 ± 21	90 ± 25	n.s.
pH	7.35 ± 0.06	7.36 ± 0.08	n.s.	7.29 ± 0.09	7.33 ± 0.02	n.s.
pCO$_2$ (mmHg)	39.7 ± 5.9	36.4 ± 2.8	n.s.	35.7 ± 2.5	37.5 ± 3.3	n.s.
pO$_2$ (mmHg)	120.7 ± 29.4	166.6 ± 21.7	< 0.01	131.3 ± 15.6	140.6 ± 14.7	n.s.
Na$^+$ (mmol/L)	140 ± 5	139 ± 5	n.s.	144 ± 4	144 ± 5	n.s.
K$^+$ (mmol/L)	4.88 ± 0.75	4.71 ± 0.84	n.s.	6.14 ± 1.90	5.95 ± 1.34	n.s.
Ca^{++} (mmol/L)	1.12 ± 0.08	1.11 ± 0.07	n.s.	1.10 ± 0.18	1.14 ± 0.08	n.s.
HCT (%)	43 ± 5	43 ± 6	n.s.	51 ± 8	49 ± 7	n.s.
O$_2$ Sat (%)	97.6 ± 1.3	98.3 ± 1.3	n.s.	97.3 ± 2.5	97.7 ± 1.4	n.s.

mean ± SD, HDAC9$^{+/+}$: n = 7-8, HDAC9$^{-/-}$: n = 5-6, MAP: mean arterial pressure, Mann-Whitney U test, n.s.: not significant

7 Discussion

The *HDAC9* gene locus at chromosome 7p21.1 was recently identified as a risk locus for LVS (Bellenguez et al., 2012; Traylor et al., 2012). The 7p21.1 locus shows only association with LVS and not with the other two subtypes of ischemic stroke, cardioembolism or small vessel disease. Additionally, this locus has also been associated with CAD and carotid intima-media thickness (Deloukas et al., 2013; Markus et al., 2013). HDAC inhibitors have already demonstrated neuroprotective and anti-inflammatory properties in several studies, making HDAC9 an interesting target for stroke research. In the first part of this thesis the role of HDAC9 deficiency was analyzed in a mouse model for atherosclerosis, which is the underlying pathology of LVS and CAD. In the second part, HDAC9 deficient mice were subjected to acute ischemic stroke and the functional as well as the histological outcome was investigated.

HDAC9 deficiency is atheroprotective

In the first part of this thesis, we got further insights into the biological role of HDAC9 in atherosclerosis. Our results suggest that HDAC9 inhibition is a promising therapeutic strategy for prevention of atherosclerosis.

The hypothesis of an atheroprotective effect of HDAC9 deficiency was based on data from my colleague Caroline Prell-Schicker, who demonstrated that HDAC9 mRNA levels were significantly increased in homozygous and heterozygous risk allele carriers of the METASTROKE lead SNP rs2107595 (Azghandi et al., 2015). The two other neighboring genes in the 7p21.1 region, *TWIST1* and *FERD3L*, did not show any correlations of mRNA levels with allele carrier status, making *HDAC9* the most promising candidate gene within this region. The increased HDAC9 mRNA levels in risk allele carriers led to the hypothesis that HDAC9 deficiency/inhibition should be protective. We confirmed this hypothesis, demonstrating protective effects of HDAC9 deficiency in a mouse atherosclerosis model, ApoE$^{-/-}$ mice, which were presented in manuscripts 1 and 2.

HDAC9$^{-/-}$ApoE$^{-/-}$ mice had significantly reduced atherosclerosis throughout the aorta at two time points (Azghandi et al., 2015). However, a third group of mice, which was fed a high-cholesterol Western-type diet, showed no difference in plaque size between HDAC9$^{-/-}$ApoE$^{-/-}$ and HDAC9$^{+/+}$ApoE$^{-/-}$ mice. These data demonstrate the importance to study different diets and time points in experimental atherosclerosis models. Our Western-type

diet data help to understand which stage of atherosclerosis is affected by HDAC9 deficiency. We conclude that HDAC9 is mainly important in early atherogenesis. This conclusion is based on the observation that (1) HDAC9 deficient mice on chow diet had more initial lesions than wild-type littermates, (2) the degree of plaque size reduction got smaller with increased age (18-week-old vs 28-week-old mice) and (3) in Western-type diet fed mice with more advanced plaques differences in plaque size between HDAC9$^{+/+}$ApoE$^{-/-}$ and HDAC9$^{-/-}$ApoE$^{-/-}$ mice could no longer be detected. The atheroprotective effect of HDAC9 deficiency was also demonstrated by another group in a second atherosclerosis model, LDLR$^{-/-}$ mice (Cao et al., 2014), showing that the phenotype is very robust, reproducible and independent of the atherosclerosis model. LDLR$^{-/-}$ mice have to be fed a high-cholesterol diet to develop atherosclerotic lesions in contrast to ApoE deficient mice which develop atherosclerotic lesions spontaneously on a chow diet. Another difference between the two mouse models is that for bone marrow transplantation into ApoE deficient mice, the donor bone marrow has to be ApoE deficient in contrast to donors for LDLR$^{-/-}$ mice where the bone marrow can have an LDLR wild-type genotype (Linton et al., 1995; Herijgers et al., 1997). This shows that these two models differ in the mechanism inducing atherosclerosis, but the reproducible effect of HDAC9 deficiency in both models makes HDAC9 inhibition a very promising strategy for humans.

HDAC9 deficiency influences monocyte/macrophage dynamics

HDACs are known to play an important role in inflammation and immunity (Shakespear et al., 2011). Several studies have shown an involvement of HDACs in innate immunity. Classical HDACs influence macrophage and dendritic cell function by targeting Toll-like receptor and IFN-γ signaling (Shakespear et al., 2011). Recent studies showed that HDACs such as HDAC3 and HDAC7 regulate inflammatory gene expression in macrophages (Chen et al., 2012; Shakespear et al., 2013). Macrophages contribute to the different stages of atherosclerosis by inducing inflammatory processes, forming foam cells and eventually the necrotic core of an advanced plaque (Moore et al., 2013). Macrophages can be grouped in M1 and M2 macrophages. Classically activated macrophages of the M1 type are pro-inflammatory and regarded as pro-atherogenic while M2 macrophages are characterized by anti-inflammatory cytokine profiles and are associated with wound healing and atherosclerosis regression (Moore et al., 2013).

Cao et al. observed in LDLR^{-/-} mice that HDAC9 deficient macrophages exhibited an upregulated expression of cholesterol efflux genes such as ABCA1 and ABCG1, expressed less pro-inflammatory cytokines after LPS stimulation, and demonstrated an M2-like phenotype *in vitro* (Cao et al., 2014). In ApoE deficient mice, we could show that HDAC9 deficiency leads to a Ly6C shift in monocytes/macrophages, meaning HDAC9^{-/-}ApoE^{-/-} mice had less inflammatory Ly6C+ and more resident, patrolling Ly6C- monocytes (see manuscript 2). It is known that hypercholesterolemic ApoE^{-/-} mice have an expansion of circulating monocytes, mainly due to an increase in Ly6C+ monocytes (Swirski et al., 2007). Monocytosis in atherosclerotic mice results from increased survival, continued proliferation and lower conversion rates from Ly6C+ to Ly6C- monocytes (Swirski et al., 2007). Besides a Ly6C shift to more Ly6C- monocytes, we observed a reduced monocyte frequency in HDAC9^{-/-}ApoE^{-/-} mice in comparison to HDAC9^{+/+}ApoE^{-/-} mice.

Additional analysis of survival, proliferation and conversion rates of HDAC9 deficient Ly6C+ monocytes could give further insights into the involvement of monocytes in the atheroprotective mechanism of HDAC9 deficiency. In our group, we are currently assessing migration and cytokine expression of macrophages exposed to different pro-inflammatory stimuli to understand how monocytes/macrophages contribute to the observed phenotype in HDAC9^{-/-}ApoE^{-/-} mice.

HDAC9 deficiency affects memory T cell distribution

Besides monocytes/macrophages, we also analyzed T cell distribution in HDAC9^{-/-}ApoE^{-/-} mice on chow and on Western-type diet using flow cytometry. We did not detect any differences in T cell frequency or in the relative amount of CD4+ and CD8+ subpopulations. HDAC9 has already been known as an important regulator of the function of regulatory T cells (Tao et al., 2007). Tao et al. showed an increase in Tregs by 50% in HDAC9 deficient mice. In contrast, we did not see any differences in frequency of Tregs in HDAC9 deficient mice without ApoE deficiency (see manuscript 2). This is probably due to different wild-type controls that were used in the studies. We always used wild-type littermates as controls in order to exclude background differences. It is not clear whether Tao et al. used normal C57BL/6 mice or littermates as controls. Furthermore, only a low number of spleens were analyzed in their study (n = 4). In our HDAC9^{-/-}ApoE^{-/-} mice, we measured a modest decrease in Treg frequencies, in chow and Western-type diet fed mice. We do not believe,

however, that this decrease has a physiological importance or that it means that HDAC9 is not important for Tregs. Tao et al. could show that Tregs have higher HDAC9 mRNA levels than effector T cells, that Treg stimulation induces nuclear export of HDAC9, and HDAC9 deficient Tregs were three- to fourfold more suppressive than controls and had increased FoxP3 acetylation (Tao et al., 2007). Therefore additional experiments are necessary to delineate the function of Tregs in HDAC9$^{-/-}$ApoE$^{-/-}$ mice.

Moreover, our FACS data revealed a very interesting difference in another T cell population, the effector memory T cells. HDAC9$^{-/-}$ApoE$^{-/-}$ mice on chow diet had significant less effector memory T cells within the CD4+ population (see manuscript 2). The decreased effector memory T cells indicate decreased activation and mobilization of T cells in HDAC9 deficient mice, which fits with the reduced atherosclerotic plaque size in chow fed HDAC9$^{-/-}$ApoE$^{-/-}$ mice. A recent study demonstrated a correlation of CD4+ effector memory T cells with the extent of atherosclerosis in animals and carotid intima-media thickness as well as coronary artery disease in humans (Ammirati et al., 2012), suggesting that effector memory T cells may represent an important immune cell population in atherogenesis.

Our data from monocytes/macrophages and T cells in HDAC9$^{-/-}$ApoE$^{-/-}$ mice show that both innate and adaptive immunity might play an important role in the atheroprotective effect mediated by HDAC9 deficiency.

HDAC9 deficiency worsens ischemic stroke outcome

All identified loci in the METASTROKE data set showed only association with one ischemic stroke subtype, emphasizing the importance of distinguishing the different stroke subtypes from each other (Traylor et al., 2012). The *HDAC9* gene region showed exclusive association with large vessel stroke, where the underlying pathology is atherosclerosis. This is why we analyzed the effects of HDAC9 deficiency in a mouse atherosclerosis model. However, several studies have already demonstrated beneficial effects of HDAC inhibitors in models for stroke and neurodegenerative diseases (Kazantsev and Thompson, 2008; Shein and Shohami, 2011). In the second part of this thesis, the role of HDAC9 in ischemic stroke outcome was analyzed by using the MCAo model in HDAC9 deficient mice (see manuscript 3). Surprisingly, HDAC9 deficient mice demonstrated larger infarct volumes 24 hours and 7 days after ischemic stroke. The increase in infarct volume was also reflected in worse neurological scores. We checked blood pressure, blood gases and vascular anatomy

(MCA territory as well as the degree of collateralization between the anterior and posterior cerebral circulation) and did not detect any differences. Also brain edema formation and reperfusion were not affected by HDAC9 deficiency. The detailed mechanism of increased infarct volume and worse functional outcome is still unclear but we hypothesize that the worse outcome is based on increased cell death due to our finding of elevated numbers of TUNEL positive cells in peri-ischemic areas of HDAC9 deficient mice. Moreover, another study already demonstrated that an HDAC9 isoform, lacking the deacetylase domain, is important for neuronal survival *in vitro* (Morrison et al., 2006). We also detected increased levels of HDAC9 in peri-infarct regions of wild-type mice in the first hours after stroke, indicating that cells may upregulate HDAC9 to counteract cell death signaling.

Since the promising atheroprotective results of HDAC9 deficiency make HDAC9 a potential drug target to prevent atherosclerosis, development of HDAC9 inhibitors should consider negative effects of these inhibitors in the brain. The potential patient target group for HDAC9 inhibitors are people at risk for atherosclerosis who are also at risk for stroke. Therefore it is important to understand in more detail the effect of such inhibitors on the brain.

HDAC9 belongs to the class IIa HDACs for which the exact mechanism of repression has not been fully discovered. Class IIa HDACs have a minimal catalytic activity and therefore regulate transcription by interacting with other multiprotein complexes containing class I HDACs, like HDAC3 (Fischle et al., 2002; Lahm et al., 2007). HDAC9 has several isoforms including some without a deacetylase domain, demonstrating that catalytic activity is not necessary for its function (Petrie et al., 2003). This could also explain why pan HDAC inhibitors are neuroprotective while HDAC9 deficiency worsens neuronal cell death. The catalytic activity of HDAC9 may not be important for its function in neuronal survival. Therefore it is of utmost importance to understand the molecular mechanism underlying the atheroprotective effect of HDAC9 deficiency in comparison with the neuroprotective effect of HDAC9.

Outlook

Since the results of this thesis make HDAC9 a potential drug target for atherosclerosis and stroke prevention, the exact mechanisms underlying its effects have to be discovered. On the one hand, responsible cell types for the atheroprotective effect of HDAC9 deficiency have to be identified. The data reported in this thesis suggest that a combined effect of several cell types is responsible for the reduced atherosclerosis phenotype in HDAC9$^{-/-}$ApoE$^{-/-}$ mice. In our group several *in vitro* approaches are under investigation to test different cell types, including macrophages, T cells but also smooth muscle and endothelial cells. My colleague Yaw Asare has already obtained promising results, showing that also smooth muscle cells and endothelial cells express less atherogenic molecules after HDAC9 knockdown in combination with inflammatory stimulation. Besides the cell type, the underlying pathway by which inhibition of HDAC9 influences inflammatory signaling has to be elucidated. These experiments can be done in animal models but the results have to be transferred to humans. Immune cells seem like a promising target considering the HDAC9 expression data in human PBMCs and my own data showing that monocytes and effector memory T cells are candidate cells for HDAC9 inhibition. My colleague Caroline Prell-Schicker has already investigated FoxP3 and HDAC9 expression in Tregs isolated from risk allele carriers of the rs2107595 lead SNP. However, she did not detect any differences in expression. Based on the results of this thesis, we now plan to investigate other immune cell types in risk allele carriers of rs2107595, such as monocytes and CD4+ effector T cells. Another interesting question, which our group is addressing, is how variants at this locus regulate HDAC9 expression. For another locus, the 1p13 locus, which was found to be associated with myocardial infarction and plasma low-density lipoprotein cholesterol by GWAS, Musunuru et al. could show how noncoding variants can lead to a clinical phenotype. The risk allele creates a new transcription binding site for C/EBP transcription factors which leads to increased liver-specific expression of the transporter protein Sortilin (Musunuru et al., 2010). Our lead SNP rs2107595 is located in a DNase I hypersensitivity cluster and histone modification hotspot, indicating a regulatory function (Azghandi et al., 2015). Indeed, the TRANSFAC database (Wingender et al., 2000) predicts that the risk allele of rs2107595 disrupts a binding site for the E2F3 transcription factor. This is a new project under investigation in our group.

Conclusion

In summary, the results of this thesis give insights into the beneficial effect of HDAC9 deficiency in atherosclerosis. We provide further evidence that *HDAC9* is the disease-relevant gene at the 7p21.1 locus associated with LVS and CAD, demonstrating how GWAS can identify new target genes for complex diseases. We could show that HDAC9 deficiency reduces early atherogenesis and propose an immune-cell mediated mechanism by both innate and adaptive immunity. HDAC9 deficiency has an effect on monocyte/macrophage dynamics as well as on effector memory T cells. Our results suggest that pharmacological inhibition of HDAC9 might be a promising therapeutic strategy for the prevention of atherosclerosis and LVS. Additional experiments are necessary to discover the mechanism by which variants at this locus regulate HDAC9 expression and how HDAC9 influences inflammatory signaling in the identified immune cell types.

In addition to atherosclerosis, we also investigated ischemic stroke outcome in HDAC9 deficient mice. HDAC9 deficiency seems to aggravate infarct volume and neurological outcome after acute ischemic stroke, indicating that HDAC9 has a neuroprotective function in the brain. Therefore the data presented in this thesis strongly suggest that potential negative effects of HDAC9 inhibitors on the brain have to be considered in the development of respective compounds.

8 References

Adams HP, Jr., Bendixen BH, Kappelle LJ, Biller J, Love BB, Gordon DL, Marsh EE, 3rd (1993). Classification of subtype of acute ischemic stroke. Definitions for use in a multicenter clinical trial. TOAST. Trial of Org 10172 in Acute Stroke Treatment. *Stroke.* 24(1): 35-41.

Ait-Oufella H, Sage AP, Mallat Z, Tedgui A (2014). Adaptive (T and B cells) immunity and control by dendritic cells in atherosclerosis. *Circ Res.* 114(10): 1640-1660.

Ait-Oufella H, Salomon BL, Potteaux S, Robertson AK, Gourdy P, Zoll J, Merval R, Esposito B, Cohen JL, Fisson S, Flavell RA, Hansson GK, Klatzmann D, Tedgui A, Mallat Z (2006). Natural regulatory T cells control the development of atherosclerosis in mice. *Nat Med.* 12(2): 178-180.

Akimova T, Ge G, Golovina T, Mikheeva T, Wang L, Riley JL, Hancock WW (2010). Histone/protein deacetylase inhibitors increase suppressive functions of human FOXP3+ Tregs. *Clin Immunol.* 136(3): 348-363.

Allfrey VG, Faulkner R, Mirsky AE (1964). Acetylation and Methylation of Histones and Their Possible Role in the Regulation of Rna Synthesis. *Proc Natl Acad Sci U S A.* 51: 786-794.

Ammirati E, Cianflone D, Vecchio V, Banfi M, Vermi AC, De Metrio M, Grigore L, Pellegatta F, Pirillo A, Garlaschelli K, Manfredi AA, Catapano AL, Maseri A, Palini AG, Norata GD (2012). Effector Memory T cells Are Associated With Atherosclerosis in Humans and Animal Models. *J Am Heart Assoc.* 1(1): 27-41.

Auffray C, Fogg D, Garfa M, Elain G, Join-Lambert O, Kayal S, Sarnacki S, Cumano A, Lauvau G, Geissmann F (2007). Monitoring of blood vessels and tissues by a population of monocytes with patrolling behavior. *Science.* 317(5838): 666-670.

Azghandi S, Prell C, van der Laan SW, Schneider M, Malik R, Berer K, Gerdes N, Pasterkamp G, Weber C, Haffner C, Dichgans M (2015). Deficiency of the Stroke Relevant HDAC9 Gene Attenuates Atherosclerosis in Accord With Allele-Specific Effects at 7p21.1. *Stroke.* 46(1): 197-202.

Bellenguez C, Bevan S, Gschwendtner A, Spencer CC, Burgess AI, Pirinen M, Jackson CA, Traylor M, Strange A, Su Z, Band G, Syme PD, Malik R, Pera J, Norrving B, et al. (2012). Genome-wide association study identifies a variant in HDAC9 associated with large vessel ischemic stroke. *Nat Genet.* 44(3): 328-333.

Bevan S, Traylor M, Adib-Samii P, Malik R, Paul NL, Jackson C, Farrall M, Rothwell PM, Sudlow C, Dichgans M, Markus HS (2012). Genetic heritability of ischemic stroke and the contribution of previously reported candidate gene and genomewide associations. *Stroke.* 43(12): 3161-3167.

Boring L, Gosling J, Cleary M, Charo IF (1998). Decreased lesion formation in CCR2-/- mice reveals a role for chemokines in the initiation of atherosclerosis. *Nature.* 394(6696): 894-897.

Brass LM, Isaacsohn JL, Merikangas KR, Robinette CD (1992). A study of twins and stroke. *Stroke.* 23(2): 221-223.

Cao Q, Rong S, Repa JJ, Clair RS, Parks JS, Mishra N (2014). Histone deacetylase 9 represses cholesterol efflux and alternatively activated macrophages in atherosclerosis development. *Arterioscler Thromb Vasc Biol.* 34(9): 1871-1879.

Chang S, McKinsey TA, Zhang CL, Richardson JA, Hill JA, Olson EN (2004). Histone deacetylases 5 and 9 govern responsiveness of the heart to a subset of stress signals and play redundant roles in heart development. *Mol Cell Biol.* 24(19): 8467-8476.

Chen X, Barozzi I, Termanini A, Prosperini E, Recchiuti A, Dalli J, Mietton F, Matteoli G, Hiebert S, Natoli G (2012). Requirement for the histone deacetylase Hdac3 for the inflammatory gene expression program in macrophages. *Proc Natl Acad Sci U S A.* 109(42): E2865-2874.

Cybulsky MI, Gimbrone MA, Jr. (1991). Endothelial expression of a mononuclear leukocyte adhesion molecule during atherogenesis. *Science.* 251(4995): 788-791.

Cybulsky MI, Iiyama K, Li H, Zhu S, Chen M, Iiyama M, Davis V, Gutierrez-Ramos JC, Connelly PW, Milstone DS (2001). A major role for VCAM-1, but not ICAM-1, in early atherosclerosis. *J Clin Invest.* 107(10): 1255-1262.

Dansky HM, Charlton SA, Harper MM, Smith JD (1997). T and B lymphocytes play a minor role in atherosclerotic plaque formation in the apolipoprotein E-deficient mouse. *Proc Natl Acad Sci U S A.* 94(9): 4642-4646.

de Zoeten EF, Wang L, Sai H, Dillmann WH, Hancock WW (2010). Inhibition of HDAC9 increases T regulatory cell function and prevents colitis in mice. *Gastroenterology.* 138(2): 583-594.

Deloukas P, Kanoni S, Willenborg C, Farrall M, Assimes TL, Thompson JR, Ingelsson E, Saleheen D, Erdmann J, Goldstein BA, Stirrups K, Konig IR, Cazier JB, Johansson A, Hall AS, et al. (2013). Large-scale association analysis identifies new risk loci for coronary artery disease. *Nat Genet.* 45(1): 25-33.

Dichgans M, Malik R, Konig IR, Rosand J, Clarke R, Gretarsdottir S, Thorleifsson G, Mitchell BD, Assimes TL, Levi C, O'Donnell CJ, Fornage M, Thorsteinsdottir U, Psaty BM, Hengstenberg C, et al. (2014). Shared genetic susceptibility to ischemic stroke and coronary artery disease: a genome-wide analysis of common variants. *Stroke.* 45(1): 24-36.

Dichgans M, Markus HS (2005). Genetic association studies in stroke: methodological issues and proposed standard criteria. *Stroke.* 36(9): 2027-2031.

Donnan GA, Fisher M, Macleod M, Davis SM (2008). Stroke. *Lancet.* 371(9624): 1612-1623.

Drechsler M, Megens RT, van Zandvoort M, Weber C, Soehnlein O (2010). Hyperlipidemia-triggered neutrophilia promotes early atherosclerosis. *Circulation.* 122(18): 1837-1845.

El Ghouzzi V, Lajeunie E, Le Merrer M, Cormier-Daire V, Renier D, Munnich A, Bonaventure J (1999). Mutations within or upstream of the basic helix-loop-helix domain of the TWIST gene are specific to Saethre-Chotzen syndrome. *Eur J Hum Genet.* 7(1): 27-33.

Falkenberg KJ, Johnstone RW (2014). Histone deacetylases and their inhibitors in cancer, neurological diseases and immune disorders. *Nat Rev Drug Discov.* 13(9): 673-691.

Faraco G, Pancani T, Formentini L, Mascagni P, Fossati G, Leoni F, Moroni F, Chiarugi A (2006). Pharmacological inhibition of histone deacetylases by suberoylanilide hydroxamic acid specifically alters gene expression and reduces ischemic injury in the mouse brain. *Mol Pharmacol.* 70(6): 1876-1884.

Feigin VL, Forouzanfar MH, Krishnamurthi R, Mensah GA, Connor M, Bennett DA, Moran AE, Sacco RL, Anderson L, Truelsen T, O'Donnell M, Venketasubramanian N, Barker-Collo S, Lawes CM, Wang W, et al. (2014). Global and regional burden of stroke during 1990-2010: findings from the Global Burden of Disease Study 2010. *Lancet.* 383(9913): 245-254.

Ferrante RJ, Kubilus JK, Lee J, Ryu H, Beesen A, Zucker B, Smith K, Kowall NW, Ratan RR, Luthi-Carter R, Hersch SM (2003). Histone deacetylase inhibition by sodium butyrate chemotherapy ameliorates the neurodegenerative phenotype in Huntington's disease mice. *J Neurosci.* 23(28): 9418-9427.

Findeisen HM, Gizard F, Zhao Y, Qing H, Heywood EB, Jones KL, Cohn D, Bruemmer D (2011). Epigenetic regulation of vascular smooth muscle cell proliferation and neointima formation by histone deacetylase inhibition. *Arterioscler Thromb Vasc Biol.* 31(4): 851-860.

Finn AV, Nakano M, Narula J, Kolodgie FD, Virmani R (2010). Concept of vulnerable/unstable plaque. *Arterioscler Thromb Vasc Biol.* 30(7): 1282-1292.

Fischle W, Dequiedt F, Hendzel MJ, Guenther MG, Lazar MA, Voelter W, Verdin E (2002). Enzymatic activity associated with class II HDACs is dependent on a multiprotein complex containing HDAC3 and SMRT/N-CoR. *Mol Cell.* 9(1): 45-57.

Frostegard J, Ulfgren AK, Nyberg P, Hedin U, Swedenborg J, Andersson U, Hansson GK (1999). Cytokine expression in advanced human atherosclerotic plaques: dominance of pro-inflammatory (Th1) and macrophage-stimulating cytokines. *Atherosclerosis.* 145(1): 33-43.

Getz GS, Reardon CA (2012). Animal models of atherosclerosis. *Arterioscler Thromb Vasc Biol.* 32(5): 1104-1115.

Goldstein LB, Adams R, Alberts MJ, Appel LJ, Brass LM, Bushnell CD, Culebras A, Degraba TJ, Gorelick PB, Guyton JR, Hart RG, Howard G, Kelly-Hayes M, Nixon JV, Sacco RL (2006). Primary prevention of ischemic stroke: a guideline from the American Heart Association/American Stroke Association Stroke Council: cosponsored by the Atherosclerotic Peripheral Vascular Disease Interdisciplinary Working Group; Cardiovascular Nursing Council; Clinical Cardiology Council; Nutrition, Physical Activity, and Metabolism Council; and the Quality of Care and Outcomes Research Interdisciplinary Working Group: the American Academy of Neurology affirms the value of this guideline. *Stroke.* 37(6): 1583-1633.

Grau AJ, Weimar C, Buggle F, Heinrich A, Goertler M, Neumaier S, Glahn J, Brandt T, Hacke W, Diener HC (2001). Risk factors, outcome, and treatment in subtypes of ischemic stroke: the German stroke data bank. *Stroke.* 32(11): 2559-2566.

Gretarsdottir S, Thorleifsson G, Manolescu A, Styrkarsdottir U, Helgadottir A, Gschwendtner A, Kostulas K, Kuhlenbaumer G, Bevan S, Jonsdottir T, Bjarnason H, Saemundsdottir J, Palsson S, Arnar DO, Holm H, et al. (2008). Risk variants for atrial fibrillation on chromosome 4q25 associate with ischemic stroke. *Ann Neurol.* 64(4): 402-409.

Gschwendtner A, Bevan S, Cole JW, Plourde A, Matarin M, Ross-Adams H, Meitinger T, Wichmann E, Mitchell BD, Furie K, Slowik A, Rich SS, Syme PD, MacLeod MJ, Meschia JF, et al. (2009). Sequence variants on chromosome 9p21.3 confer risk for atherosclerotic stroke. *Ann Neurol.* 65(5): 531-539.

Gu L, Okada Y, Clinton SK, Gerard C, Sukhova GK, Libby P, Rollins BJ (1998). Absence of monocyte chemoattractant protein-1 reduces atherosclerosis in low density lipoprotein receptor-deficient mice. *Mol Cell.* 2(2): 275-281.

Gudbjartsson DF, Holm H, Gretarsdottir S, Thorleifsson G, Walters GB, Thorgeirsson G, Gulcher J, Mathiesen EB, Njolstad I, Nyrnes A, Wilsgaard T, Hald EM, Hveem K, Stoltenberg C, Kucera G, et al. (2009). A sequence variant in ZFHX3 on 16q22 associates with atrial fibrillation and ischemic stroke. *Nat Genet.* 41(8): 876-878.

Haberland M, Montgomery RL, Olson EN (2009). The many roles of histone deacetylases in development and physiology: implications for disease and therapy. *Nat Rev Genet.* 10(1): 32-42.

Hacke W, Kaste M, Bluhmki E, Brozman M, Davalos A, Guidetti D, Larrue V, Lees KR, Medeghri Z, Machnig T, Schneider D, von Kummer R, Wahlgren N, Toni D (2008). Thrombolysis with alteplase 3 to 4.5 hours after acute ischemic stroke. *N Engl J Med.* 359(13): 1317-1329.

Hansson GK (2005). Inflammation, atherosclerosis, and coronary artery disease. *N Engl J Med.* 352(16): 1685-1695.

Herijgers N, Van Eck M, Groot PH, Hoogerbrugge PM, Van Berkel TJ (1997). Effect of bone marrow transplantation on lipoprotein metabolism and atherosclerosis in LDL receptor-knockout mice. *Arterioscler Thromb Vasc Biol.* 17(10): 1995-2003.

Hirschhorn JN, Lohmueller K, Byrne E, Hirschhorn K (2002). A comprehensive review of genetic association studies. *Genet Med.* 4(2): 45-61.

Ionita MG, van den Borne P, Catanzariti LM, Moll FL, de Vries JP, Pasterkamp G, Vink A, de Kleijn DP (2010). High neutrophil numbers in human carotid atherosclerotic plaques are associated with characteristics of rupture-prone lesions. *Arterioscler Thromb Vasc Biol.* 30(9): 1842-1848.

Jonasson L, Holm J, Skalli O, Bondjers G, Hansson GK (1986). Regional accumulations of T cells, macrophages, and smooth muscle cells in the human atherosclerotic plaque. *Arteriosclerosis.* 6(2): 131-138.

Jovin TG, Chamorro A, Cobo E, de Miquel MA, Molina CA, Rovira A, San Roman L, Serena J, Abilleira S, Ribo M, Millan M, Urra X, Cardona P, Lopez-Cancio E, Tomasello A, et al. (2015). Thrombectomy within 8 hours after symptom onset in ischemic stroke. *N Engl J Med.* 372(24): 2296-2306.

Kazantsev AG, Thompson LM (2008). Therapeutic application of histone deacetylase inhibitors for central nervous system disorders. *Nat Rev Drug Discov.* 7(10): 854-868.

Kee HJ, Kwon JS, Shin S, Ahn Y, Jeong MH, Kook H (2011). Trichostatin A prevents neointimal hyperplasia via activation of Kruppel like factor 4. *Vascul Pharmacol.* 55(5-6): 127-134.

Kee HJ, Sohn IS, Nam KI, Park JE, Qian YR, Yin Z, Ahn Y, Jeong MH, Bang YJ, Kim N, Kim JK, Kim KK, Epstein JA, Kook H (2006). Inhibition of histone deacetylation blocks cardiac hypertrophy induced by angiotensin II infusion and aortic banding. *Circulation.* 113(1): 51-59.

Kim HJ, Rowe M, Ren M, Hong JS, Chen PS, Chuang DM (2007). Histone deacetylase inhibitors exhibit anti-inflammatory and neuroprotective effects in a rat permanent ischemic model of stroke: multiple mechanisms of action. *J Pharmacol Exp Ther.* 321(3): 892-901.

Klingenberg R, Gerdes N, Badeau RM, Gistera A, Strodthoff D, Ketelhuth DF, Lundberg AM, Rudling M, Nilsson SK, Olivecrona G, Zoller S, Lohmann C, Luscher TF, Jauhiainen M, Sparwasser T, et al. (2013). Depletion of FOXP3+ regulatory T cells promotes hypercholesterolemia and atherosclerosis. *J Clin Invest.* 123(3): 1323-1334.

Kook H, Lepore JJ, Gitler AD, Lu MM, Wing-Man Yung W, Mackay J, Zhou R, Ferrari V, Gruber P, Epstein JA (2003). Cardiac hypertrophy and histone deacetylase-dependent transcriptional repression mediated by the atypical homeodomain protein Hop. *J Clin Invest.* 112(6): 863-871.

Lahm A, Paolini C, Pallaoro M, Nardi MC, Jones P, Neddermann P, Sambucini S, Bottomley MJ, Lo Surdo P, Carfi A, Koch U, De Francesco R, Steinkuhler C, Gallinari P (2007). Unraveling the hidden catalytic activity of vertebrate class IIa histone deacetylases. *Proc Natl Acad Sci U S A.* 104(44): 17335-17340.

Langley B, D'Annibale MA, Suh K, Ayoub I, Tolhurst A, Bastan B, Yang L, Ko B, Fisher M, Cho S, Beal MF, Ratan RR (2008). Pulse inhibition of histone deacetylases induces complete resistance to oxidative death in cortical neurons without toxicity and reveals a role for cytoplasmic p21(waf1/cip1) in cell cycle-independent neuroprotection. *J Neurosci.* 28(1): 163-176.

Lanktree MB, Hegele RA, Yusuf S, Anand SS (2009). Multi-ethnic genetic association study of carotid intima-media thickness using a targeted cardiovascular SNP microarray. *Stroke.* 40(10): 3173-3179.

Lemmens R, Buysschaert I, Geelen V, Fernandez-Cadenas I, Montaner J, Schmidt H, Schmidt R, Attia J, Maguire J, Levi C, Jood K, Blomstrand C, Jern C, Wnuk M, Slowik A, et al. (2010). The association of the 4q25 susceptibility variant for atrial fibrillation with stroke is limited to stroke of cardioembolic etiology. *Stroke.* 41(9): 1850-1857.

Linton MF, Atkinson JB, Fazio S (1995). Prevention of atherosclerosis in apolipoprotein E-deficient mice by bone marrow transplantation. *Science.* 267(5200): 1034-1037.

Lozano R, Naghavi M, Foreman K, Lim S, Shibuya K, Aboyans V, Abraham J, Adair T, Aggarwal R, Ahn SY, Alvarado M, Anderson HR, Anderson LM, Andrews KG, Atkinson C, et al. (2012). Global and regional mortality from 235 causes of death for 20 age groups in 1990 and 2010: a systematic analysis for the Global Burden of Disease Study 2010. *Lancet.* 380(9859): 2095-2128.

Lusis AJ (2000). Atherosclerosis. *Nature.* 407(6801): 233-241.

Lusis AJ, Fogelman AM, Fonarow GC (2004). Genetic basis of atherosclerosis: part I: new genes and pathways. *Circulation.* 110(13): 1868-1873.

Mallat Z, Besnard S, Duriez M, Deleuze V, Emmanuel F, Bureau MF, Soubrier F, Esposito B, Duez H, Fievet C, Staels B, Duverger N, Scherman D, Tedgui A (1999). Protective role of interleukin-10 in atherosclerosis. *Circ Res.* 85(8): e17-24.

Mallat Z, Gojova A, Marchiol-Fournigault C, Esposito B, Kamate C, Merval R, Fradelizi D, Tedgui A (2001). Inhibition of transforming growth factor-beta signaling accelerates atherosclerosis and induces an unstable plaque phenotype in mice. *Circ Res.* 89(10): 930-934.

Mansour AA, Khazanov-Zisman S, Netser Y, Klar A, Ben-Arie N (2014). Nato3 plays an integral role in dorsoventral patterning of the spinal cord by segregating floor plate/p3 fates via Nkx2.2 suppression and Foxa2 maintenance. *Development.* 141(3): 574-584.

Marks PA, Breslow R (2007). Dimethyl sulfoxide to vorinostat: development of this histone deacetylase inhibitor as an anticancer drug. *Nat Biotechnol.* 25(1): 84-90.

Markus HS, Makela KM, Bevan S, Raitoharju E, Oksala N, Bis JC, O'Donnell C, Hainsworth A, Lehtimaki T (2013). Evidence HDAC9 genetic variant associated with ischemic stroke increases risk via promoting carotid atherosclerosis. *Stroke.* 44(5): 1220-1225.

Marson AG, Al-Kharusi AM, Alwaidh M, Appleton R, Baker GA, Chadwick DW, Cramp C, Cockerell OC, Cooper PN, Doughty J, Eaton B, Gamble C, Goulding PJ, Howell SJ, Hughes A, et al. (2007). The SANAD study of effectiveness of valproate, lamotrigine, or topiramate for generalised and unclassifiable epilepsy: an unblinded randomised controlled trial. *Lancet.* 369(9566): 1016-1026.

Marteau JB, Zaiou M, Siest G, Visvikis-Siest S (2005). Genetic determinants of blood pressure regulation. *J Hypertens.* 23(12): 2127-2143.

Matsuyama A, Shimazu T, Sumida Y, Saito A, Yoshimatsu Y, Seigneurin-Berny D, Osada H, Komatsu Y, Nishino N, Khochbin S, Horinouchi S, Yoshida M (2002). In vivo destabilization of dynamic microtubules by HDAC6-mediated deacetylation. *EMBO J.* 21(24): 6820-6831.

McKinsey TA, Zhang CL, Lu J, Olson EN (2000). Signal-dependent nuclear export of a histone deacetylase regulates muscle differentiation. *Nature.* 408(6808): 106-111.

Miraoui H, Marie PJ (2010). Pivotal role of Twist in skeletal biology and pathology. *Gene.* 468(1-2): 1-7.

Moore KJ, Sheedy FJ, Fisher EA (2013). Macrophages in atherosclerosis: a dynamic balance. *Nat Rev Immunol.* 13(10): 709-721.

Morrison BE, Majdzadeh N, Zhang X, Lyles A, Bassel-Duby R, Olson EN, D'Mello SR (2006). Neuroprotection by histone deacetylase-related protein. *Mol Cell Biol.* 26(9): 3550-3564.

Mozaffarian D, Benjamin EJ, Go AS, Arnett DK, Blaha MJ, Cushman M, de Ferranti S, Despres JP, Fullerton HJ, Howard VJ, Huffman MD, Judd SE, Kissela BM, Lackland DT, Lichtman JH, et al. (2015). Heart disease and stroke statistics--2015 update: a report from the American Heart Association. *Circulation.* 131(4): e29-322.

Murray CJ, Vos T, Lozano R, Naghavi M, Flaxman AD, Michaud C, Ezzati M, Shibuya K, Salomon JA, Abdalla S, Aboyans V, Abraham J, Ackerman I, Aggarwal R, Ahn SY, et al. (2012). Disability-adjusted life years (DALYs) for 291 diseases and injuries in 21 regions, 1990-2010: a systematic analysis for the Global Burden of Disease Study 2010. *Lancet.* 380(9859): 2197-2223.

Musunuru K, Strong A, Frank-Kamenetsky M, Lee NE, Ahfeldt T, Sachs KV, Li X, Li H, Kuperwasser N, Ruda VM, Pirruccello JP, Muchmore B, Prokunina-Olsson L, Hall JL, Schadt EE, et al. (2010). From noncoding variant to phenotype via SORT1 at the 1p13 cholesterol locus. *Nature.* 466(7307): 714-719.

Nakashima Y, Plump AS, Raines EW, Breslow JL, Ross R (1994). ApoE-deficient mice develop lesions of all phases of atherosclerosis throughout the arterial tree. *Arterioscler Thromb.* 14(1): 133-140.

Nakashima Y, Raines EW, Plump AS, Breslow JL, Ross R (1998). Upregulation of VCAM-1 and ICAM-1 at atherosclerosis-prone sites on the endothelium in the ApoE-deficient mouse. *Arterioscler Thromb Vasc Biol.* 18(5): 842-851.

Olesen J, Gustavsson A, Svensson M, Wittchen HU, Jonsson B (2012). The economic cost of brain disorders in Europe. *Eur J Neurol.* 19(1): 155-162.

Ono Y, Nakatani T, Minaki Y, Kumai M (2010). The basic helix-loop-helix transcription factor Nato3 controls neurogenic activity in mesencephalic floor plate cells. *Development.* 137(11): 1897-1906.

Paulsson G, Zhou X, Tornquist E, Hansson GK (2000). Oligoclonal T cell expansions in atherosclerotic lesions of apolipoprotein E-deficient mice. *Arterioscler Thromb Vasc Biol.* 20(1): 10-17.

Petrie K, Guidez F, Howell L, Healy L, Waxman S, Greaves M, Zelent A (2003). The histone deacetylase 9 gene encodes multiple protein isoforms. *J Biol Chem.* 278(18): 16059-16072.

Plump AS, Smith JD, Hayek T, Aalto-Setala K, Walsh A, Verstuyft JG, Rubin EM, Breslow JL (1992). Severe hypercholesterolemia and atherosclerosis in apolipoprotein E-deficient mice created by homologous recombination in ES cells. *Cell.* 71(2): 343-353.

Rajavashisth TB, Andalibi A, Territo MC, Berliner JA, Navab M, Fogelman AM, Lusis AJ (1990). Induction of endothelial cell expression of granulocyte and macrophage colony-stimulating factors by modified low-density lipoproteins. *Nature.* 344(6263): 254-257.

Ross R, Harker L (1976). Hyperlipidemia and atherosclerosis. *Science.* 193(4258): 1094-1100.

Rotzius P, Thams S, Soehnlein O, Kenne E, Tseng CN, Bjorkstrom NK, Malmberg KJ, Lindbom L, Eriksson EE (2010). Distinct infiltration of neutrophils in lesion shoulders in ApoE-/- mice. *Am J Pathol.* 177(1): 493-500.

Sacco RL, Kasner SE, Broderick JP, Caplan LR, Connors JJ, Culebras A, Elkind MS, George MG, Hamdan AD, Higashida RT, Hoh BL, Janis LS, Kase CS, Kleindorfer DO, Lee JM, et al. (2013). An updated definition of stroke for the 21st century: a statement for healthcare professionals from the American Heart Association/American Stroke Association. *Stroke.* 44(7): 2064-2089.

Saver JL, Goyal M, Bonafe A, Diener HC, Levy EI, Pereira VM, Albers GW, Cognard C, Cohen DJ, Hacke W, Jansen O, Jovin TG, Mattle HP, Nogueira RG, Siddiqui AH, et al. (2015). Stent-retriever thrombectomy after intravenous t-PA vs. t-PA alone in stroke. *N Engl J Med.* 372(24): 2285-2295.

Seshadri S, Wolf PA (2007). Lifetime risk of stroke and dementia: current concepts, and estimates from the Framingham Study. *Lancet Neurol.* 6(12): 1106-1114.

Shahbazian MD, Grunstein M (2007). Functions of site-specific histone acetylation and deacetylation. *Annu Rev Biochem.* 76: 75-100.

Shakespear MR, Halili MA, Irvine KM, Fairlie DP, Sweet MJ (2011). Histone deacetylases as regulators of inflammation and immunity. *Trends Immunol.* 32(7): 335-343.

Shakespear MR, Hohenhaus DM, Kelly GM, Kamal NA, Gupta P, Labzin LI, Schroder K, Garceau V, Barbero S, Iyer A, Hume DA, Reid RC, Irvine KM, Fairlie DP, Sweet MJ (2013). Histone deacetylase 7 promotes Toll-like receptor 4-dependent proinflammatory gene expression in macrophages. *J Biol Chem.* 288(35): 25362-25374.

Shein NA, Shohami E (2011). Histone deacetylase inhibitors as therapeutic agents for acute central nervous system injuries. *Mol Med.* 17(5-6): 448-456.

Skalen K, Gustafsson M, Rydberg EK, Hulten LM, Wiklund O, Innerarity TL, Boren J (2002). Subendothelial retention of atherogenic lipoproteins in early atherosclerosis. *Nature.* 417(6890): 750-754.

Stemme S, Faber B, Holm J, Wiklund O, Witztum JL, Hansson GK (1995). T lymphocytes from human atherosclerotic plaques recognize oxidized low density lipoprotein. *Proc Natl Acad Sci U S A.* 92(9): 3893-3897.

Stemme S, Holm J, Hansson GK (1992). T lymphocytes in human atherosclerotic plaques are memory cells expressing CD45RO and the integrin VLA-1. *Arterioscler Thromb.* 12(2): 206-211.

Stoneman V, Braganza D, Figg N, Mercer J, Lang R, Goddard M, Bennett M (2007). Monocyte/macrophage suppression in CD11b diphtheria toxin receptor transgenic mice differentially affects atherogenesis and established plaques. *Circ Res.* 100(6): 884-893.

Stylianou IM, Bauer RC, Reilly MP, Rader DJ (2012). Genetic basis of atherosclerosis: insights from mice and humans. *Circ Res.* 110(2): 337-355.

Swirski FK, Libby P, Aikawa E, Alcaide P, Luscinskas FW, Weissleder R, Pittet MJ (2007). Ly-6Chi monocytes dominate hypercholesterolemia-associated monocytosis and give rise to macrophages in atheromata. *J Clin Invest.* 117(1): 195-205.

Tao R, de Zoeten EF, Ozkaynak E, Chen C, Wang L, Porrett PM, Li B, Turka LA, Olson EN, Greene MI, Wells AD, Hancock WW (2007). Deacetylase inhibition promotes the generation and function of regulatory T cells. *Nat Med.* 13(11): 1299-1307.

The National Institute of Neurological Disorders and Stroke rt-PA Stroke Study Group (1995). Tissue plasminogen activator for acute ischemic stroke. The National Institute of Neurological Disorders and Stroke rt-PA Stroke Study Group. *N Engl J Med.* 333(24): 1581-1587.

Traylor M, Farrall M, Holliday EG, Sudlow C, Hopewell JC, Cheng YC, Fornage M, Ikram MA, Malik R, Bevan S, Thorsteinsdottir U, Nalls MA, Longstreth W, Wiggins KL, Yadav S, et al. (2012). Genetic risk factors for ischaemic stroke and its subtypes (the METASTROKE collaboration): a meta-analysis of genome-wide association studies. *Lancet Neurol.* 11(11): 951-962.

van Leeuwen M, Gijbels MJ, Duijvestijn A, Smook M, van de Gaar MJ, Heeringa P, de Winther MP, Tervaert JW (2008). Accumulation of myeloperoxidase-positive neutrophils in atherosclerotic lesions in LDLR-/- mice. *Arterioscler Thromb Vasc Biol.* 28(1): 84-89.

Wang WY, Barratt BJ, Clayton DG, Todd JA (2005). Genome-wide association studies: theoretical and practical concerns. *Nat Rev Genet.* 6(2): 109-118.

Weber C, Zernecke A, Libby P (2008). The multifaceted contributions of leukocyte subsets to atherosclerosis: lessons from mouse models. *Nat Rev Immunol.* 8(10): 802-815.

Whitman SC, Ravisankar P, Elam H, Daugherty A (2000). Exogenous interferon-gamma enhances atherosclerosis in apolipoprotein E-/- mice. *Am J Pathol.* 157(6): 1819-1824.

Wingender E, Chen X, Hehl R, Karas H, Liebich I, Matys V, Meinhardt T, Pruss M, Reuter I, Schacherer F (2000). TRANSFAC: an integrated system for gene expression regulation. *Nucleic Acids Res.* 28(1): 316-319.

Yan K, Cao Q, Reilly CM, Young NL, Garcia BA, Mishra N (2011). Histone deacetylase 9 deficiency protects against effector T cell-mediated systemic autoimmunity. *J Biol Chem.* 286(33): 28833-28843.

Yildirim F, Gertz K, Kronenberg G, Harms C, Fink KB, Meisel A, Endres M (2008). Inhibition of histone deacetylation protects wildtype but not gelsolin-deficient mice from ischemic brain injury. *Exp Neurol.* 210(2): 531-542.

Zampetaki A, Zeng L, Margariti A, Xiao Q, Li H, Zhang Z, Pepe AE, Wang G, Habi O, deFalco E, Cockerill G, Mason JC, Hu Y, Xu Q (2010). Histone deacetylase 3 is critical in endothelial survival and atherosclerosis development in response to disturbed flow. *Circulation.* 121(1): 132-142.

Zhang CL, McKinsey TA, Chang S, Antos CL, Hill JA, Olson EN (2002). Class II histone deacetylases act as signal-responsive repressors of cardiac hypertrophy. *Cell.* 110(4): 479-488.

Zhang R, Brennan ML, Fu X, Aviles RJ, Pearce GL, Penn MS, Topol EJ, Sprecher DL, Hazen SL (2001). Association between myeloperoxidase levels and risk of coronary artery disease. *JAMA.* 286(17): 2136-2142.

Zhou X, Nicoletti A, Elhage R, Hansson GK (2000). Transfer of CD4(+) T cells aggravates atherosclerosis in immunodeficient apolipoprotein E knockout mice. *Circulation.* 102(24): 2919-2922.

9 Acknowledgments

First and foremost, I would like to thank my supervisor PD Dr. Christof Haffner. I am very grateful for his guidance, motivation and especially his patience during the last years. I thank him for all the advice and support he gave me.

I would also like to thank Prof. Dr. Martin Dichgans for the opportunity to work in his laboratory and for giving me a very interesting project to work on. He was always supportive and open to new ideas. I appreciated the trust Prof. Dr. Martin Dichgans and PD Dr. Christof Haffner put in me and my work.

I am very thankful to Prof. Dr. Nikolaus Plesnila who constantly supported, encouraged, and motivated me with his enthusiasm. I really appreciated to be also a part of his team and that he always had an open door for discussions.

I would further like to acknowledge our cooperation partners (Prof. Dr. Christian Weber, Dr. Norbert Gerdes, Holger Winkels, Prof. Dr. Gerard Pasterkamp, Sander W. van der Laan, PD Dr. Gurumoorthy Krishnamoorthy, Dr. Kerstin Berer) for teaching me techniques, introducing me to the field of atherosclerosis and immunology, and exchanging data.

I am very grateful to my thesis advisory committee. I enjoyed and profited a lot from the fruitful discussions with Prof. Dr. Jochen Herms and Prof. Dr. Andreas Ladurner. I thank them for the time they spent to guide me and discuss my project.

Thanks a lot also to the Graduate School of Systemic Neurosciences for their constant support and the nice and motivating environment they created for their students. I would especially like to thank Dr. Julia Brenndörfer for her support during the last weeks when we always found solutions to finalize this thesis. I would also like to thank the Peters-Beer-Foundation for their financial support during the last year.

I am also grateful to the animal facility of the ISD (Dr. Manuela Schneider, Dr. Anne von Thaden, Peggy Kunath, Stefanie Wurster, Tamara Voss) and of the ZNP (Dr. Julia Geyer, Dr. Elisabeth Baloch, Dr. Gerda Mitteregger, Patrizia Bonert, Michaela Wellisch) for helping me to manage my mouse lines.

Special thanks I would like to express to Birgit, Melanie, Natalie and Uta for all the technical support they gave me, but also for their very constructive comments and constant encouragement which brought out the best in me. I also want to thank Marco and Farida for their motivation. They always had an open door for me and time for scientific discussion.

I would like to express my deep appreciation to Dr. Kerstin Berer. Without her, the immunological part of this thesis would not have been possible. I thank her for her patience, supervision, and the scientific and non-scientific discussions which stimulated my work and of course for all the fun we had together.

Thanks to all my colleagues, Caro, Eva, Barbara, Flavia, Matilde, Kathrin G., Pierre, Iga and Kathrin S. for our afternoon breaks, mutual motivation and consolations and their help in this project. Thanks to my friends Monika and Franziska for supporting me, always having time for me and all the chocolate cakes we made together.

I am enormously thankful to my parents for their patience, motivation, support, faith and love. Without them, this work would not have been possible.

I don`t have enough space to express my gratefulness and love to my partner, best friend and favorite colleague Dominik for his support, patience, great illustrations and for taking care of me.

Finally, I would like to thank all the proofreaders of this thesis.

10 Curriculum vitae

Personal data

Name:	Sepiede Azghandi
Date of birth:	22nd March 1990 in Gräfelfing, Germany
Nationality:	German

Education

Since 10.2011:	Fast-track PhD student at the Graduate School of Systemic Neurosciences, LMU Munich
	PhD project title: "Effect of HDAC9 Deficiency on Atherosclerosis and Stroke" in the laboratory of Prof. Dr. Martin Dichgans and Prof. Dr. Nikolaus Plesnila, Institute for Stroke and Dementia Research, Klinikum der Universität München Supervisor: PD Dr. Christof Haffner
10.2008 - 08.2011:	Bachelor of Science in "Molecular Medicine", Ulm University
	Bachelor thesis: "Effects of the toxins rotenone and 3-NP on oxidative stress and on the mitochondrial membrane potential in microglia"
09.2000 - 07.2008:	Erasmus-Grasser-Gymnasium, Munich ("Abitur", general qualification for university entrance)

Fellowships

Since 07.2014:	Fellowship of the Peters-Beer-Foundation
10.2011 - 09.2012:	GSN Fellowship for fast-track PhD students

Conferences

Role of HDAC9 deficiency in a murine model of atherosclerosis (Poster Presentation)

Advisory Board Meeting of the Institute for Stroke and Dementia Research, Munich, Germany (August 2013)

Deficiency of the stroke-relevant HDAC9 gene is atheroprotective (Oral Presentation)

European stroke organization conference, Glasgow, United Kingdom (April 2015)

Effect of HDAC9 deficiency on ischemic stroke outcome (Poster Presentation)

Brain 2015 – International Symposium on Cerebral Blood Flow, Metabolism and Function, Vancouver, Canada (June 2015)

Deficiency of the stroke-relevant HDAC9 gene is atheroprotective (Poster Presentation)

Brain 2015 – International Symposium on Cerebral Blood Flow, Metabolism and Function, Vancouver, Canada (June 2015)

11 Current publications

Deficiency of the Stroke Relevant HDAC9 Gene Attenuates Atherosclerosis in Accord With Allele-Specific Effects at 7p21.1

> **Sepiede Azghandi***, Caroline Prell*, Sander W. van der Laan, Manuela Schneider, Rainer Malik, Kerstin Berer, Norbert Gerdes, Gerard Pasterkamp, Christian Weber, Christof Haffner, Martin Dichgans
> *Stroke, January 2015, Volume 46, Issue 1, pp 197-202*

Effect of Decompressive Craniectomy on Outcome Following Subarachnoid Hemorrhage in Mice

> Dominik Bühler, **Sepiede Azghandi**, Kathrin Schüller, Nikolaus Plesnila
> *Stroke, March 2015, Volume 46, Issue 3, pp 819-826*

Eidesstattliche Versicherung

Hiermit versichere ich an Eides statt, dass ich die vorliegende Dissertation **„Effect of HDAC9 Deficiency on Atherosclerosis and Stroke"** selbstständig angefertigt habe, mich außer der angegebenen keiner weiteren Hilfsmittel bedient und alle Erkenntnisse, die aus dem Schrifttum ganz oder annähernd übernommen sind, als solche kenntlich gemacht und nach ihrer Herkunft unter Bezeichnung der Fundstelle einzeln nachgewiesen habe.

München, den _____

_____
Sepiede Azghandi

Author contributions

Die Autoren leisteten folgende Beiträge zu den Publikationen und Manuskripten:

1) Azghandi S*, Prell C*, van der Laan SW, Schneider M, Malik R, Berer K, Gerdes N, Pasterkamp G, Weber C, Haffner C, Dichgans M. **Deficiency of the Stroke Relevant HDAC9 Gene Attenuates Atherosclerosis in Accord With Allele-Specific Effects at 7p21.1.** *SA designed, acquired and analyzed the mouse experiments; CP acquired and analyzed the human gene expression data; SWvDL acquired and analyzed human atherosclerotic plaque data. MS, RM and KB worked as technical consultants and edited the manuscript. NG, GP, CW, CH and MD designed the study and edited the manuscript. SA, CP and MD wrote the manuscript.*

2) Azghandi S, Bühler D, Berer K, Dichgans M, Haffner C. **Effect of HDAC9 deficiency on atherosclerosis and immune cell homeostasis.** *SA designed the studies, performed and analyzed the experiments, and wrote the manuscript. DB worked as technical consultant and edited the manuscript. KB and CH contributed to writing of the manuscript. KB, MD and CH designed and supervised the study.*

3) Azghandi S, Bühler D, Mamrak U, Rynarzewska I, Schneider M, Haffner C, Dichgans M, Plesnila N. **Histone deacetylase 9 deficiency worsens brain damage and neurological function after experimental ischemic stroke.** *SA designed the studies, performed and analyzed the experiments, and wrote the manuscript. DB and UM performed and analyzed the experiments. IR and MS worked as technical consultants and edited the manuscript. DB and MD contributed to writing of the manuscript. NP and CH designed and supervised the study and edited the manuscript.*

Hiermit bestätige ich die angegebenen Beiträge zur Erstellung der Publikationen und Manuskripte.

München, den _____

_____
Sepiede Azghandi

_____   _____
Dr. Caroline Prell-Schicker   PD Dr. Christof Haffner
(shared first author)   (Supervisor)